宇宙線電子望遠鏡 CALET:
3 年間の軌道上観測による最新の成果

早稲田大学・理工総研 浅岡陽一
CALET共同研究者

CALET Collaboration Team

O. Adriani[25], Y. Akaike[2], K. Asano[7], Y. Asaoka[9,31], M.G. Bagliesi[29], E. Berti[25], G. Bigongiari[29], W.R. Binns[32], S. Bonechi[29], M. Bongi[25], P. Brogi[29], A. Bruno[15], J.H. Buckley[32], N. Cannady[13], G. Castellini[25], C. Checchia[26],M.L. Cherry[13], G. Collazuol[26], V. Di Felice[28], K. Ebisawa[8], H. Fuke[8], T.G. Guzik[13], T. Hams[3], N. Hasebe[31], K. Hibino[10], M. Ichimura[4], K. Ioka[34], W. Ishizaki[7], M.H. Israel[32], K. Kasahara[31], J. Kataoka[31], R. Kataoka[17], Y. Katayose[33], C. Kato[23], Y.Kawakubo[1], N. Kawanaka[30], K. Kohri [12], H.S. Krawczynski[32], J.F. Krizmanic[2], T. Lomtadze[27], P. Maestro[29], P.S. Marrocchesi[29], A.M. Messineo[27], J.W. Mitchell[15], S. Miyake[5], A.A. Moiseev[3], K. Mori[9,31], M. Mori[20], N. Mori[25], H.M. Motz[31], K. Munakata[23], H. Murakami[31], S. Nakahira[9], J. Nishimura[8], G.A De Nolfo[15], S. Okuno[10], J.F. Ormes[25], S. Ozawa[31], L. Pacini[25], F. Palma[28], V. Pal'shin[1], P. Papini[25], A.V. Penacchioni[29], B.F. Rauch[32], S.B. Ricciarini[25], K. Sakai[3], T. Sakamoto[1], M. Sasaki[3], Y. Shimizu[10], A. Shiomi[18], R. Sparvoli[28], P. Spillantini[25], F. Stolzi[29], S. Sugita[1], J.E. Suh[29], A. Sulaj[29], I. Takahashi[11], M. Takayanagi[8], M. Takita[7], T. Tamura[10], N. Tateyama[10], T. Terasawa[7], H. Tomida[8], S. Torii[31], Y. Tunesada[19], Y. Uchihori[16], S. Ueno[8], E. Vannuccini[25], J.P. Wefel[13], K. Yamaoka[14], S. Yanagita[6], A. Yoshida[1], and K. Yoshida[22]

1) Aoyama Gakuin University, Japan
2) CRESST/NASA/GSFC and Universities Space Research Association, USA
3) CRESST/NASA/GSFC and University of Maryland, USA
4) Hirosaki University, Japan
5) Ibaraki National College of Technology, Japan
6) Ibaraki University, Japan
7) ICRR, University of Tokyo, Japan
8) ISAS/JAXA Japan
9) JAXA, Japan
10) Kanagawa University, Japan
11) Kavli IPMU, University of Tokyo, Japan
12) KEK, Japan
13) Louisiana State University, USA
14) Nagoya University, Japan
15) NASA/GSFC, USA
16) National Inst. of Radiological Sciences, Japan
17) National Institute of Polar Research, Japan
18) Nihon University, Japan
19) Osaka City University, Japan
20) Ritsumeikan University, Japan
21) Saitama University, Japan
22) Shibaura Institute of Technology, Japan
23) Shinshu University, Japan
24) University of Denver, USA
25) University of Florence, IFAC (CNR) and INFN, Italy
26) University of Padova and INFN, Italy
27) University of Pisa and INFN, Italy
28) University of Rome Tor Vergata and INFN, Italy
29) University of Siena and INFN, Italy
30) University of Tokyo, Japan
31) Waseda University, Japan
32) Washington University-St. Louis, USA
33) Yokohama National University, Japan
34) Yukawa Institute for Theoretical Physics, Kyoto University, Japan

CALET Collaboration Team

O. Adriani[25], Y. Akaike[2], K. Asano[7], Y. Asaoka[9,31], M.G. Bagliesi[29], E. Berti[25], G. Bigongiari[29], W.R. Binns[32], S. Bonechi[29], M. Bongi[25], P. Brogi[29], A. Bruno[15], J.H. Buckley[32], N. Cannady[13], G. Castellini[25], C. Checchia[26],M.L. Cherry[13], G. Collazuol[26], V. Di Felice[28], K. Ebisawa[8], H. Fuke[8], T.G. Guzik[13], T. Hams[3], N. Hasebe[31], K. Hibino[10], M. Ichimura[4], K. Ioka[34], W. Ishizaki[7], M.H. Israel[32], K. Kasahara[31], J. Kataoka[31], R. Kataoka[17], Y. Katayose[33], C. Kato[23], Y.Kawakubo[1], N. Kawanaka[30], K. Kohri [12], H.S. Krawczynski[32], J.F. Krizmanic[2], T. Lomtadze[27], P. Maestro[29], P.S. Marrocchesi[29], A.M. Messineo[27], J.W. Mitchell[15], S. Miyake[5], A.A. Moiseev[3], K. Mori[9,31], M. Mori[20], N. Mori[25], H.M. Motz[31], K. Munakata[23], H. Murakami[31], S. Nakahira[9], J. Nishimura[8], G.A De Nolfo[15], S. Okuno[10], J.F. Ormes[25], S. Ozawa[31], L. Pacini[25], F. Palma[28], V. Pal'shin[1], P. Papini[25], A.V. Penacchioni[29], B.F. Rauch[32], S.B. Ricciarini[25], K. Sakai[3], T. Sakamoto[1], M. Sasaki[3], Y. Shimizu[10], A. Shiomi[18], R. Sparvoli[28], P. Spillantini[25], F. Stolzi[29], S. Sugita[1], J.E. Suh[29], A. Sulaj[29], I. Takahashi[11], M. Takayanagi[8], M. Takita[7], T. Tamura[10], N. Tateyama[10], T. Terasawa[7], H. Tomida[8], S. Torii[31], Y. Tunesada[19], Y. Uchihori[16], S. Ueno[8], E. Vannuccini[25], J.P. Wefel[13], K. Yamaoka[14], S. Yanagita[6], A. Yoshida[1], and K. Yoshida[22]

Outline

1. Introduction
2. Calibration
3. Operations
4. Results
   - Electrons
   - Hadrons
   - Gamma-Rays
   - Space Weather
5. Summary

Y.Asaoka, Y.Akaike, Y.Komiya, R.Miyata, S.Torii et al. (CALET Collaboration), Astropart. Phys. 91 (2017) 1.

Y.Asaoka, S.Ozawa, S.Torii et al. (CALET Collaboration), Astropart. Phys. 100 (2018) 29.

O.Adriani et al. (CALET Collaboration), Phys.Rev.Lett. 119 (2017) 181101.

O.Adriani et al. (CALET Collaboration), Phys.Rev.Lett. 120 (2018) 261102.

O.Adriani et al. (CALET Collab.), ApJL 829 (2016) L20.
O.Adriani et al. (CALET Collab.), ApJ 863 (2018) 160.
N.Cannady, Y.Asaoka et al. (CALET Collab.), ApJS in press.

R.Kataoka et al., JGR, 10.1002/2016GL068930 (2016).

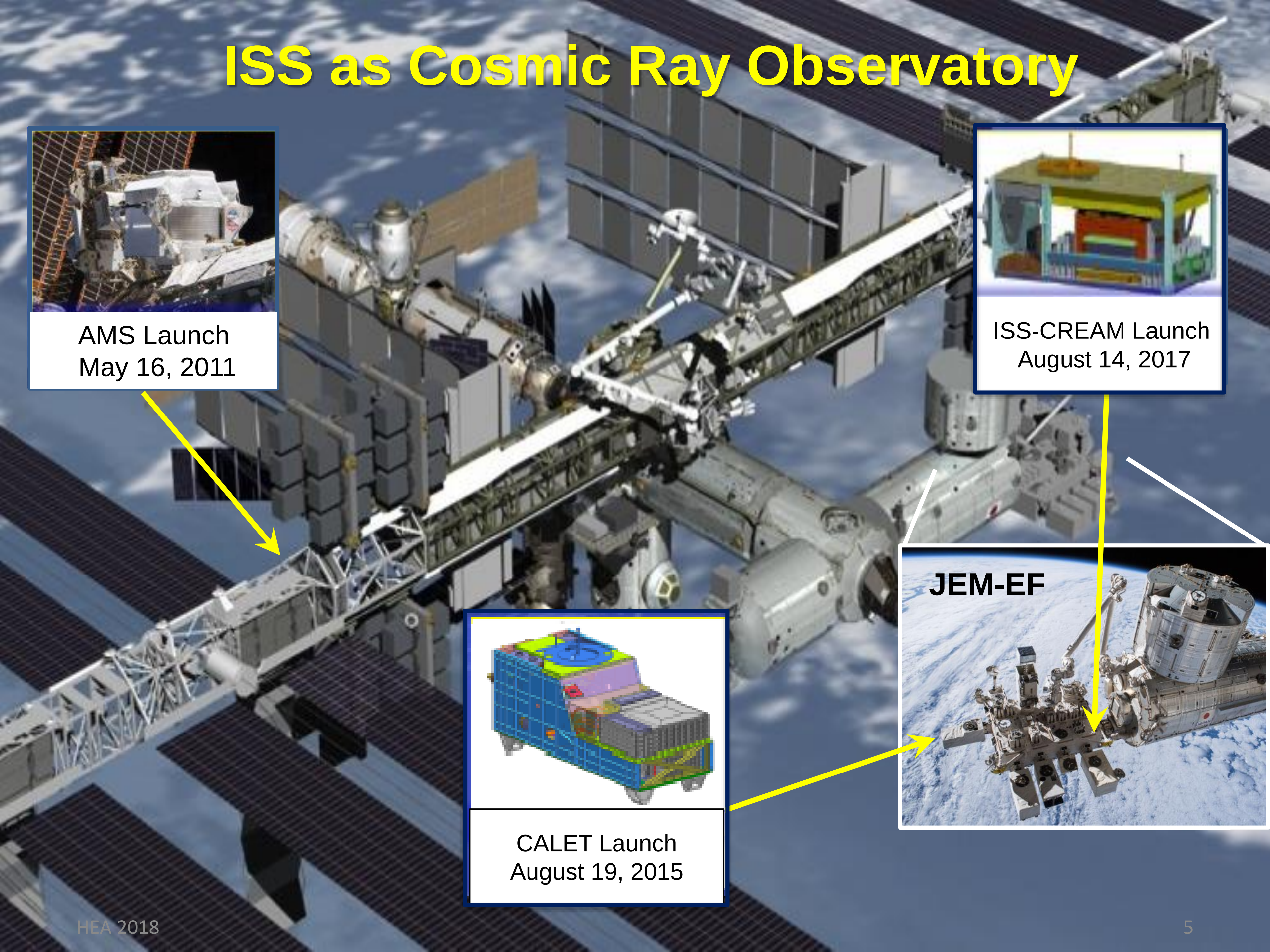
ISS as Cosmic Ray Observatory
AMS Launch
May 16, 2011
ISS-CREAM Launch
August 14, 2017
JEM-EF
CALET Launch
August 19, 2015

ISS as Cosmic Ray Observatory

AMS Launch
May 16, 2011

Magnet Spectrometer
- Various PID
- Anti-particles
- E ≤ TeV

Calorimeter
- Carbon target
- Hadrons
- Including TeV region

ISS-CREAM Launch
August 14, 2017

Calorimeter
- Fully active
- Electrons
- Including TeV region

CALET Launch
August 19, 2015

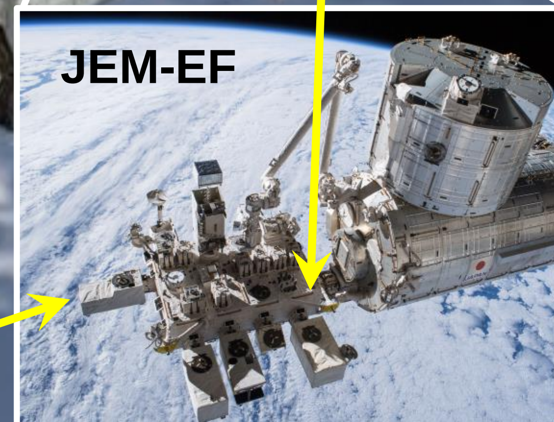

Cosmic Ray Observations at the ISS and CALET

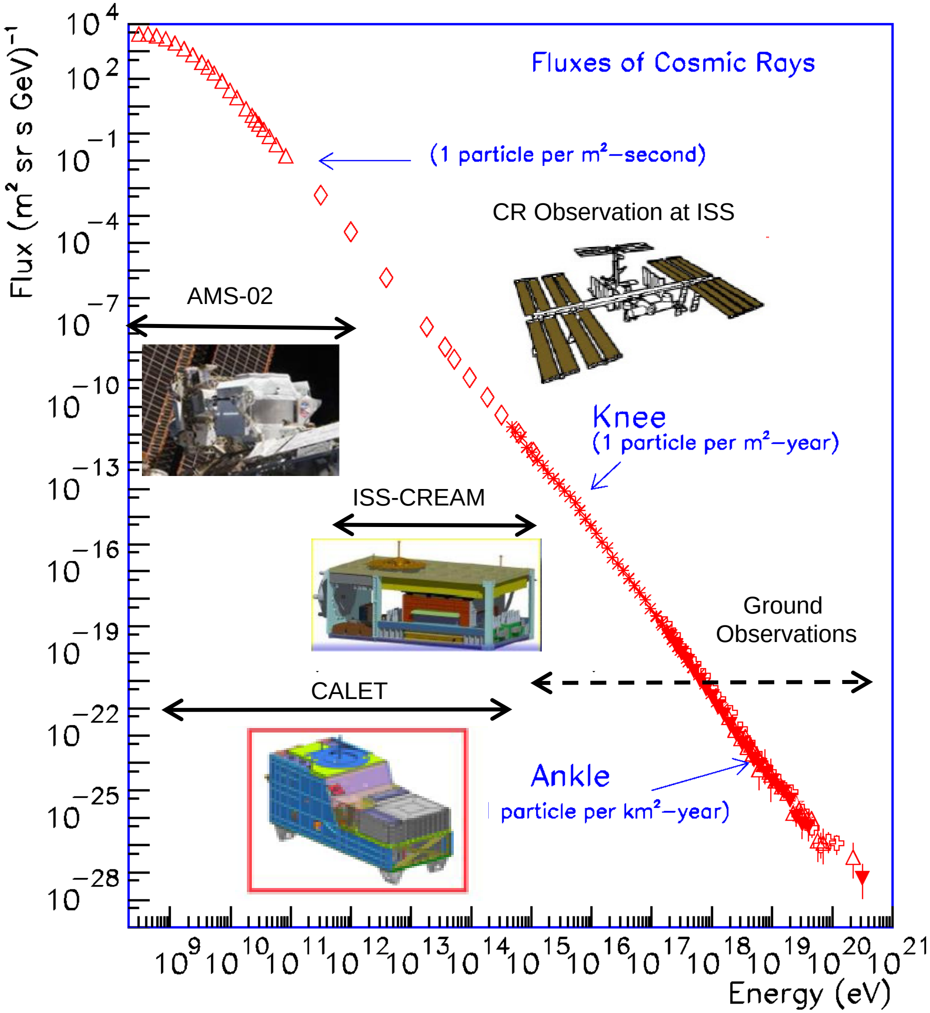

Overview of CALET Observations

- Direct cosmic ray observations in space at the highest energy region by combining:
  - ✓ A large-size detector
  - ✓ Long-term observation onboard the ISS (5 years or more is expected)
- Electron observation in 1 GeV - 20 TeV will be achieved with high energy resolution due to optimization for electron detection
  ⇨ Search for Dark Matter and Nearby Sources
- Observation of cosmic-ray nuclei will be performed in energy region from 10 GeV to 1 PeV
  ⇨ Unravelling the CR acceleration and propagation mechanism
- Detection of transient phenomena is expected in space by long-term stable observations
  ⇨ EM radiation from GW sources, Gamma-ray burst, Solar flare, etc.

CALET Payload

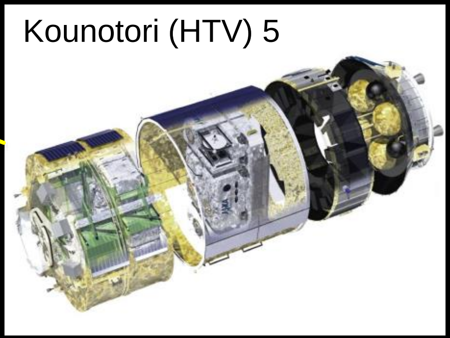

Launched on Aug. 19th, 2015 by the Japanese H2-B rocket

Emplaced on JEM-EF port #9 on Aug. 25th, 2015 (JEM-EF: Japanese Experiment Module-Exposed Facility)

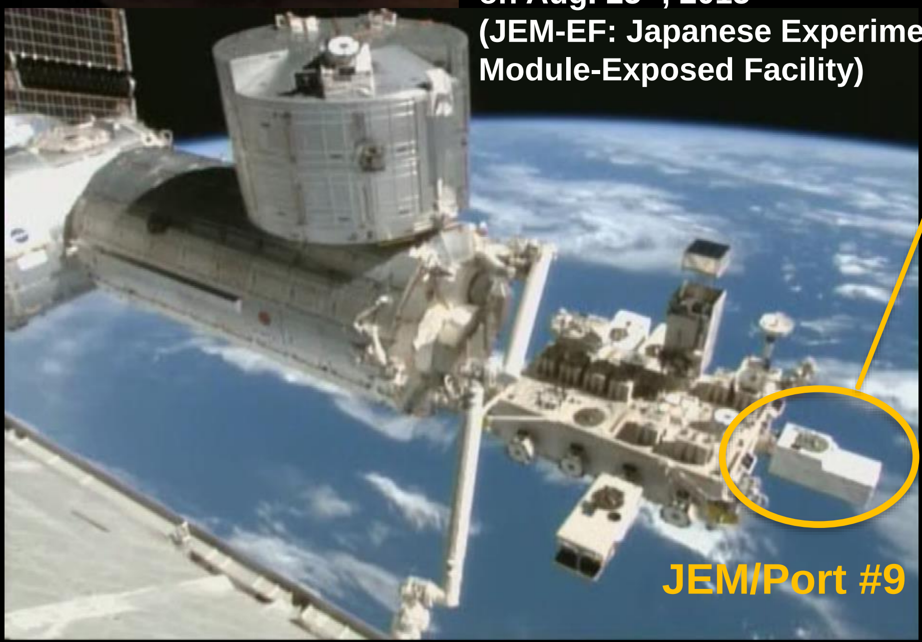

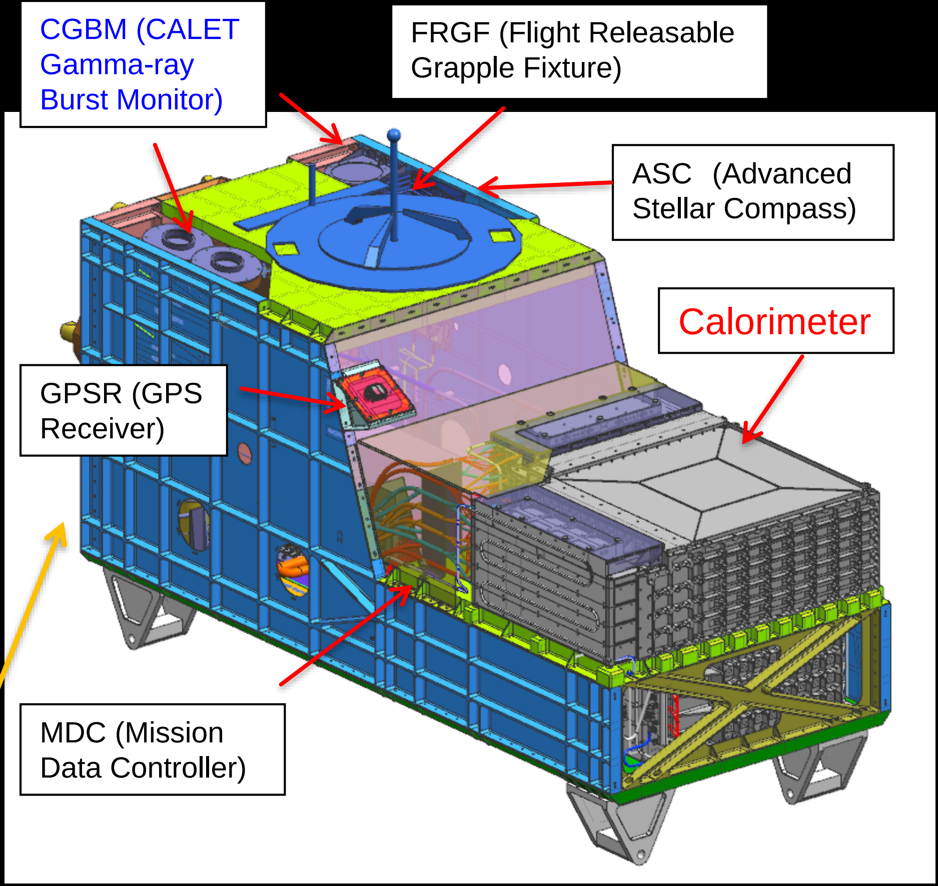

- **Mass: 612.8 kg**
- **JEM Standard Payload Size:**
  1850mm(L) × 800mm(W) × 1000mm(H)
- **Power Consumption: 507 W（max）**
- **Telemetry:**
  Medium 600 kbps (6.5GB/day) / Low 50 kbps

CALET Instrument

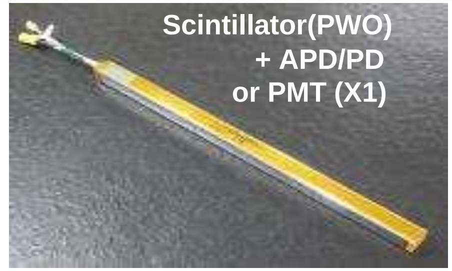

CALORIMETER

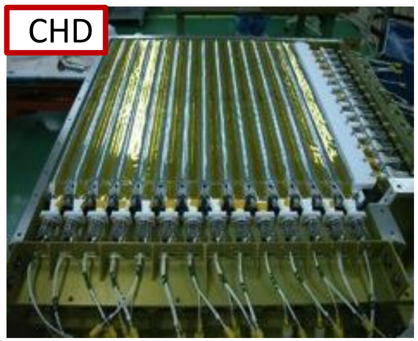

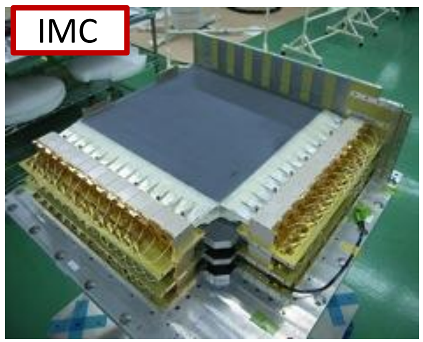

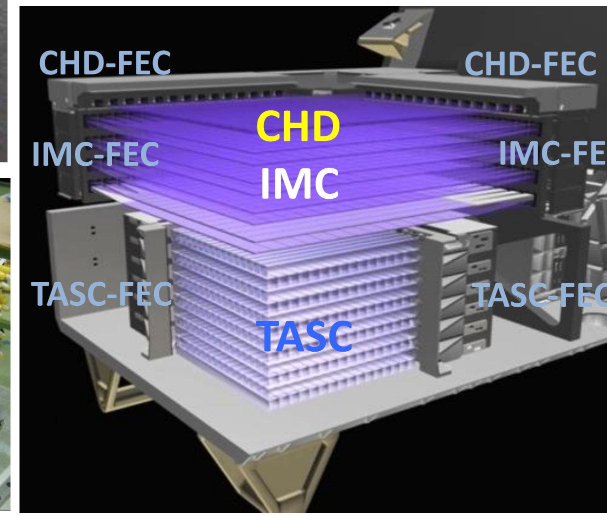

	CHD (Charge Detector)	IMC (Imaging Calorimeter)	TASC (Total Absorption Calorimeter)
Measure	**Charge (Z=1-40)**	**Tracking , Particle ID**	**Energy, e/p Separation**
Geometry (Material)	**Plastic Scintillator 14 paddles x 2 layers (X,Y): 28 paddles Paddle Size: 32 x 10 x 450 mm^3**	**448 Scifi x 16 layers (X,Y) : 7168 Scifi 7 W layers (3X_0): 0.2X_0 x 5 + 1X_0 x2 Scifi size : 1 x 1 x 448 mm^3**	**16 PWO logs x 12 layers (x,y): 192 logs log size: 19 x 20 x 326 mm^3 Total Thickness : 27 X_0 , ~1.2 λ_I**
Readout	**PMT+CSA**	**64-anode PMT+ ASIC**	**APD/PD+CSA PMT+CSA (for Trigger)@top layer**

Event Examples of High-Energy Showers

Electron, E=3.05 TeV

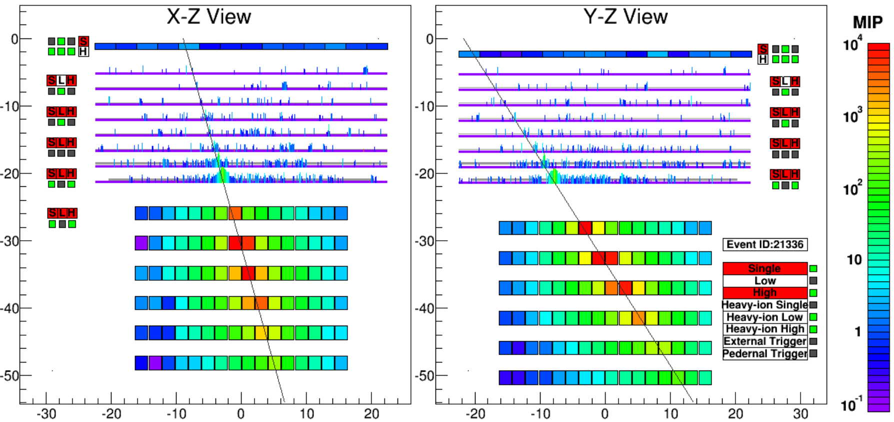

fully contained even at 3TeV

Proton, ΔE=2.89 TeV

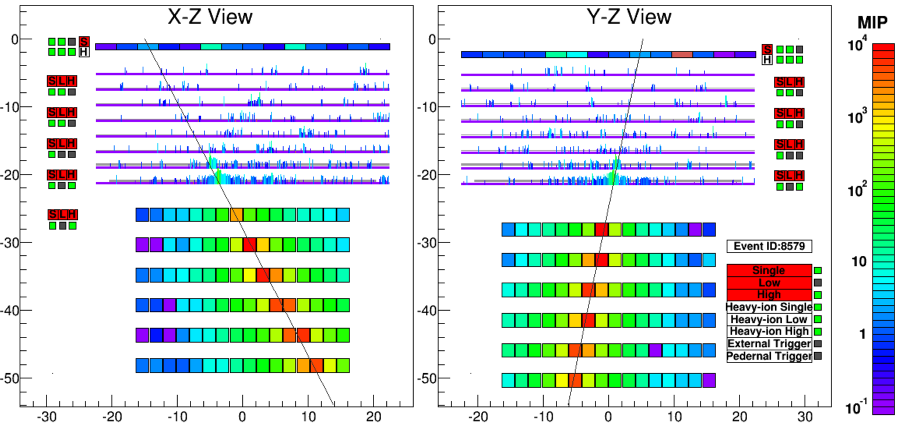

clear difference from electron shower

Fe(Z=26), ΔE=9.3 TeV

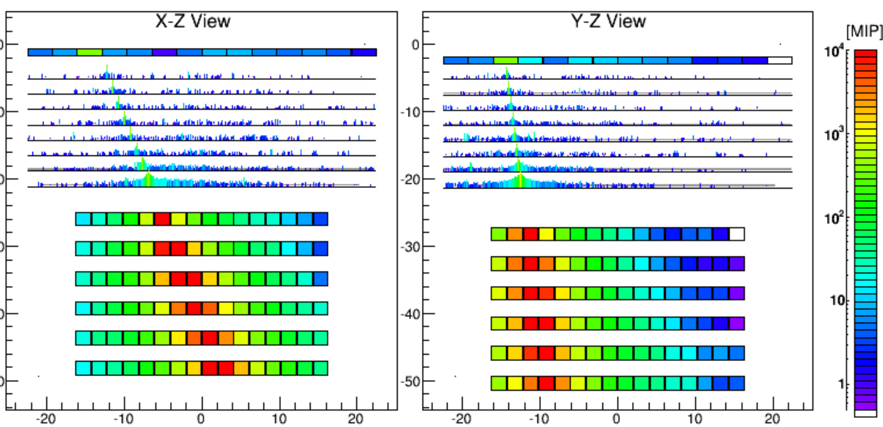

energy deposit in CHD consistent with Fe

Gamma-ray, E=44.3 GeV

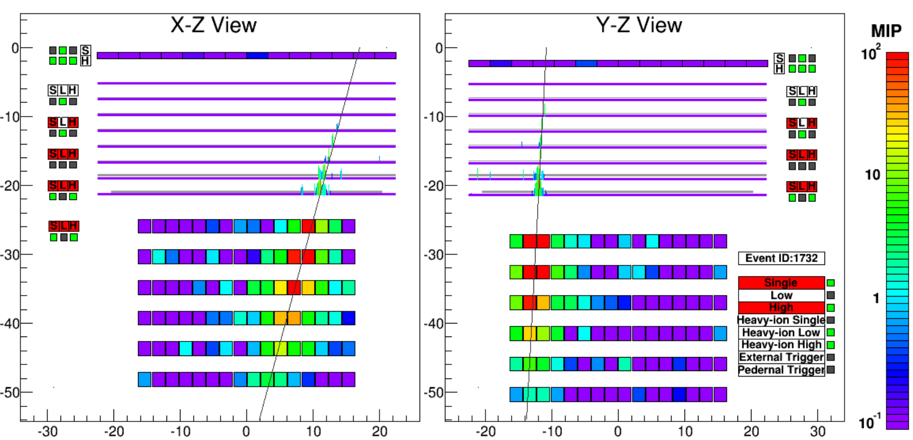

no energy deposit before pair production

Observation with High Energy Trigger (>10GeV)

Y.Asaoka, S.Ozawa, S.Torii et al. (CALET Collaboration), Astropart. Phys. 100 (2018) 29.

Observation by High Energy Trigger for 1023 days : Oct.13, 2015 – Jul. 31, 2018

- The exposure, SΩT, has reached to ~89.6 m^2 sr day for electron observations by continuous and stable operations.
- Total number of triggered events is ~670 million with a live time fraction of 84.0 %.

Accumulated observation time (live, dead)

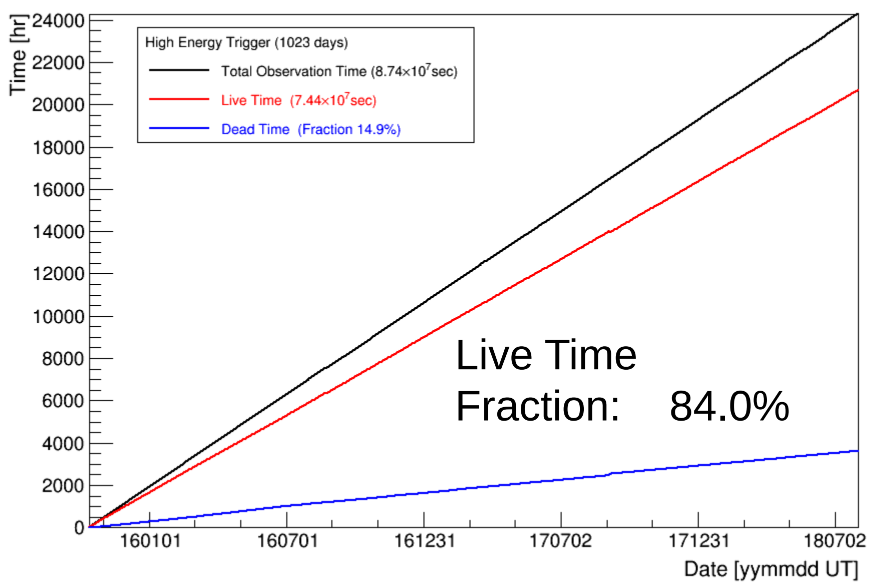

Accumulated triggered event number

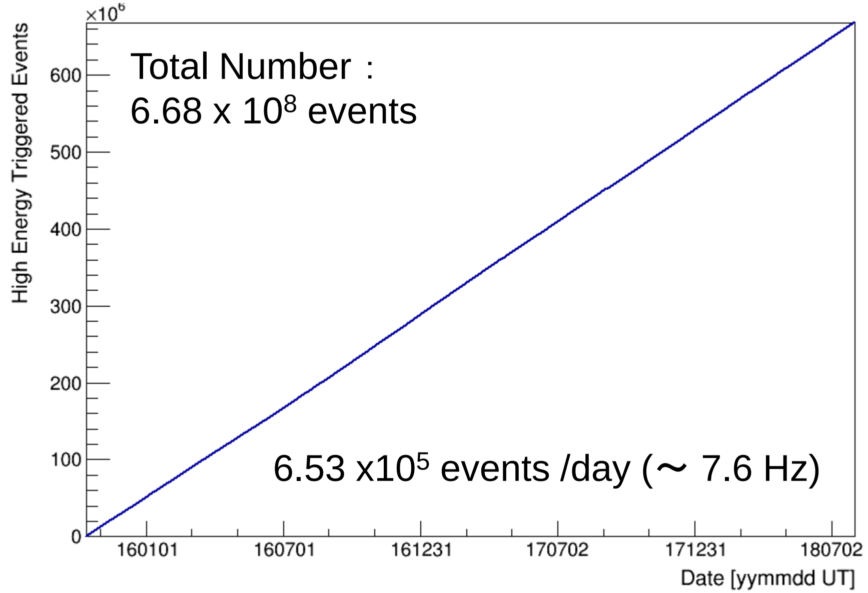

TASC Energy Deposit Distribution of All Triggered-Events by Observation for 1023 days

Y.Asaoka, Y.Akaike, Y.Komiya, R.Miyata, S.Torii et al. (CALET Collaboration), Astropart. Phys. 91 (2017) 1.

Distribution of deposit energies in TASC observed in 2015.10.13—2018.7.31

Energies are calibrated but non-reconstructed

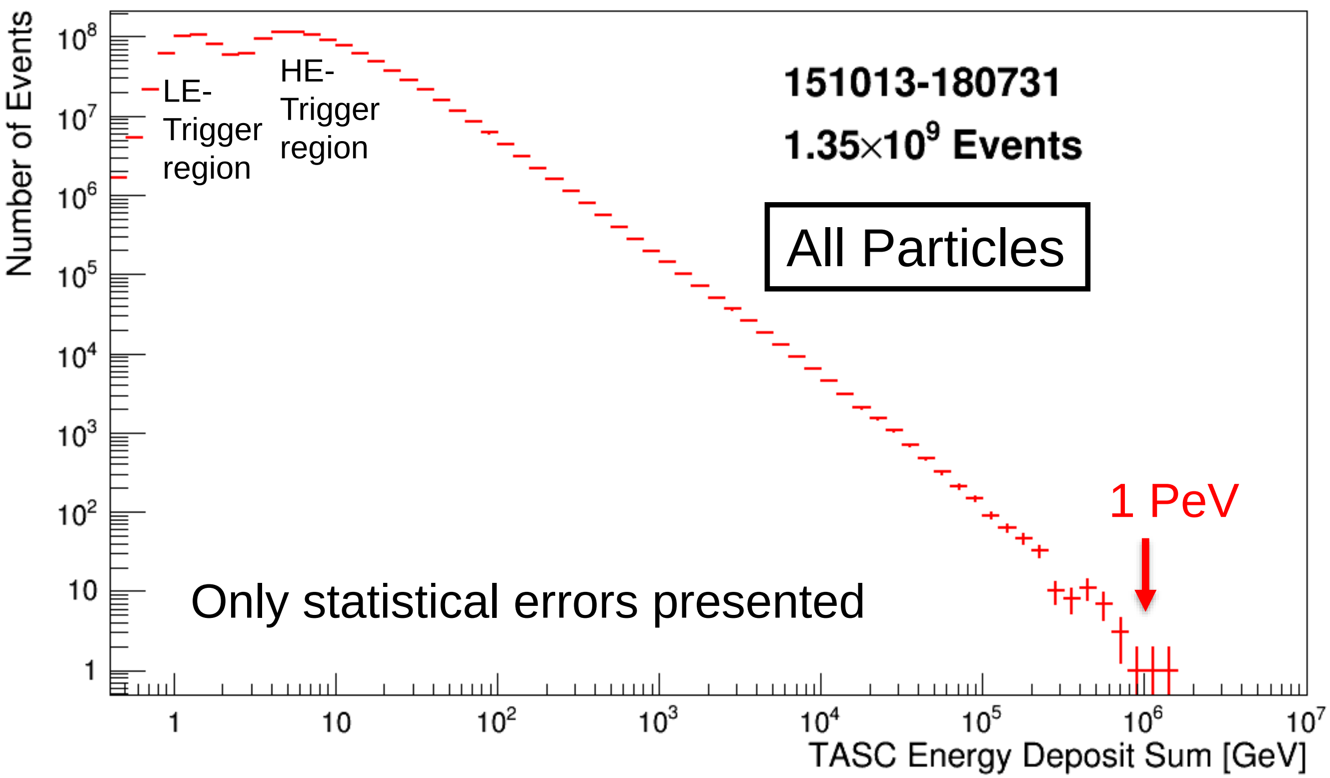

The TASC energy measurements have successfully been carried out in the dynamic range of 1 GeV – 1 PeV.

All-Electron (e^++e^-)

O.Adriani et al. (CALET collaboration), Phys. Rev. Lett. 119 (2017) 181101

O.Adriani et al. (CALET collaboration), Phys. Rev. Lett. 120 (2018) 261102

Electron Identification

Simple Two Parameter Cut

F_E: Energy fraction of the bottom layer sum to the whole energy deposit sum in TASC

R_E: Lateral spread of energy deposit in TASC-X1

Separation Parameter K is defined as follows:

$$K = \log_{10}(F_E) + 0.5\ R_E\ (/cm)$$

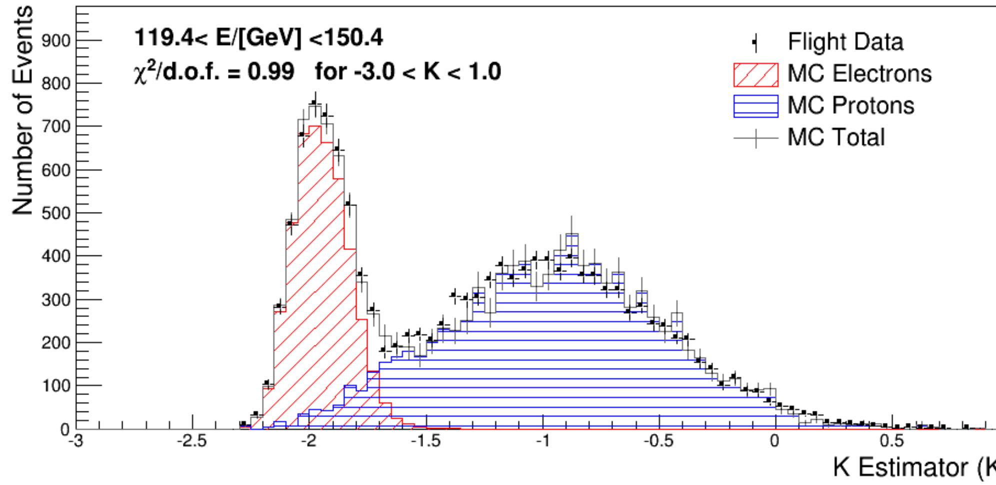

Boosted Decision Trees

In addition to the two parameters making up K, TASC and IMC shower profile fits are used as discriminating variables.

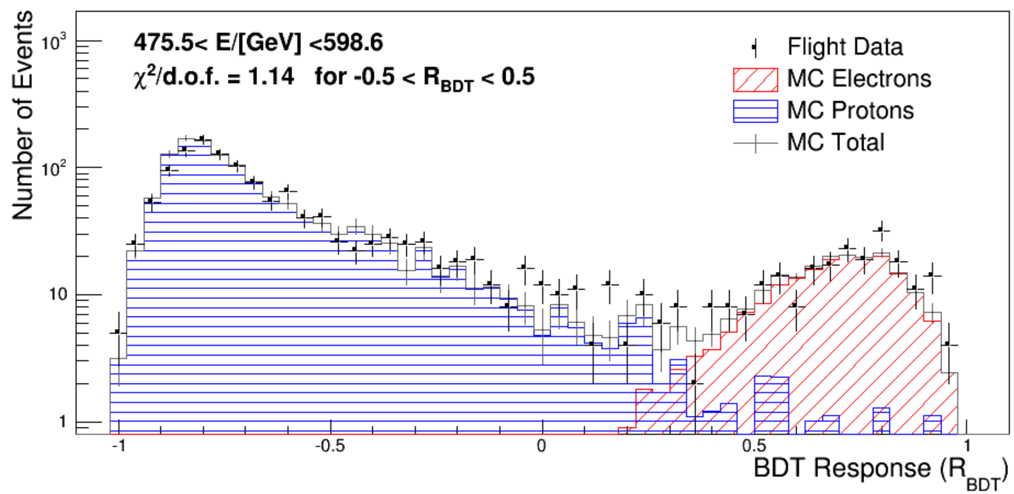

E<475GeV: Simple two parameter cut
E>475GeV: BDT cut

} the small difference in resultant spectrum between two methods are taken into account in the systematic error.

⇒ Contamination is ~5% up to 1TeV, and 10~15% in the 1—3 TeV region.

All-Electron Spectrum Measured with CALET from 10 GeV to 3 TeV

CALET: PRL 119 (2017) 181101, 3 November 2017

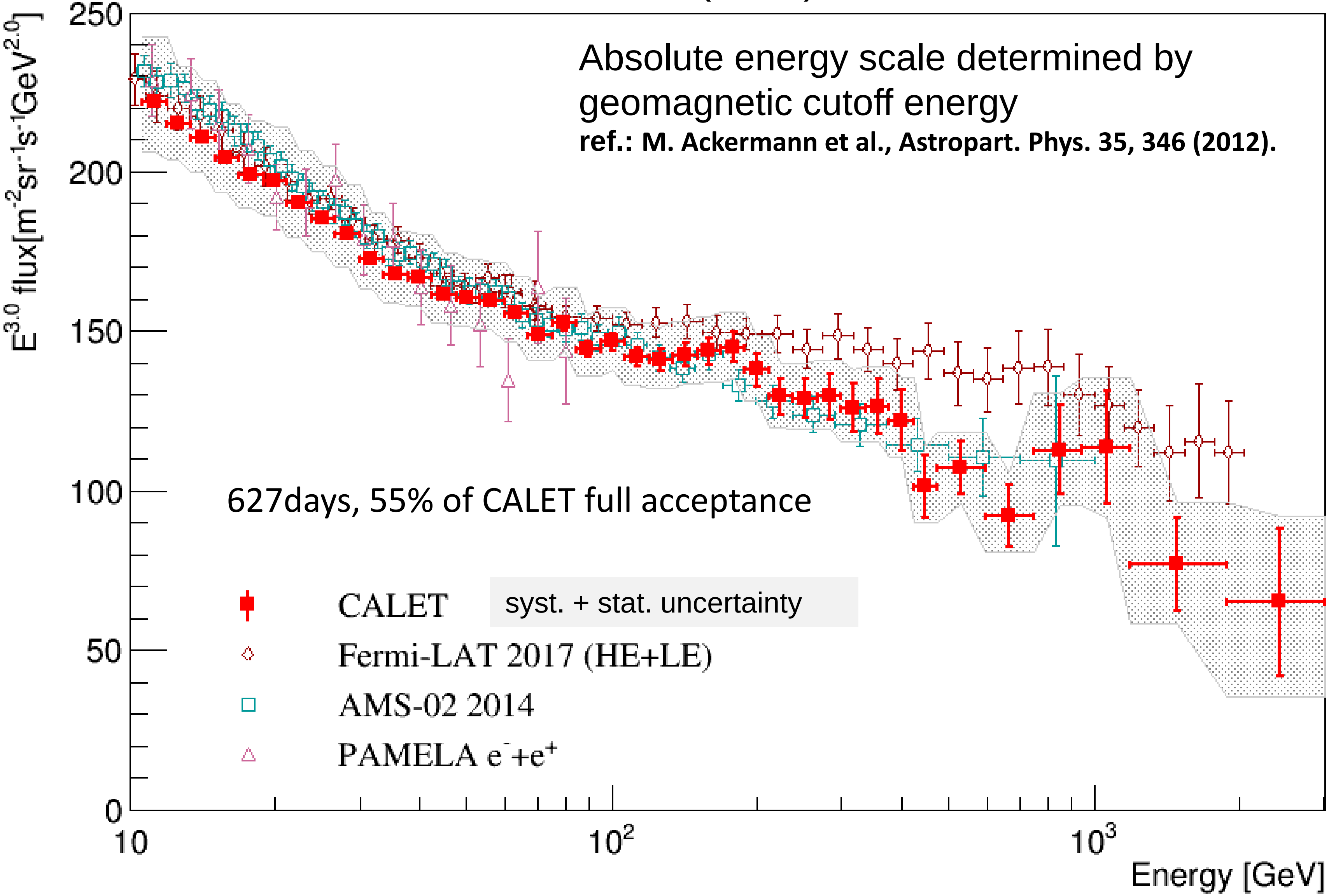

All-Electron Spectrum Comparison w/ DAMPE

and other space based experiments

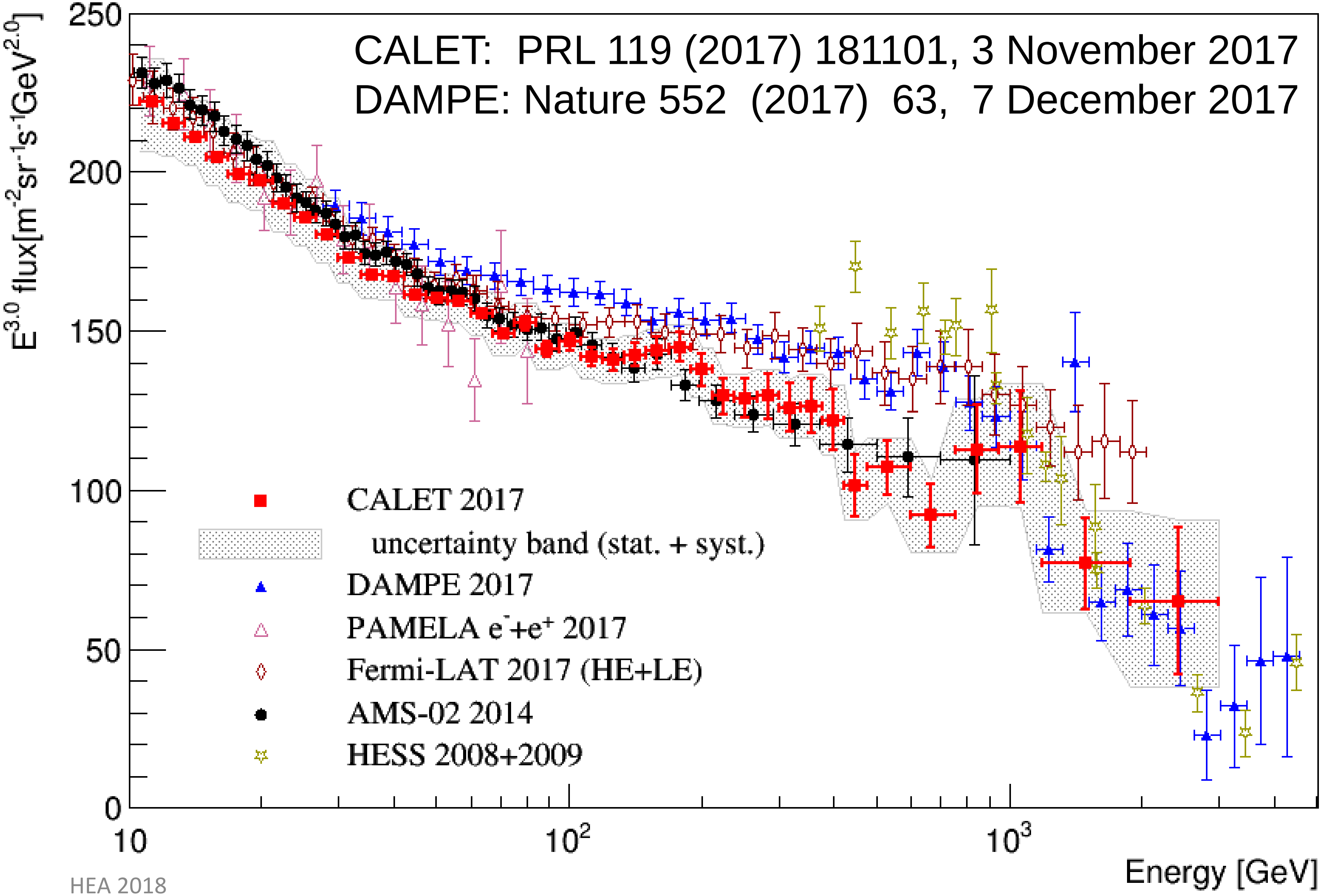

All-Electron Spectrum Comparison w/ DAMPE

and other space based experiments

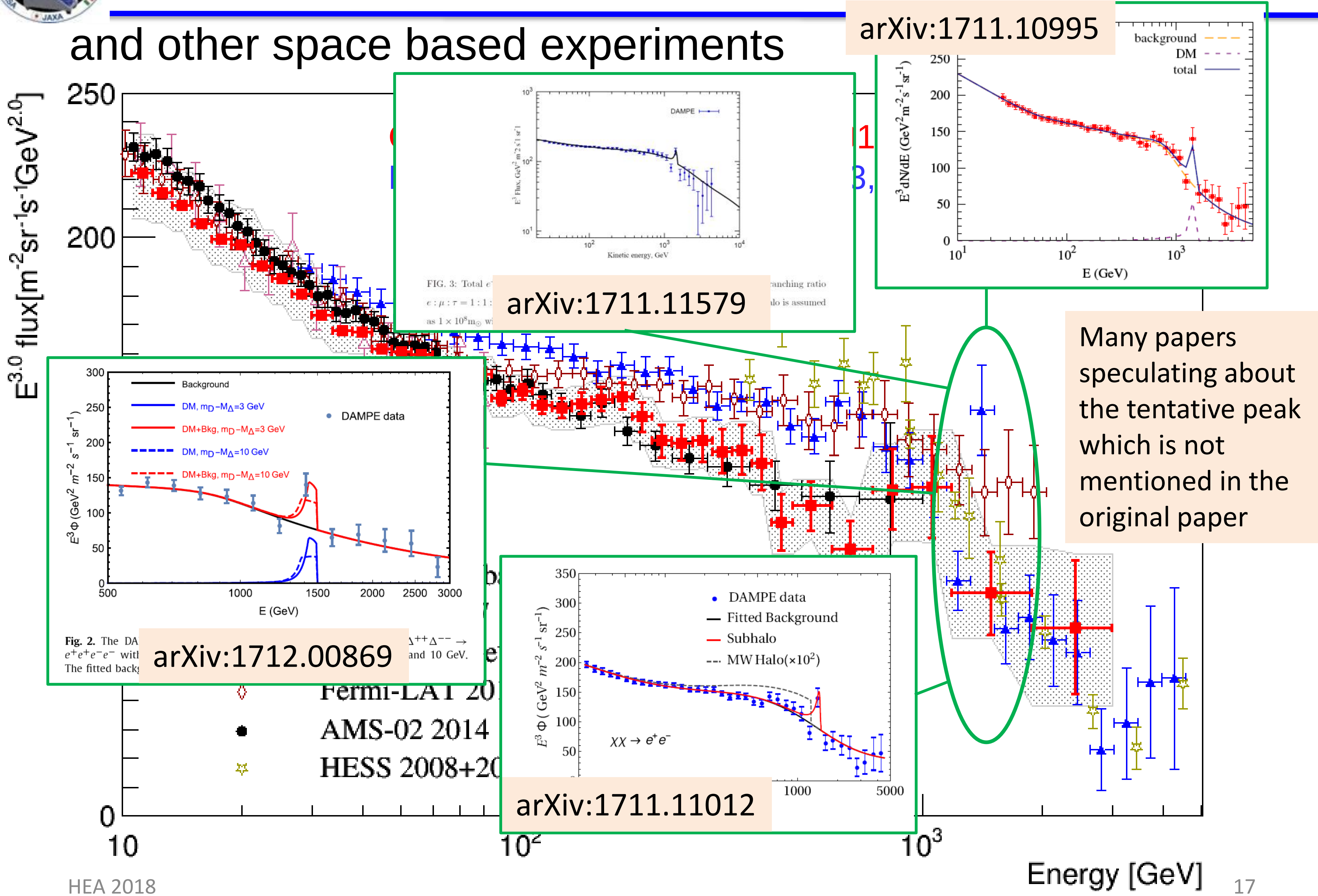

Many papers speculating about the tentative peak which is not mentioned in the original paper

All-Electron Spectrum Comparison w/ DAMPE

and other space based experiments

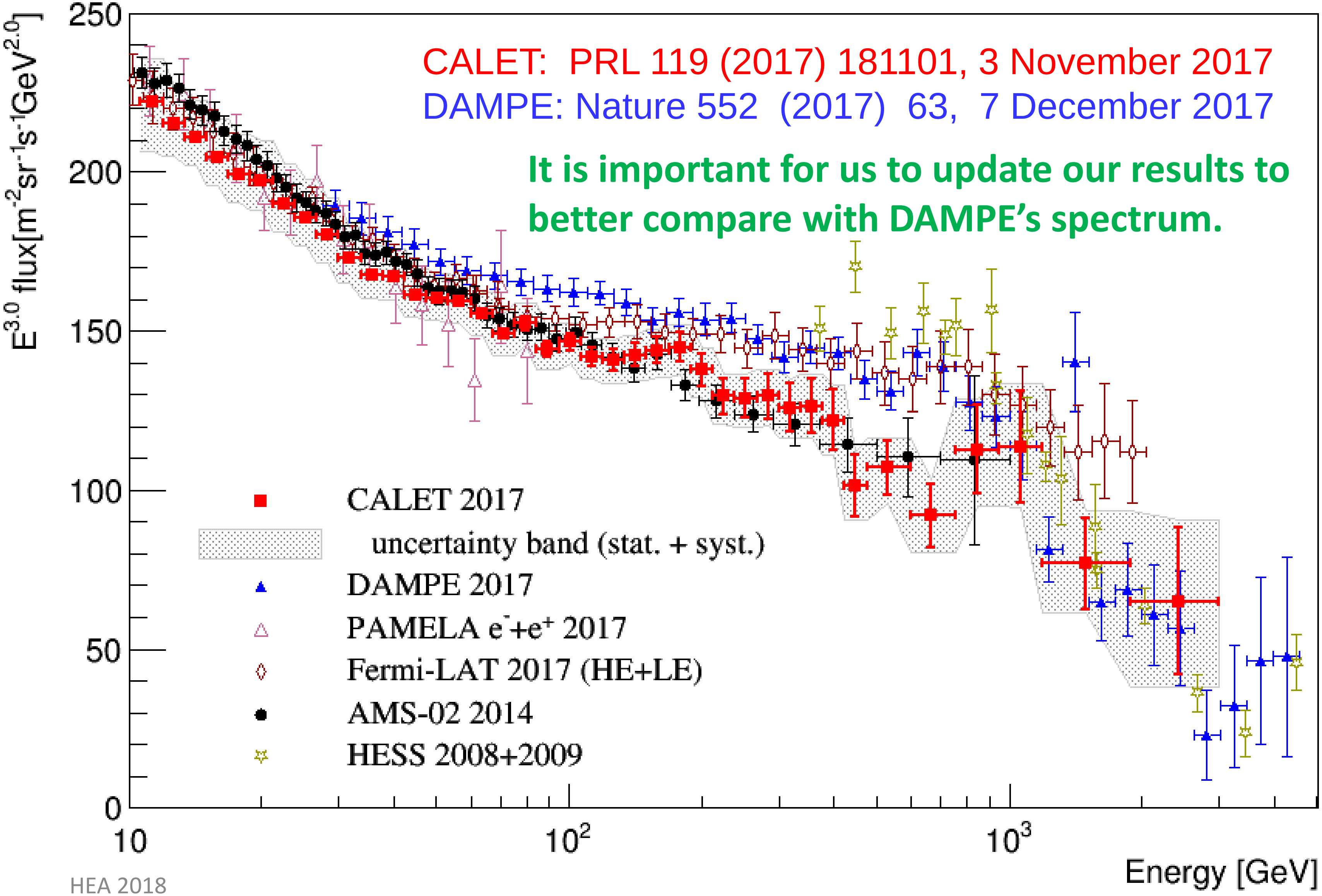

Extending the Analysis to Full Acceptance

Analyzed Flight Data:

- 780 days (October 13, 2015 to November 30, 2017)
- Full CALET acceptance at the high energy region (Acceptance A+B+C+D; 1040cm^{2}sr). In the low energy region fully contained events are used (A+B; 550cm^{2}sr)

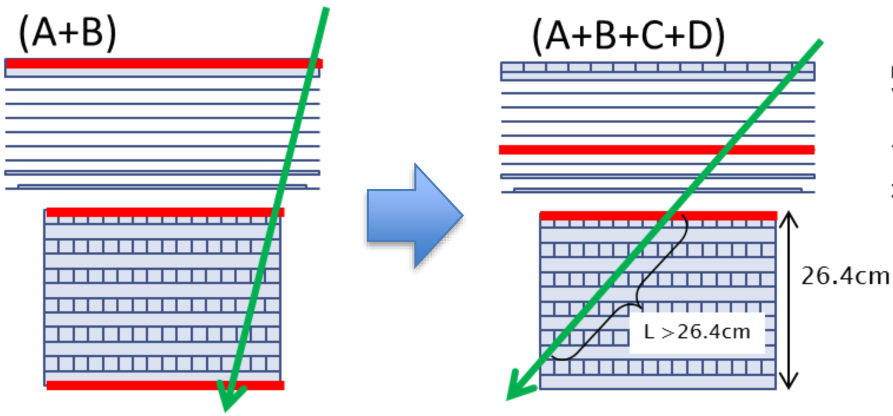

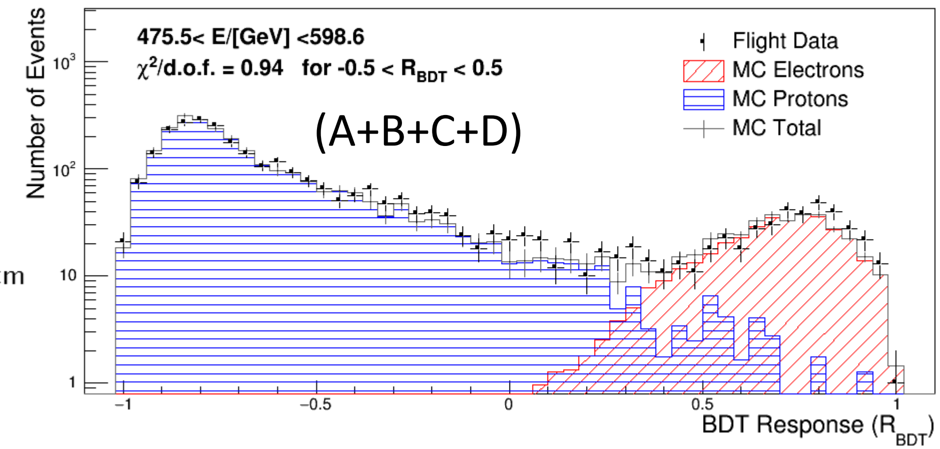

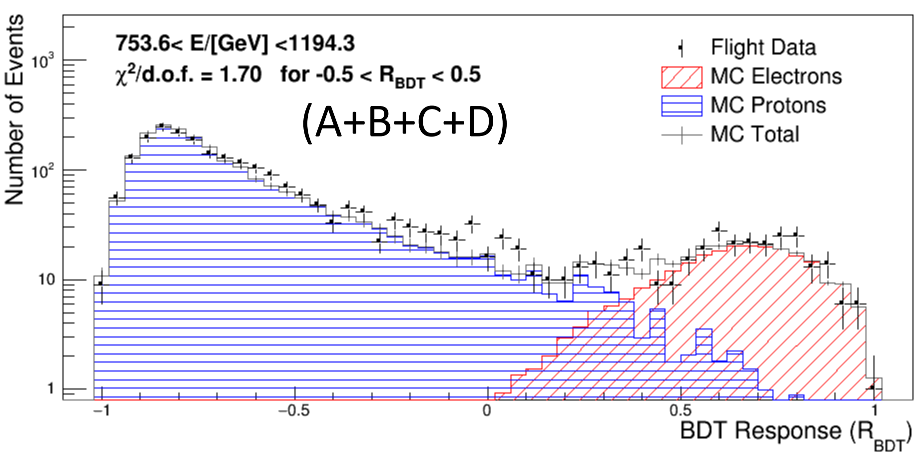

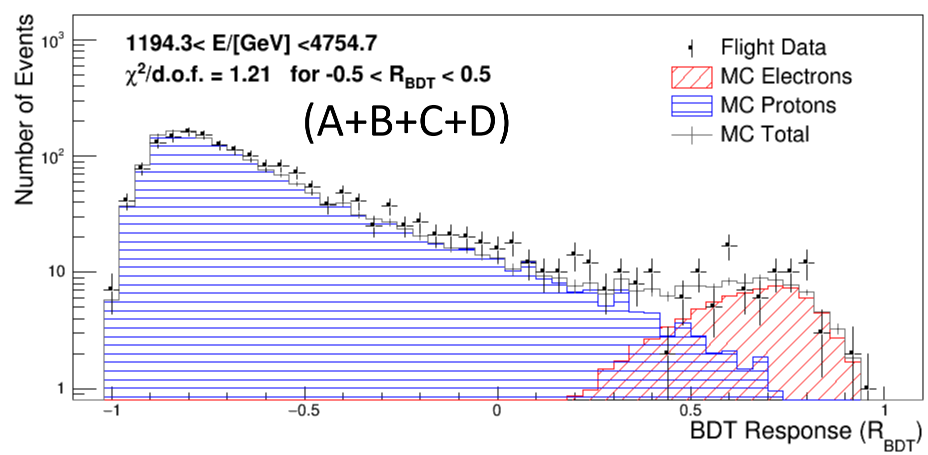

Systematic Uncertainties

(other than energy scale uncertainty)

Stability of resultant flux are analyzed by scanning parameter space

Normalization:
- Live time
- Radiation environment
- Long-term stability
- Quality cuts

- Energy dependent:
  - 2 independent tracking
  - charge ID
  - electron ID (K-Cut vs BDT)
  - **BDT stability** (vs efficiency & training)
  - MC model (EPICS vs Geant4)

Flux Ratio vs Efficiency for BDT @ 1TeV

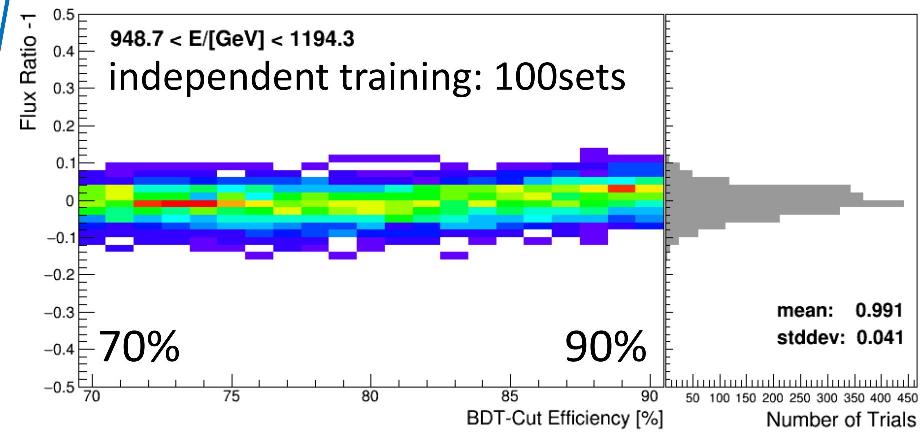

Energy Dependence of BDT stability

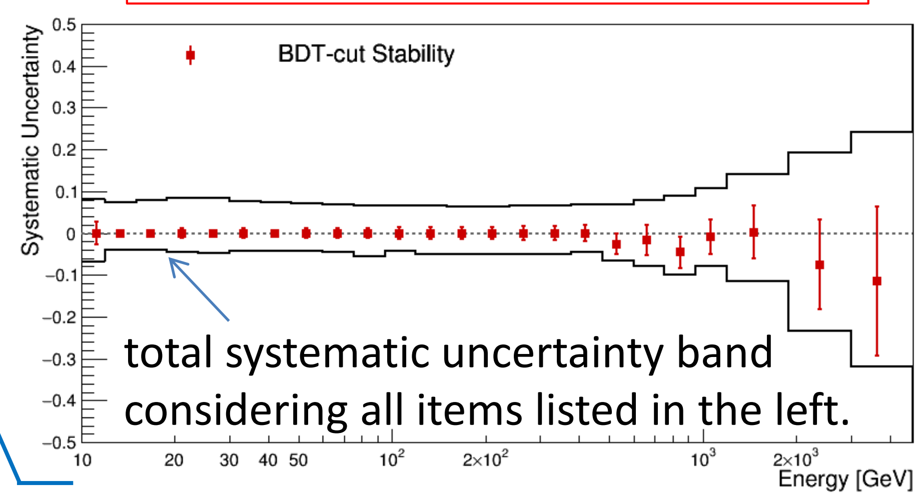

Extended Measurement by CALET

Approximately doubled statistics above 500GeV by using full acceptance of CALET

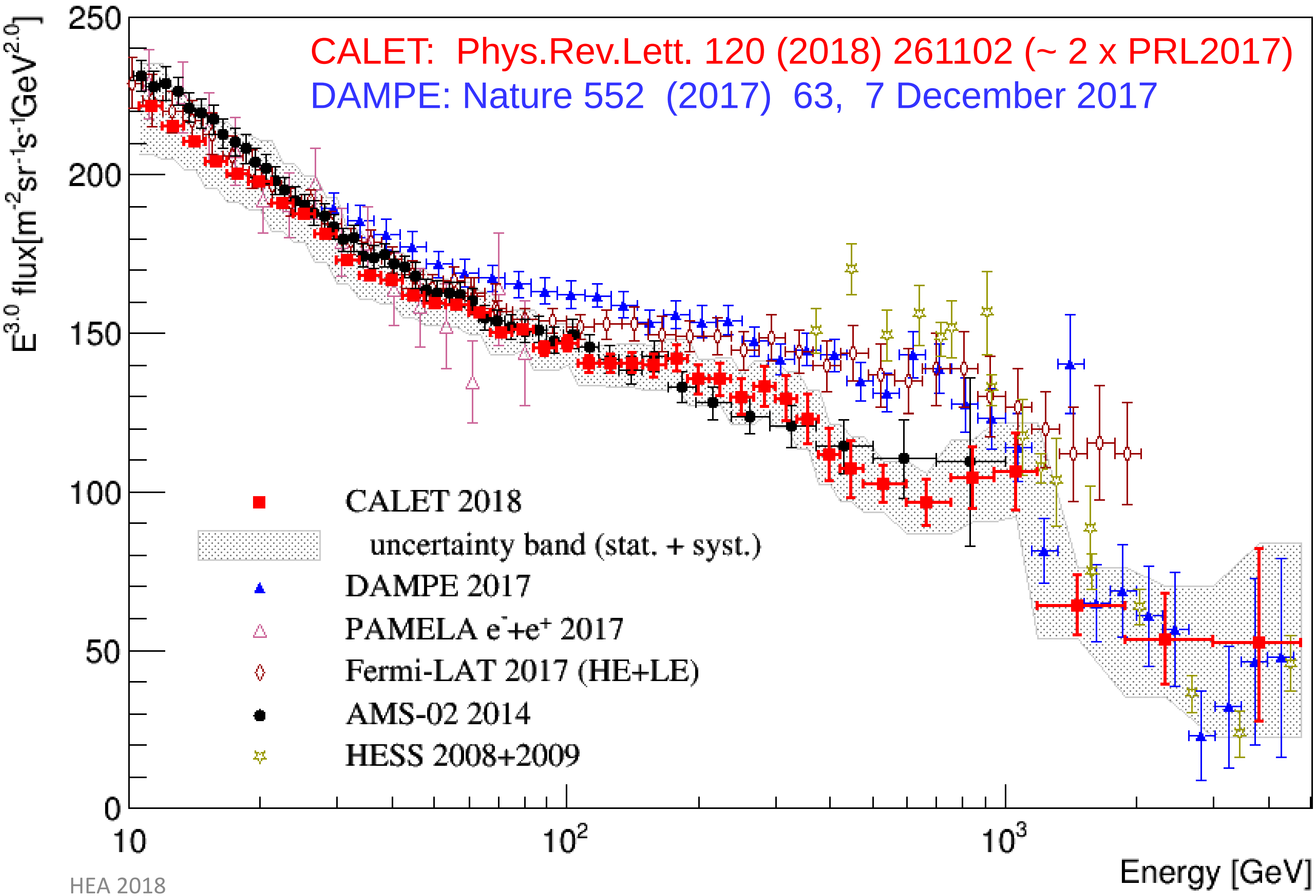

Extended Measurement by CALET

Approximately doubled statistics above 500GeV by using full acceptance of CALET

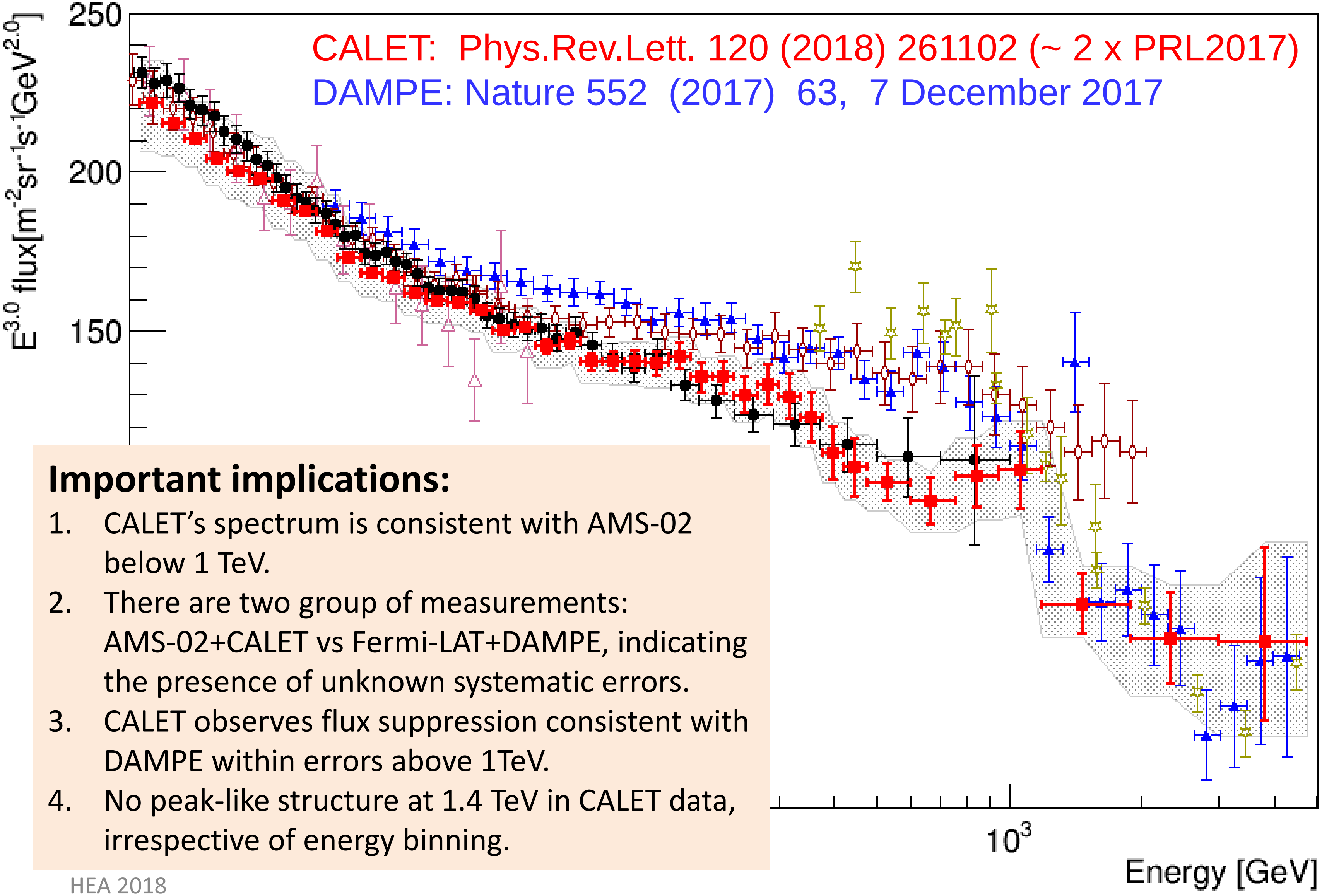

Important implications:

1. CALET's spectrum is consistent with AMS-02 below 1 TeV.
2. There are two group of measurements: AMS-02+CALET vs Fermi-LAT+DAMPE, indicating the presence of unknown systematic errors.
3. CALET observes flux suppression consistent with DAMPE within errors above 1TeV.
4. No peak-like structure at 1.4 TeV in CALET data, irrespective of energy binning.

Comparison with DAMPE's result

Here, we have adopted the same energy binning as DAMPE.

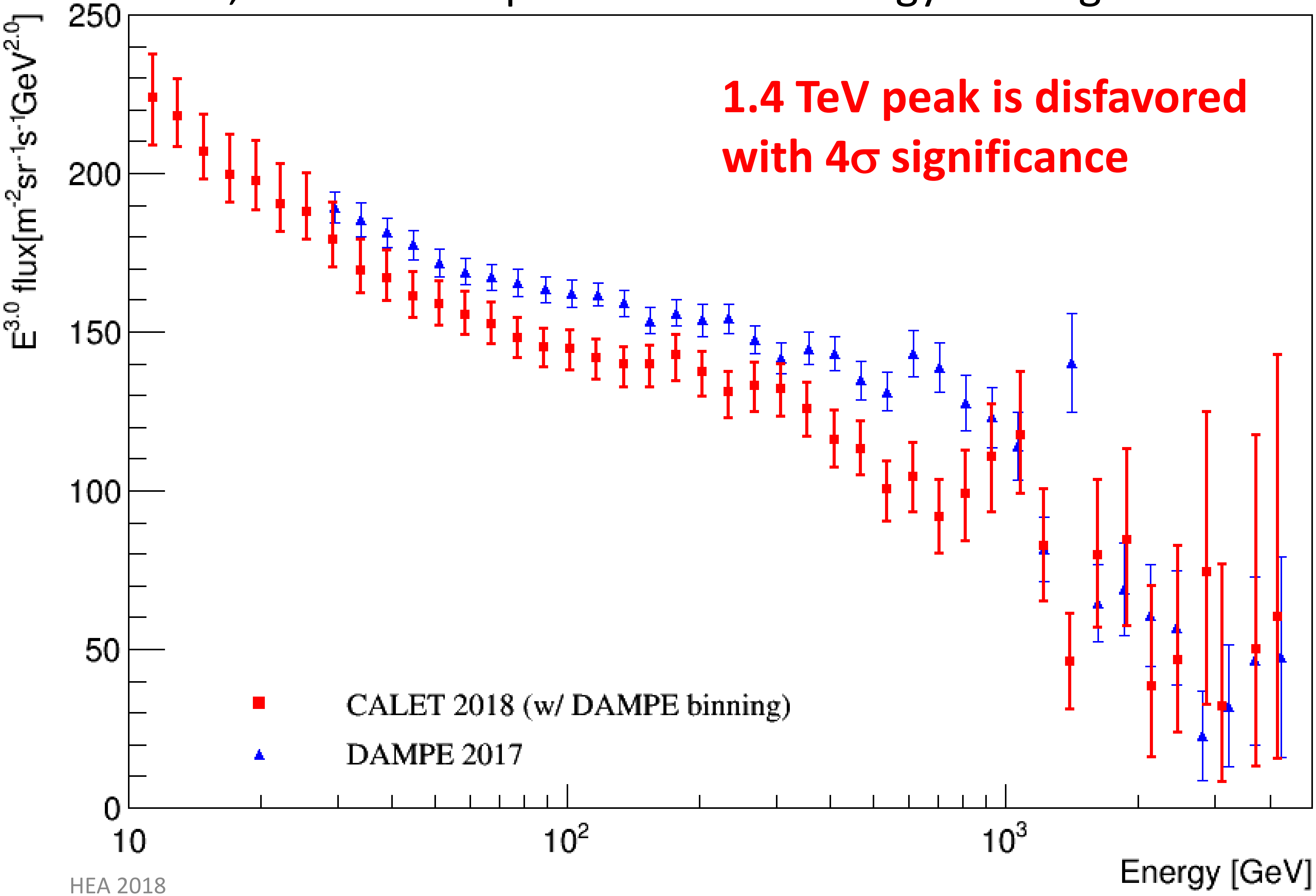

Comparison with DAMPE's result

What happens if we shifted our energy binning…

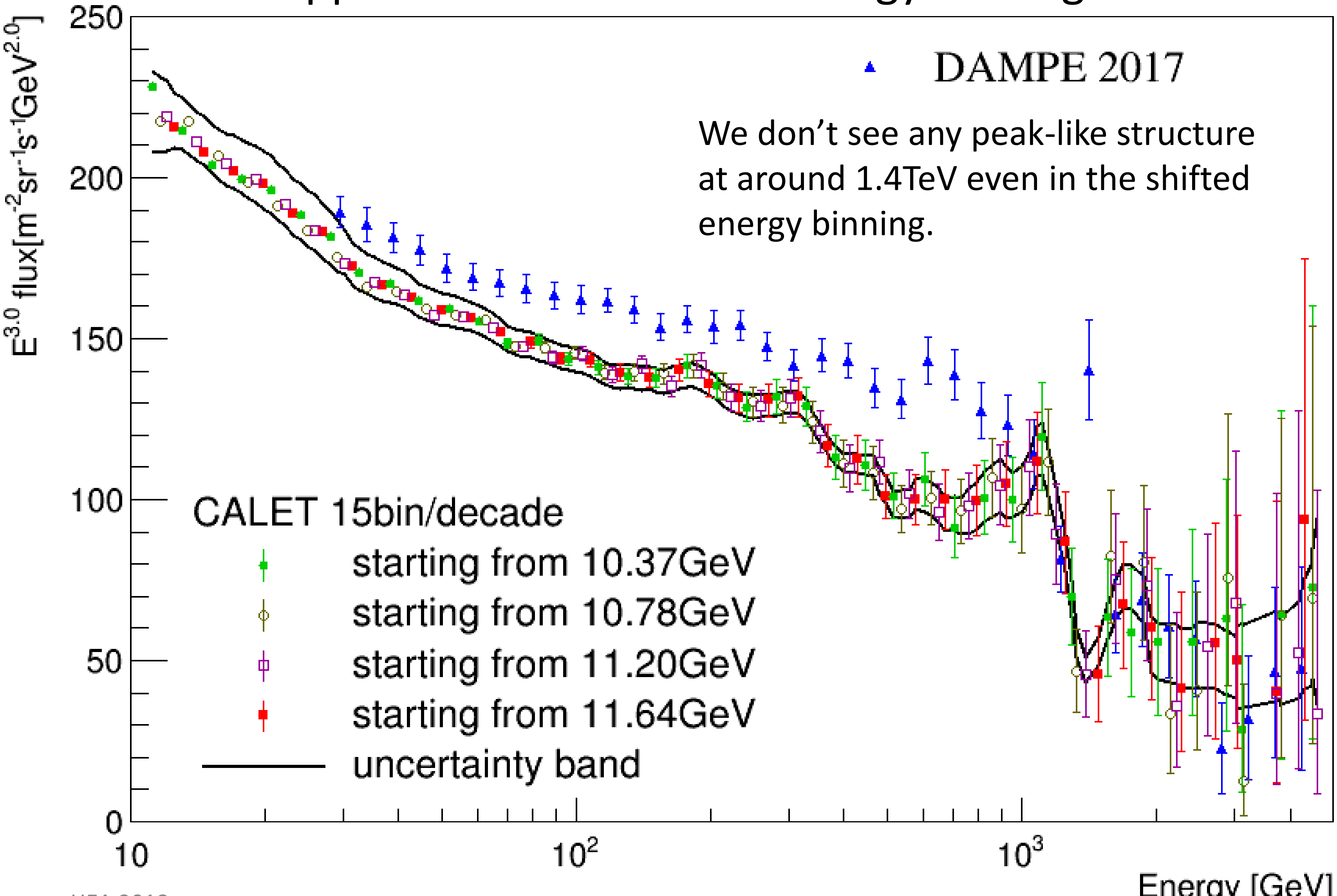

Extended Measurement by CALET

Approximately doubled statistics above 500GeV by using full acceptance of CALET

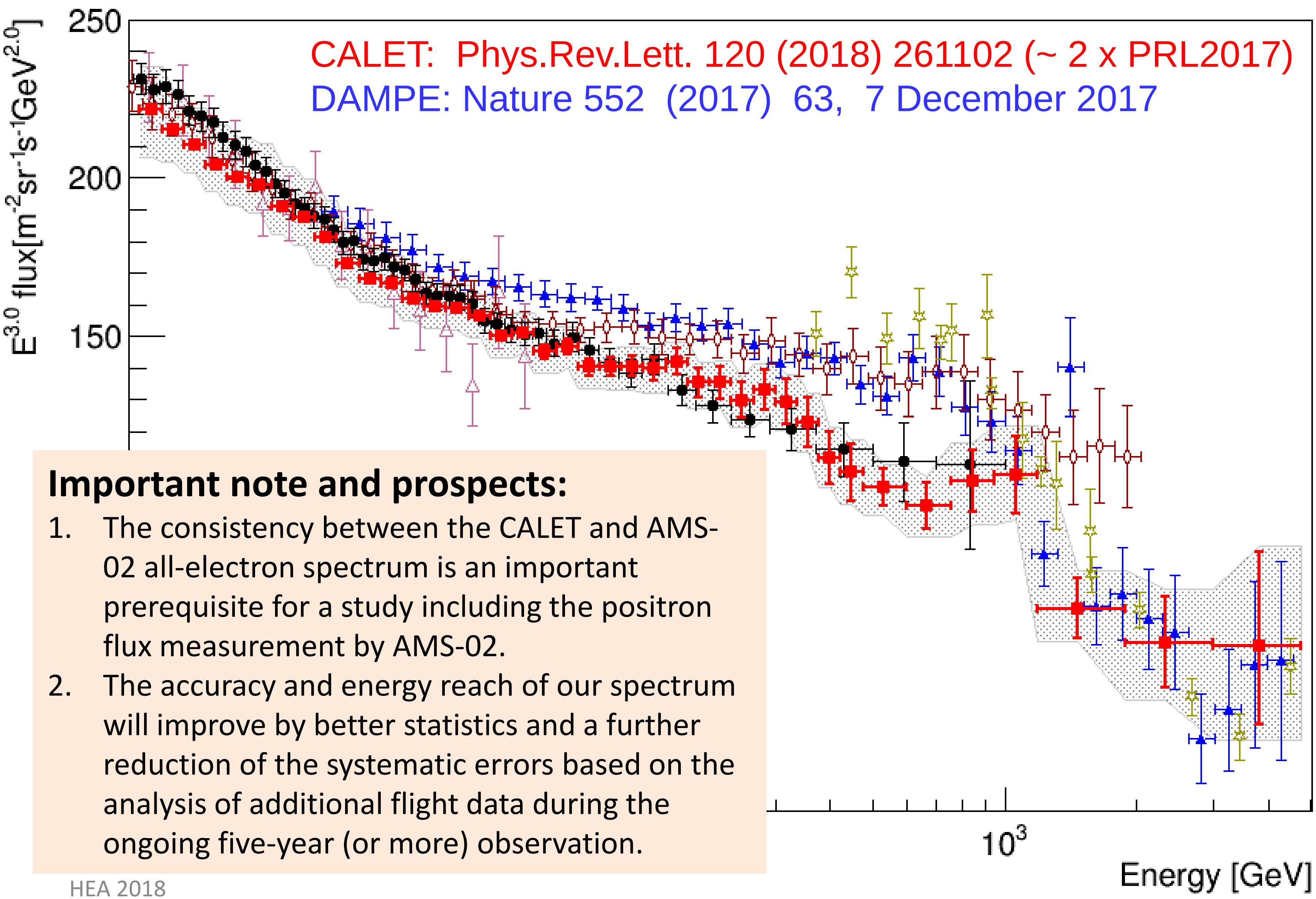

Important note and prospects:

1. The consistency between the CALET and AMS-02 all-electron spectrum is an important prerequisite for a study including the positron flux measurement by AMS-02.
2. The accuracy and energy reach of our spectrum will improve by better statistics and a further reduction of the systematic errors based on the analysis of additional flight data during the ongoing five-year (or more) observation.

Hadrons & Gamma-Rays

O.Adriani et al. (CALET Collab.), ApJL 829 (2016) L20.
O.Adriani et al. (CALET Collab.), ApJ 863 (2018) 160.
N.Cannady, Y.Asaoka et al. (CALET Collab.),
ApJS in press.

Preliminary Flux of Primary Components

Flux measurement:

$$\Phi(E) = \frac{N(E)}{S\Omega\varepsilon(E)T\Delta E}$$

N(*E*): Events in unfolded energy bin
SΩ : Geometrical acceptance
T : Live time
ε(*E*) : Efficiency
ΔE : Energy bin width

Observation period:
2015.10.13 – 2017.10.31 (750 days)
Selected events: ~13 million

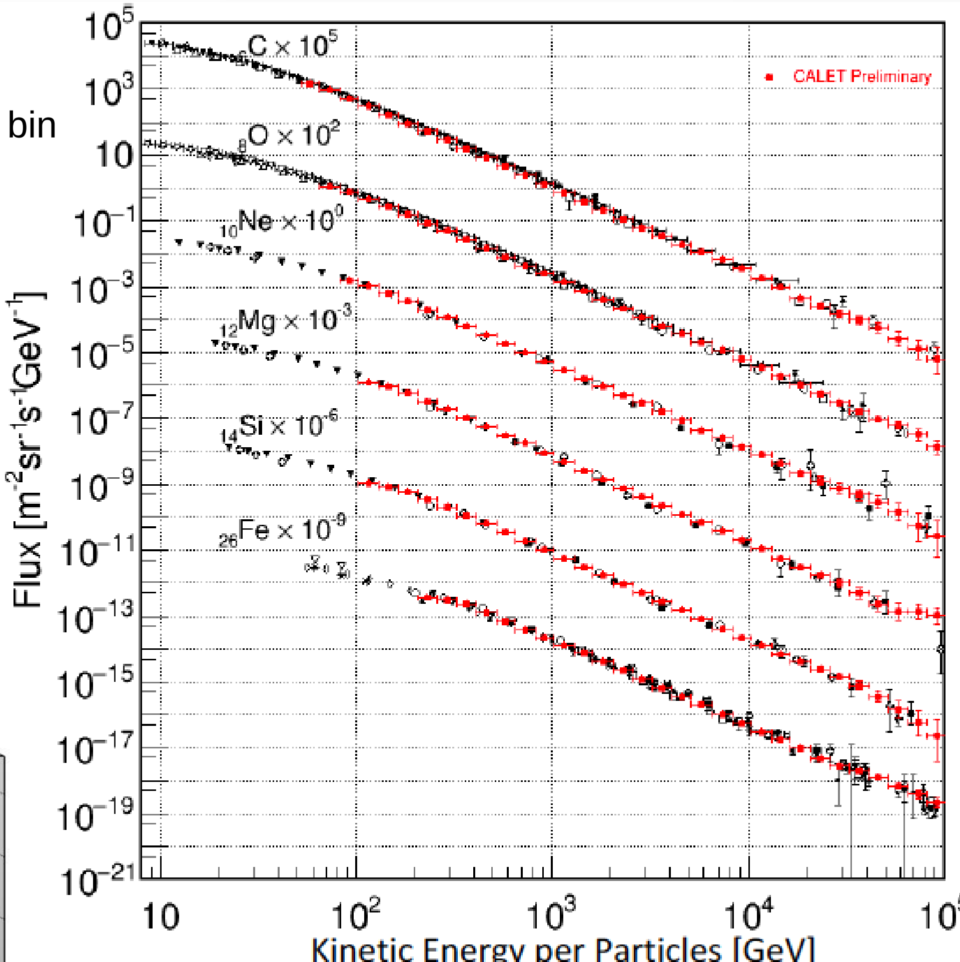

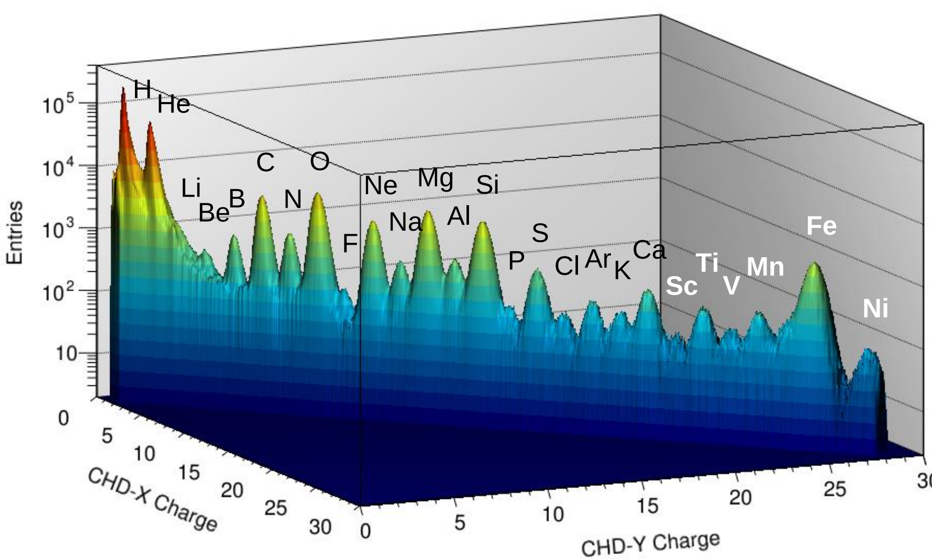

Charge Separation only with CHD

Clear separation of protons, helium to iron and nickel (up to Z=40).

Preliminary Energy Spectra of Carbon and Oxygen

(2 independent CALET analyses)

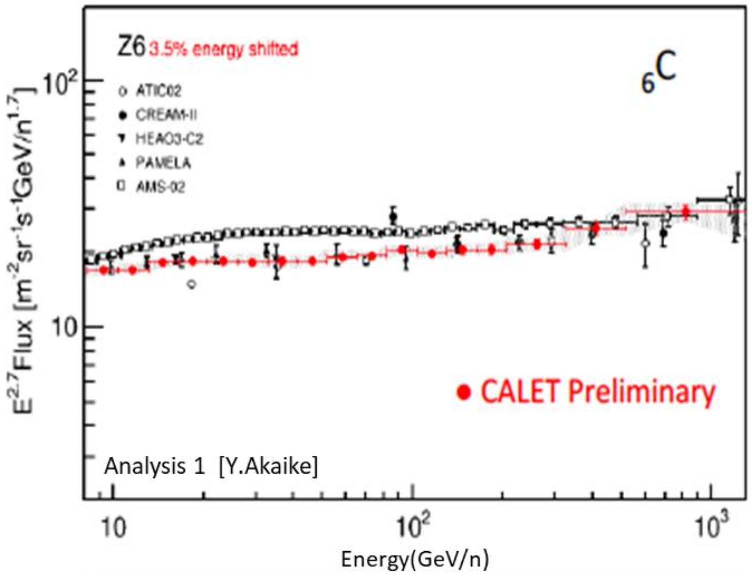

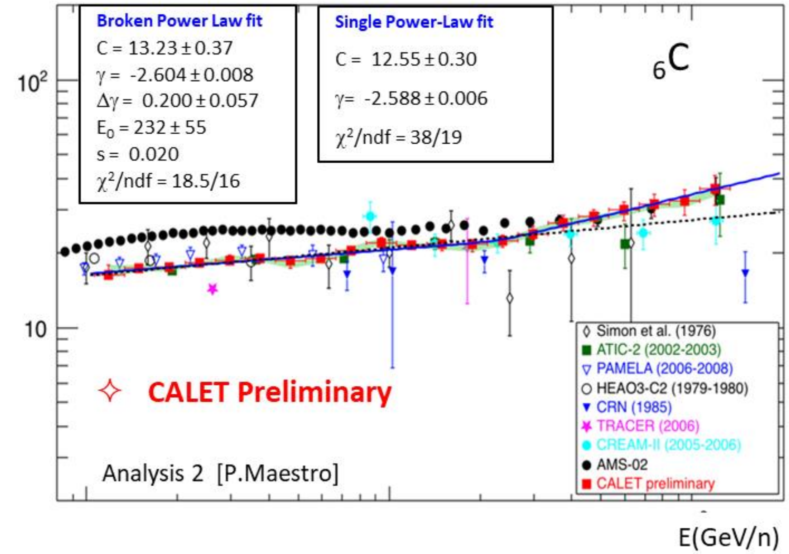

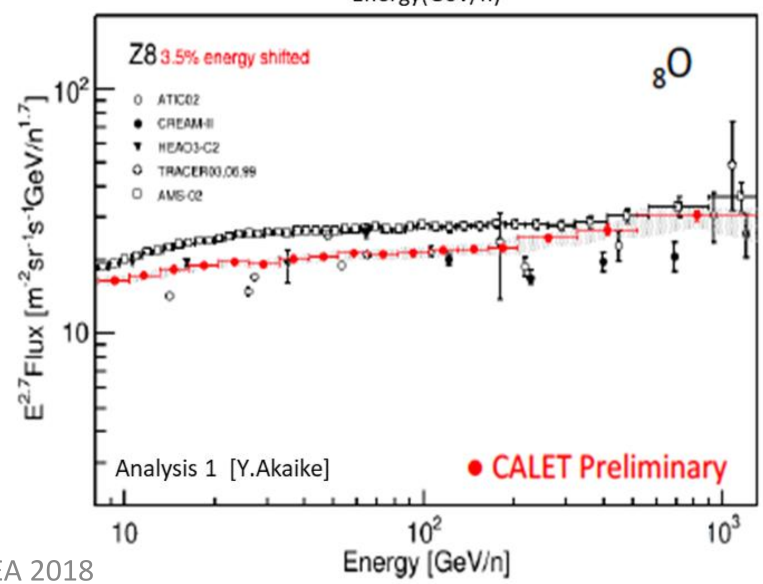

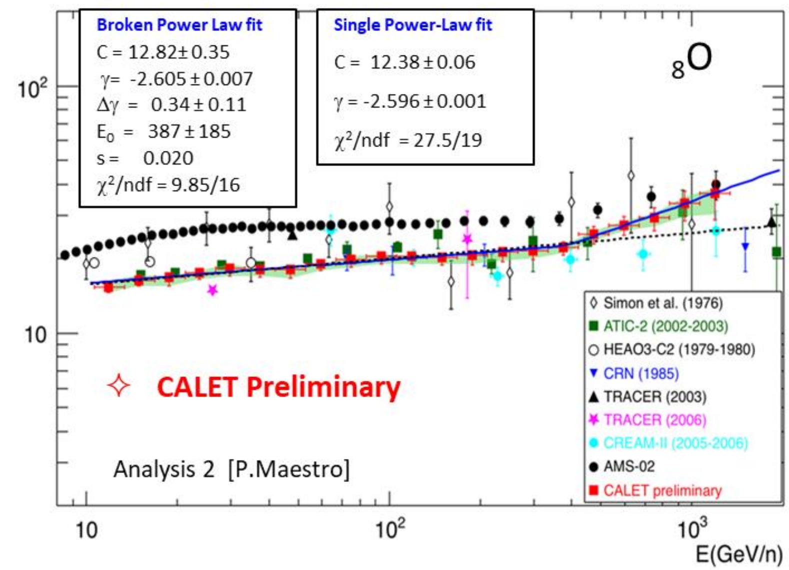

CALET γ–ray Sky in LE (>1GeV) Trigger

Analysis methodology:
N.Cannady, Y.Asaoka et al.
(CALET Collab.), ApJS in press.

Exposure map

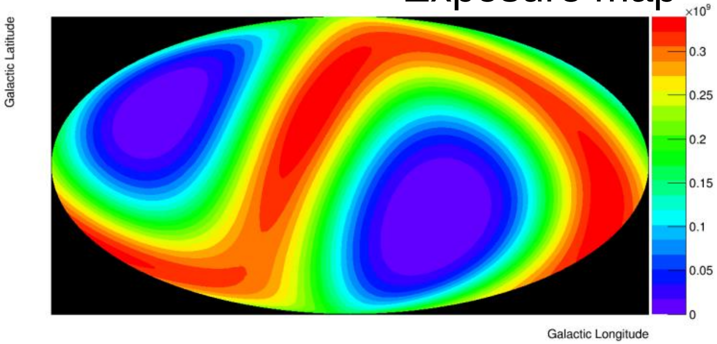

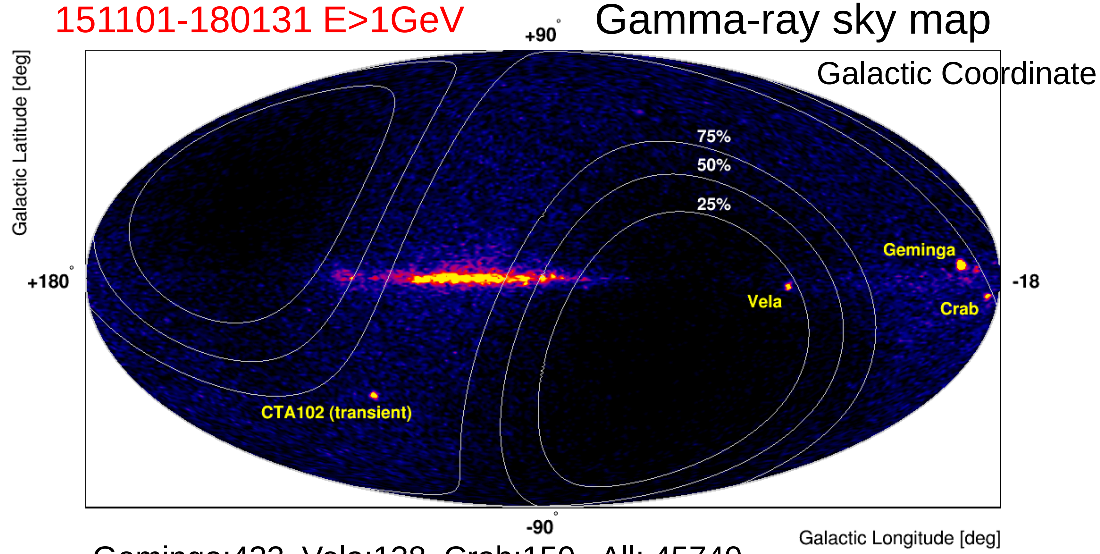

Geminga:432 Vela:138 Crab:150 All: 45740

Galactic diffuse gamma-rays

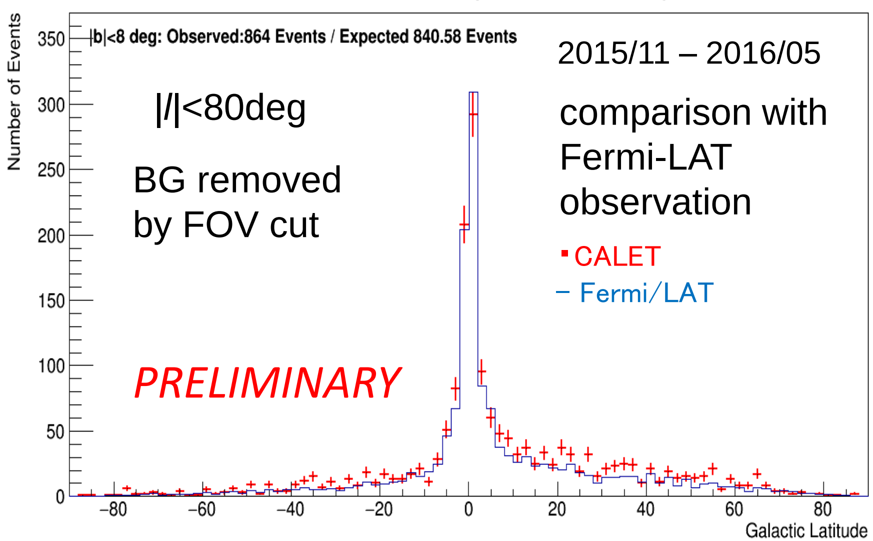

Gamma-ray energy spectrum

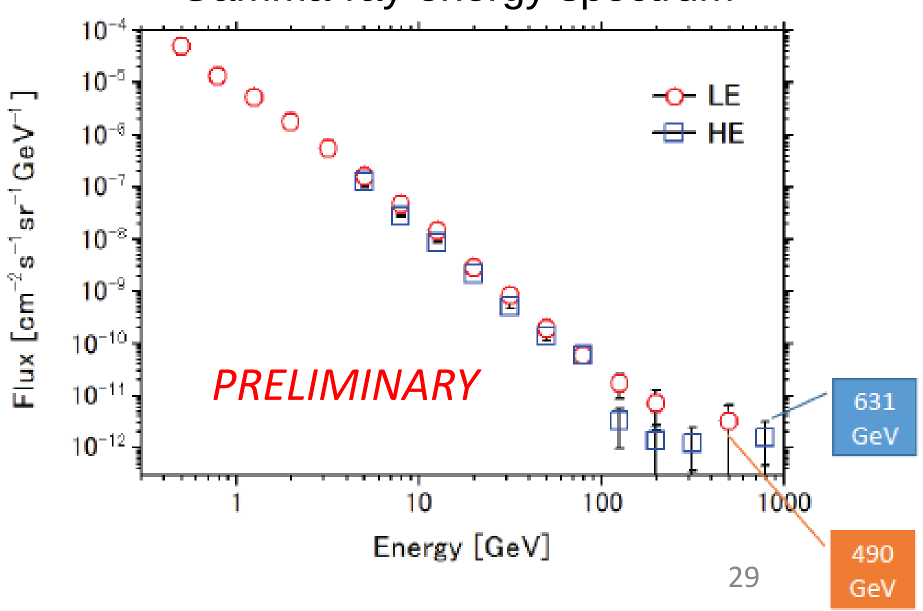

CALET UPPER LIMITS ON X-RAY AND GAMMA-RAY COUNTERPARTS OF GW 151226

Astrophysical Journal Letters 829:L20(5pp), 2016 September 20

The CGBM covered 32.5% and 49.1% of the GW 151226 sky localization probability in the 7 keV - 1 MeV and 40 keV - 20 MeV bands respectively. We place a 90% upper limit of 2×10^{-7} erg cm^{-2} s^{-1} in the 1 - 100 GeV band where CAL reaches 15% of the integrated LIGO probability (~1.1 sr). The CGBM 7 σ upper limits are 1.0×10^{-6} erg cm^{-2} s^{-1} (7-500 keV) and 1.8×10^{-6} erg cm^{-2} s^{-1} (50-1000 keV) for one second exposure. Those upper limits correspond to the luminosity of 3-5 $\times 10^{49}$ erg s^{-1} which is significantly lower than typical short GRBs.

CGBM light curve at the moment of the GW151226 event

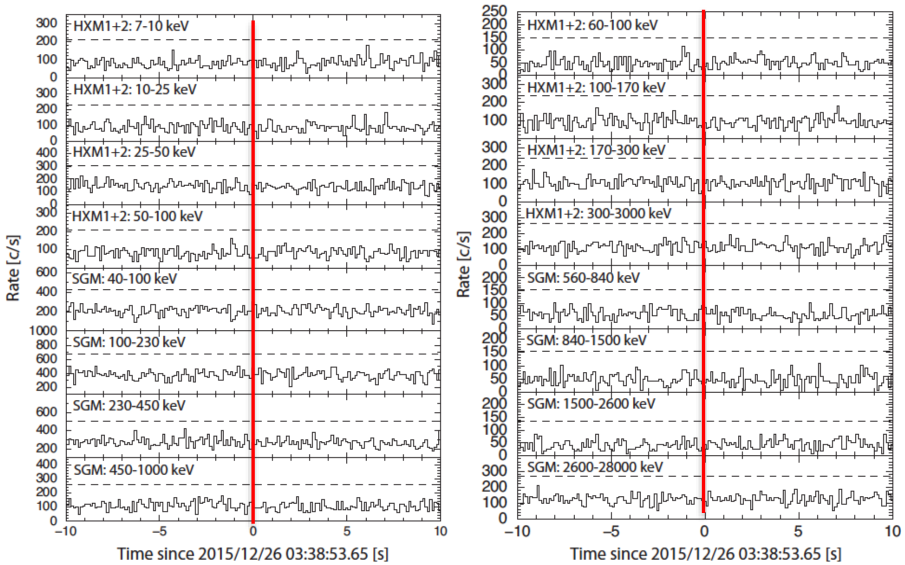

Figure 1. The CGBM light curves in 0.125 s time resolution for the high-gain data (left) and the low-gain data (right). The time is offset from the LIGO trigger time of GW 151226. The dashed-lines correspond to the 5 σ level from the mean count rate using the data of ± 10 s.

Upper limit for gamma-ray burst monitors and Calorimeter

HXM: 7-500 keV

SGM: 50-1000 keV

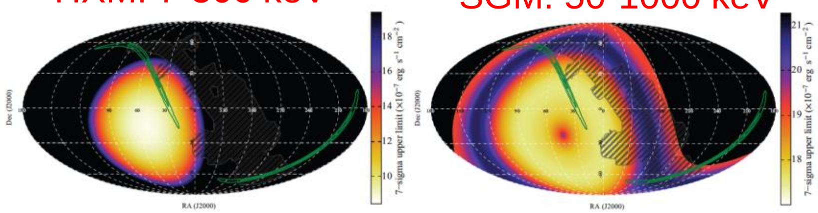

Figure 2. The sky maps of the 7 σ upper limit for HXM (left) and SGM (right). The assumed spectrum for estimating the upper limit is a typical BATSE S-GRBs (see text for details). The energy bands are 7-500 keV for HXM and 50-1000 keV for SGM. The GW 151226 probability map is shown in green contours. The shadow of ISS is shown in black hatches.

Calorimeter: 1-100 GeV

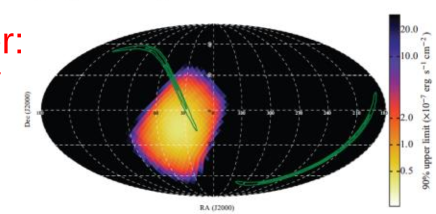

Figure 3. The sky map of the 90% upper limit for CAL in the 1-100 GeV band. A power-law model with a photon index of −2 is used to calculate the upper limit. The GW 151226 probability map is shown in green contours.

Updated analysis incl. all GW candidates in O2: O.Adriani et al. (CALET Collab.), ApJ 863 (2018) 160.

Summary and Future Prospects

- CALET was successfully launched on Aug. 19, 2015, and the detector is being very stable for observation since Oct. 13, 2015.
- As of July 31, 2018, total observation time is 1023 days with live time fraction to total time close to 84%. Nearly 670 million events are collected with high energy trigger (E>10 GeV)
- Careful calibrations have been adopted by using "MIP" signals of the non-interacting p & He events, and the linearity in the energy measurements up to 10^6 MIPs is established by using observed events.
- All electron spectrum has been extended in statistics and in the energy range up to 4.8TeV. This result is published in PRL again on June 2018.
- Preliminary analysis of nuclei have successfully been carried out to obtain the energy spectra in the energy range: Protons in 55 GeV~22 TeV, Ne-Fe in 500 GeV~100 TeV.
- CALET's CGBM detected nearly 60 GRBs (~20 % short GRB among them) per year in the energy range of 7keV-20 MeV, as expected (not included in this talk). Follow-up observation of the GW events is carried out and published in ApJL.
- GW counterpart searches with CALET calorimeter were extended to cover the whole LIGO/Virgo O2 and published in ApJ. In addition, onboard performance of gamma-ray observation will be published in ApJS (currently in press).
- The so far excellent performance of CALET and the outstanding quality of the data suggest that a 5-year observation period is likely to provide a wealth of new interesting results.

Backup

Spectral Analysis with Extended CALET Result

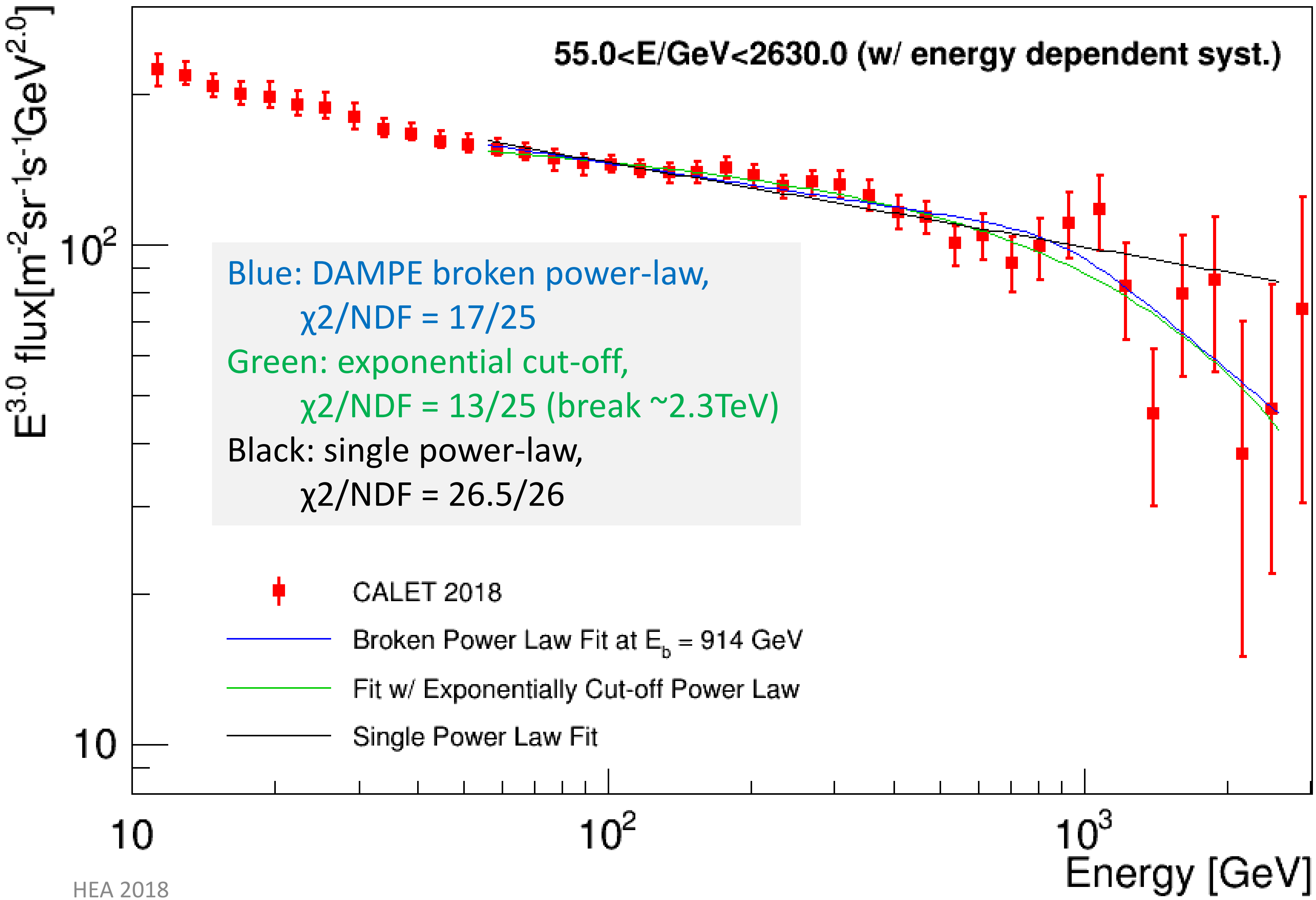

TASC Energy Measurement in Dynamic Range of 1-10^6 MIP

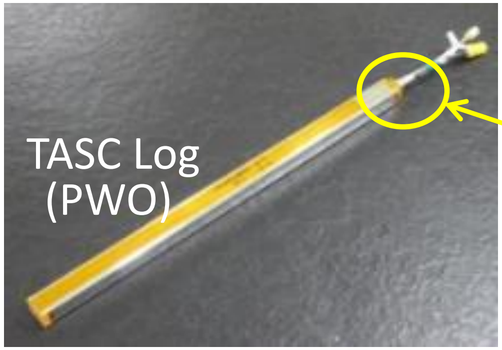

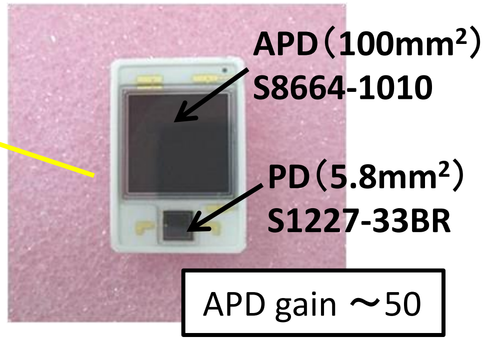

"MIP" peak in PWO: Obs. vs. MC

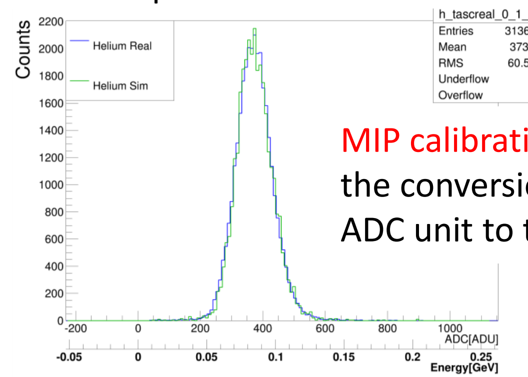

MIP calibration determines the conversion factor from ADC unit to the energy

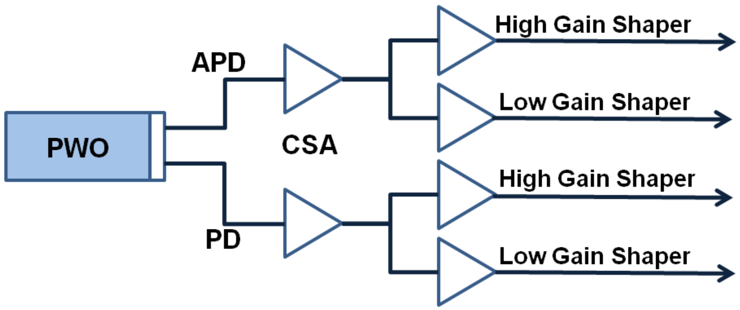

The whole dynamic range was calibrated by UV laser irradiation on ground :
1) The linearity of each gain range is confirmed in the range of 1.4-2.5 %.
2) Each channel covers from 1 MIP to 10^6 MIPs.

APD-H	APD-L	PD-H	PD-L
1.4%	1.5%	2.5%	2.2%

The correlation between adjacent gain ranges is calibrated by using in-flight data in each channel.

APD-H APD-L	APD-L PD-H	PD-H PD-L
0.1%	0.7%	0.1%

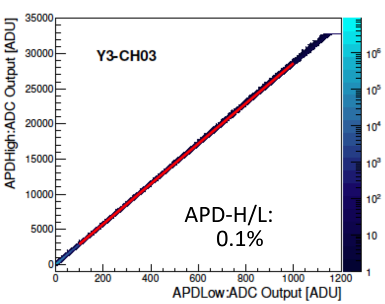

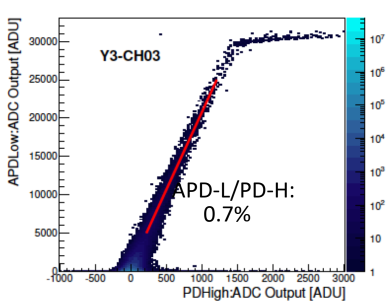

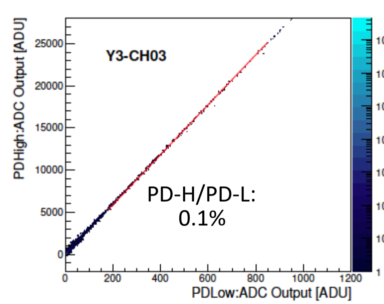

Example of energy distribution in one PWO log

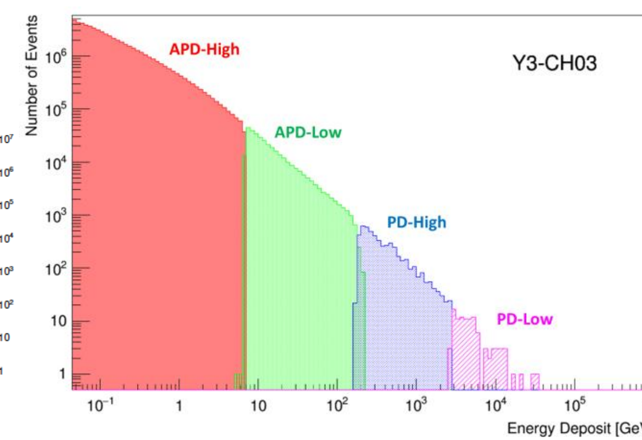

Electron Efficiency and Proton Rejection

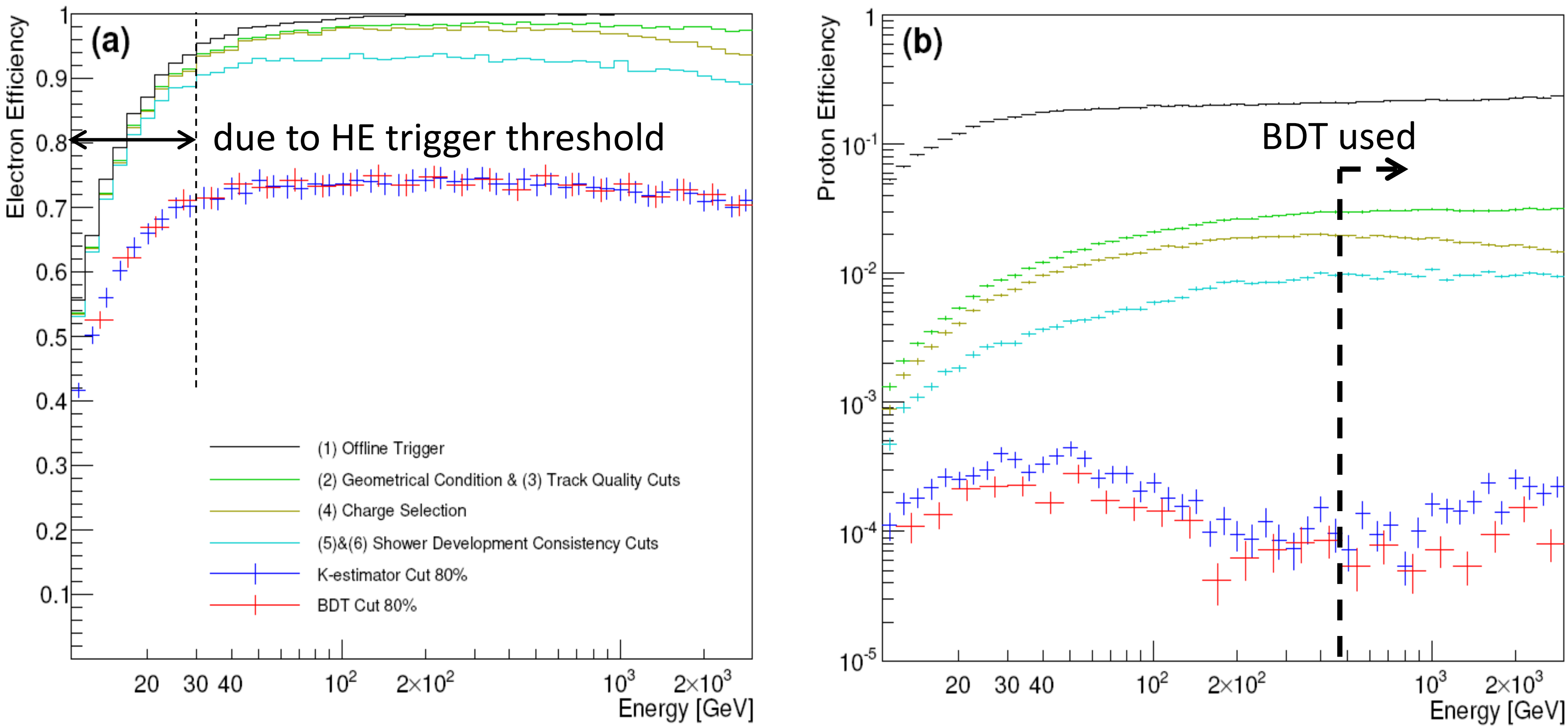

- Constant and high efficiency is the key point in our analysis.
- Simple two parameter (BDT) cut is used in the energy region E<475GeV (E>475GeV) while the small difference in resultant spectrum between two methods are taken into account in the systematic uncertainty.
- Contamination is ~5% up to 1TeV, and 10~15% in the 1—3 TeV region.

Preliminary Ultra Heavy Nuclei Measurements (26 < Z ≤ 40)

Onboard trigger for UH events

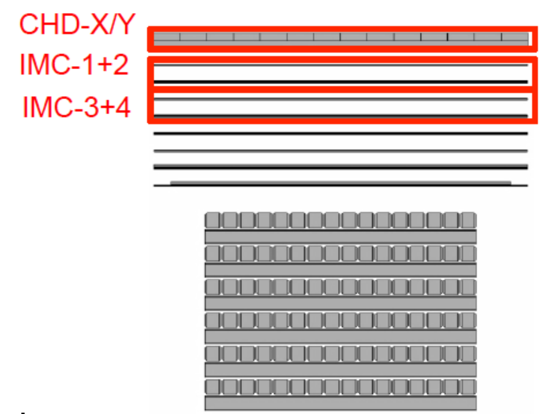

- CALET measures the relative abundances of ultra heavy nuclei through ${}_{40}$Zr
- Trigger for ultra heavy nuclei:
  - signals of only CHD, IMC1+2 and IMC3+4 are required

    ➡ an expanded geometrical acceptance (4000 cm^{2}sr)
- Energy threshold depends on the geomagnetic cutoff rigidity

<u>Data analysis</u>

- ☐ Event Selection: Vertical cutoff rigidity > 4GV & Zenith Angle < 60 degrees
- ☐ Contamination from neighboring charge are determined by multiple-Gaussian function

Charge distribution

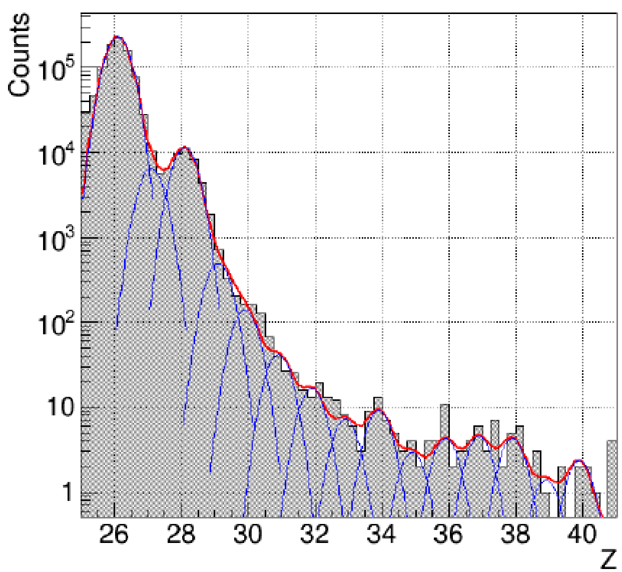

Relative abundance (Fe=1)

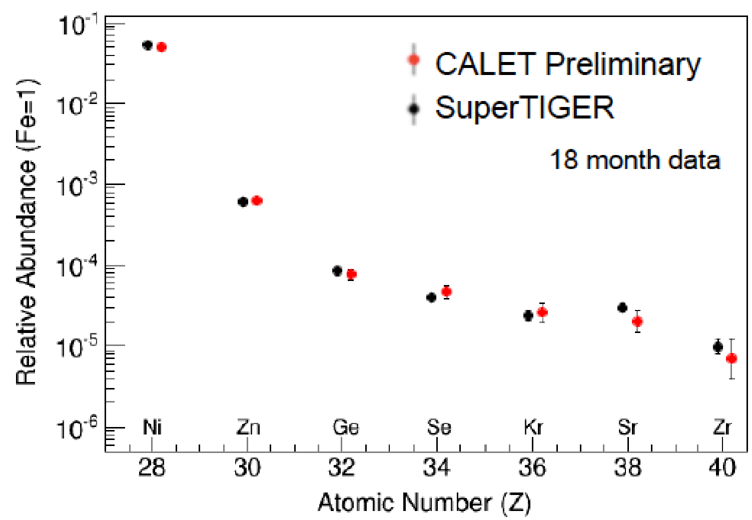

CALET's first publication NOT for Cosmic Rays

Accepted article online 25 APR 2016

Geophysical Research Letters

Relativistic electron precipitation at International Space Station: Space weather monitoring by Calorimetric Electron Telescope

Ryuho Kataoka[1,2], Yoichi Asaoka[3], Shoji Torii[3,4], Toshio Terasawa[5], Shunsuke Ozawa[4], Tadahisa Tamura[6], Yuki Shimizu[6], Yosui Akaike[4], and Masaki Mori[7]

[1]Space and Upper Atmospheric Sciences Group, National Institute of Polar Research, Tachikawa, Japan, [2]Department of Polar Science, School of Multidisciplinary Sciences, SOKENDAI (Graduate University for Advanced Studies), Tachikawa, Japan, [3]Research Institute for Science and Engineering, Waseda University, Shinjuku, Japan, [4]Department of Physics, Waseda University, Shinjuku, Japan, [5]Institute for Cosmic Ray Research, University of Tokyo, Kashiwa, Japan, [6]Institute of Physics, Kanagawa University, Yokohama, Japan, [7]Department of Physical Sciences, Ritsumeikan University, Kusatsu, Japan

Abstract The charge detector (CHD) of the Calorimetric Electron Telescope (CALET) on board the International Space Station (ISS) has a huge geometric factor for detecting MeV electrons and is sensitive to relativistic electron precipitation (REP) events. During the first 4 months, CALET CHD observed REP events mainly at the dusk to midnight sector near the plasmapause, where the trapped radiation belt electrons can be efficiently scattered by electromagnetic ion cyclotron (EMIC) waves. Here we show that interesting 5–20 s periodicity regularly exists during the REP events at ISS, which is useful to diagnose the wave-particle interactions associated with the nonlinear wave growth of EMIC-triggered emissions.

Space Weather is now a new topic of the CALET science !!

Relativistic Electron Precipitation

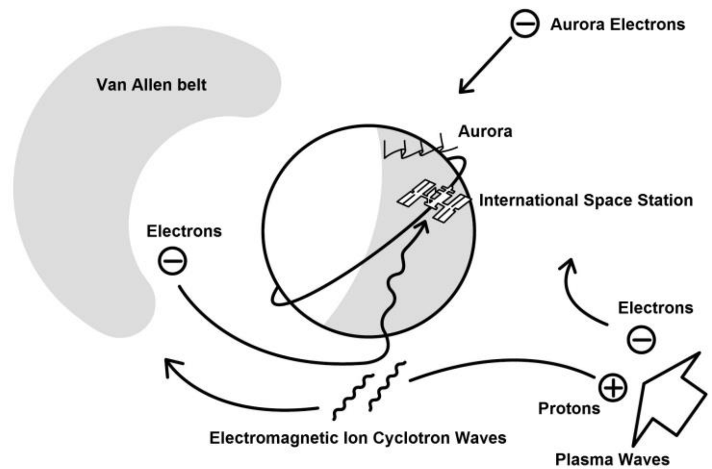

CHD X and Y count rate increase by REP

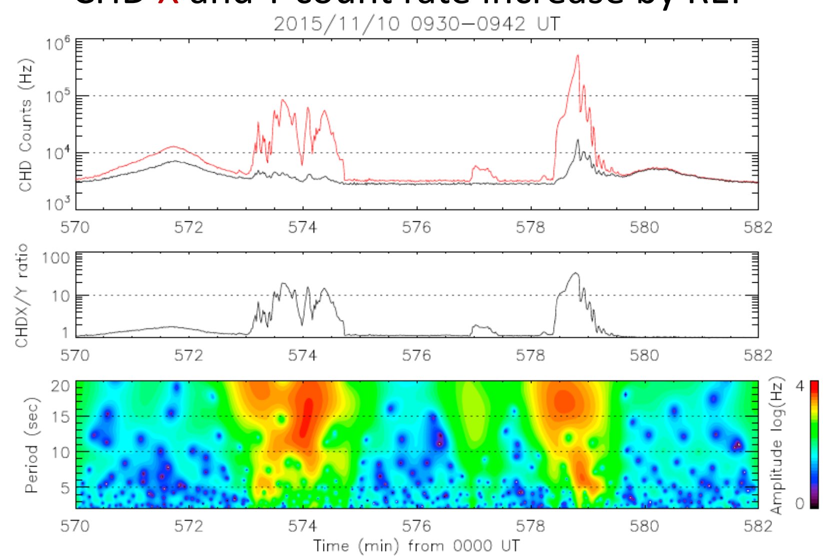

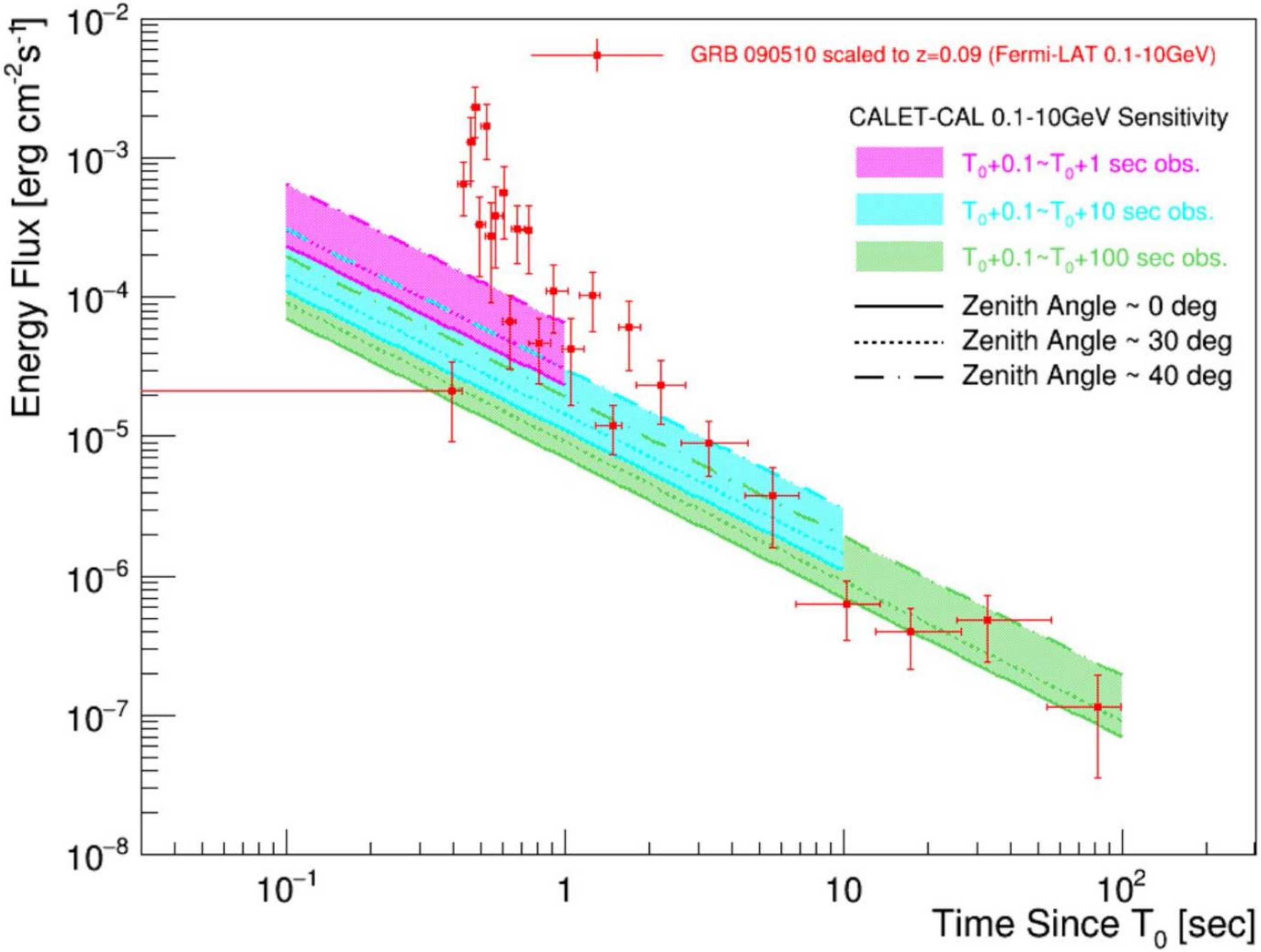

Figure 8. *CALET*/CAL sensitivity to obtain 1 event for a transient source assuming the energy spectrum proportional to $E^{-2}t^{-1}$, where E is the energy and t is the time after T_0, in the energy region 0.1–10 GeV. Despite the lack of sensitivity to sub-GeV gamma-rays in the CAL, the 0.1–1 GeV band is included in this calculation of the limit to compare to the *Fermi*-LAT light curve since the energy flux is sensitive to the range over which it is integrated. Shaded areas show energy-flux sensitivities assuming observations of 1, 10, and 100 s durations for a source around the zenith, and dotted and dotted–dashed lines show those for a source around 30° and 40° from zenith, respectively. Also shown by points are the observed light curve of GRB 090510 by *Fermi*-LAT, which is a short-hard GRB with an additional hard power-law component from 10 keV to GeV energies (Ajello et al. 2018), scaled to $z = 0.09$, the nominal redshift of the first LIGO event GW150914 as calculated by Ackermann et al. (2016).

Not Included

Attached Location (JEM-EF Port No.9) and the FOV

CALET has a Field-Of-View of 45° from its position at Port No.9. (A small part of the FOV is covered by thin structural material.

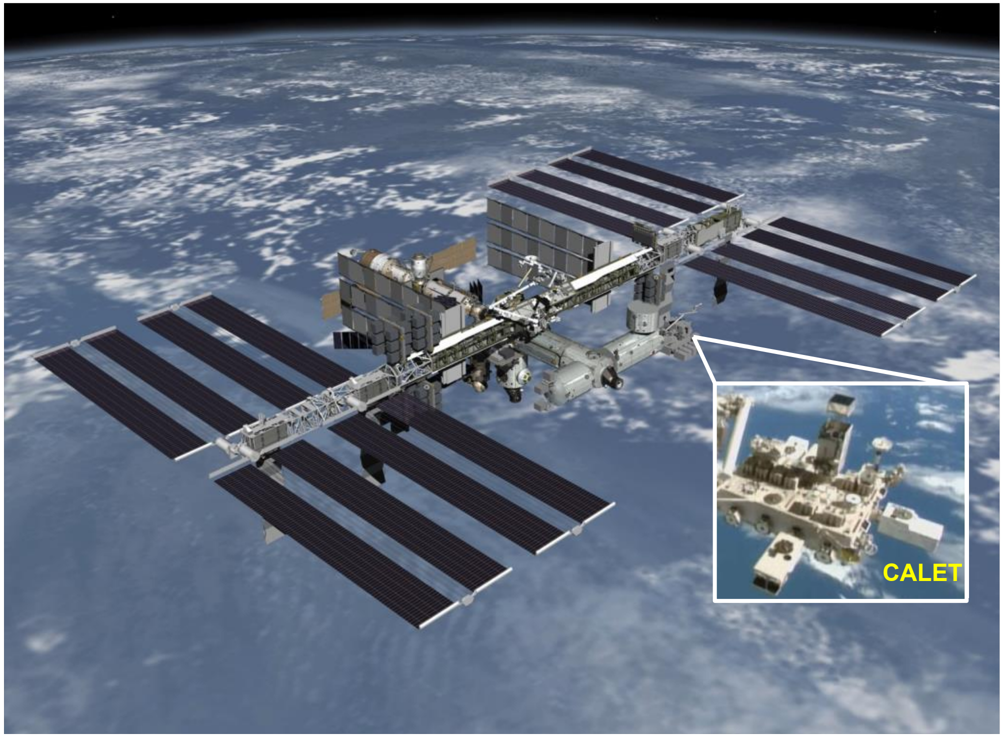

CALET located at the Port No.9
at the Japanese Experiment Module

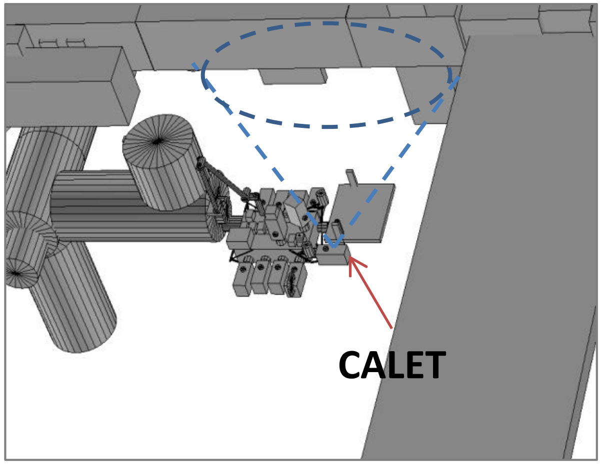

ISS simplified model

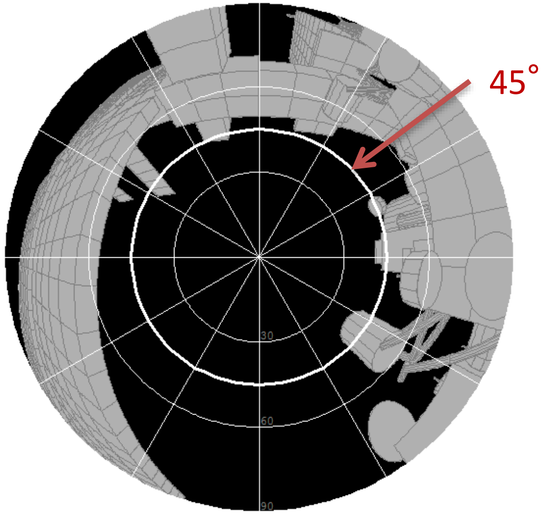

CALET FOV

All-Electron Spectrum Comparison w/ DAMPE

and other space based experiments

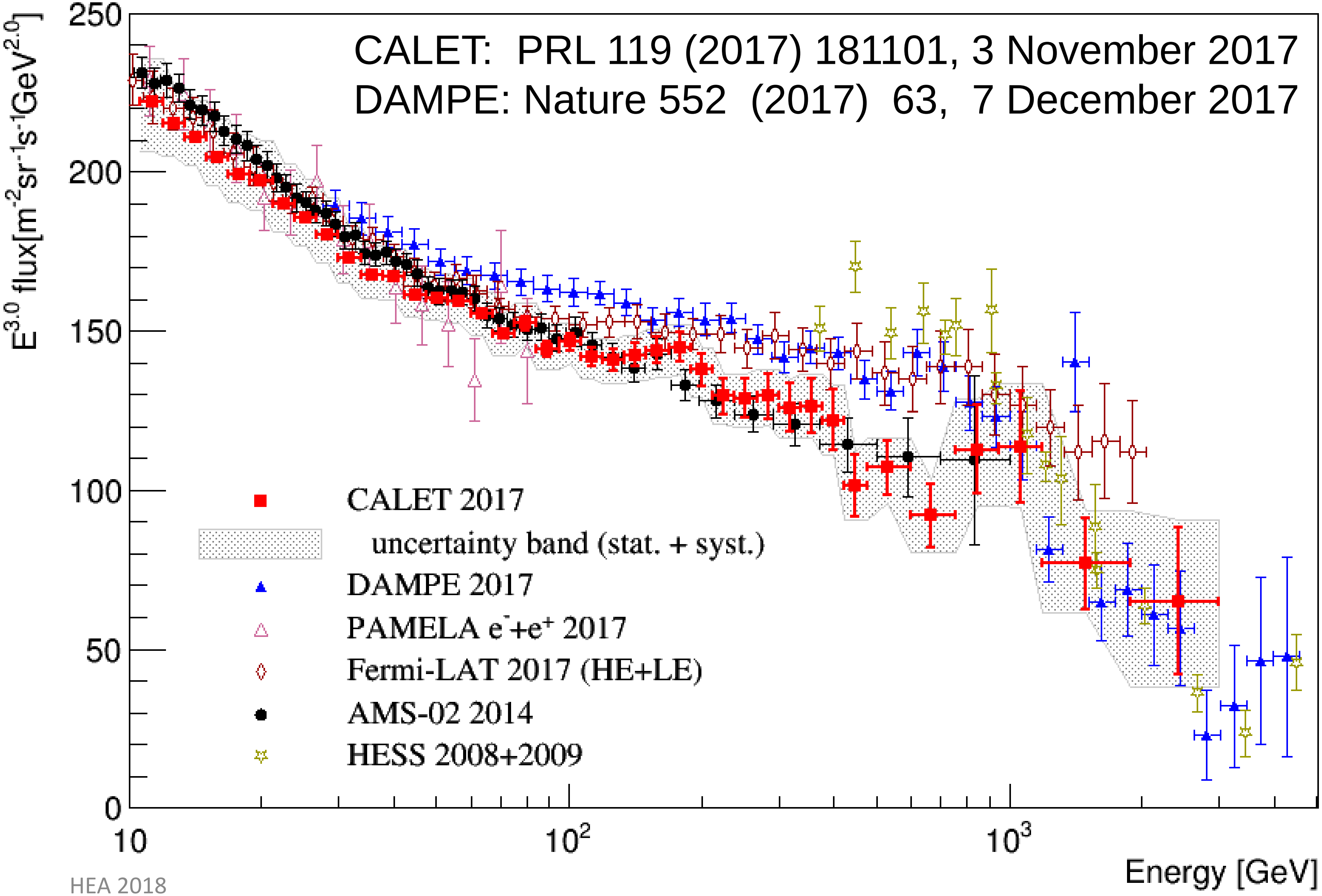

TASC Energy Measurement in Dynamic Range of 1-10^6 MIP

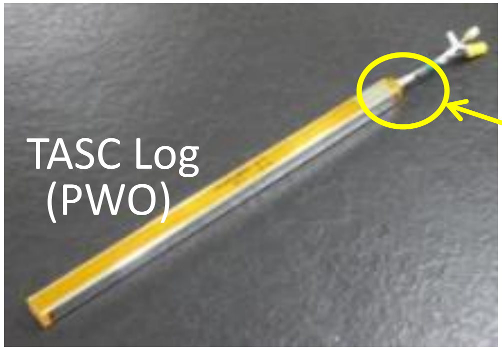

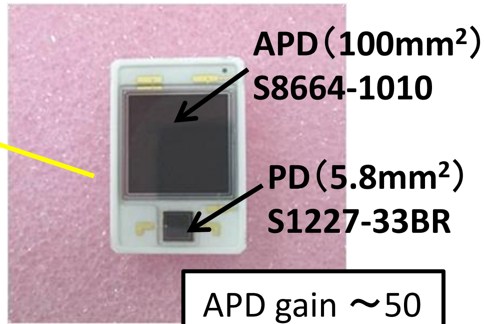

APD gain ～50

"MIP" peak in PWO: Obs. vs. MC

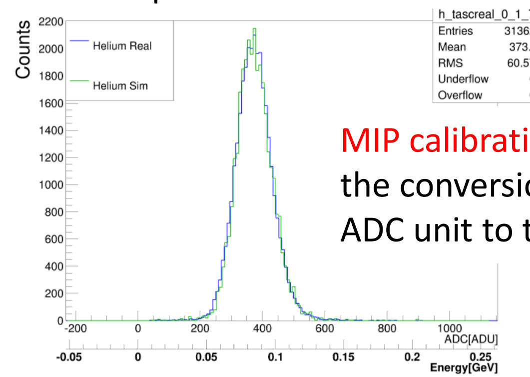

MIP calibration determines the conversion factor from ADC unit to the energy

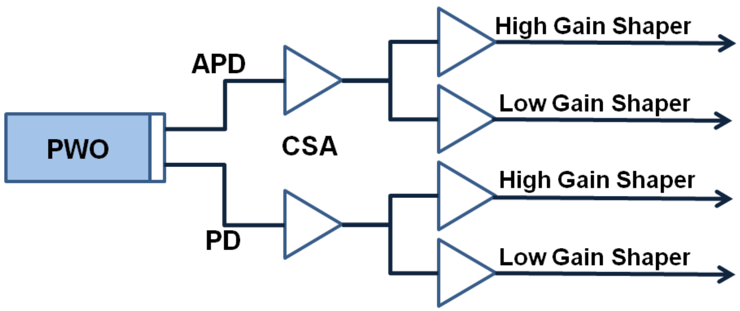

The whole dynamic range was calibrated by UV laser irradiation on ground :
1) The linearity of each gain range is confirmed in the range of 1.4-2.5 %.
2) Each channel covers from 1 MIP to 10^6 MIPs.

APD-H	APD-L	PD-H	PD-L
1.4%	1.5%	2.5%	2.2%

The correlation between adjacent gain ranges is calibrated by using in-flight data in each channel.

APD-H APD-L	APD-L PD-H	PD-H PD-L
0.1%	0.7%	0.1%

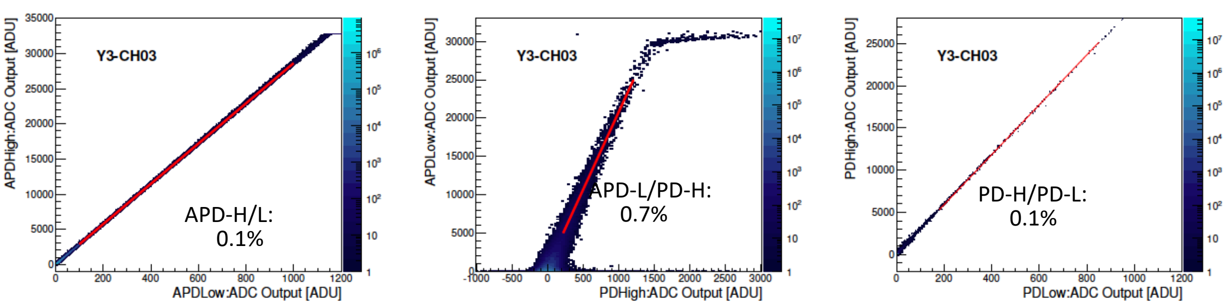

Example of energy distribution in one PWO log

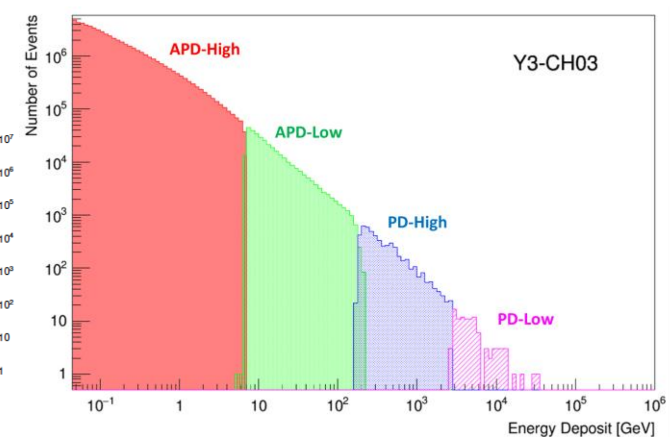

Preliminary Energy spectra of Car

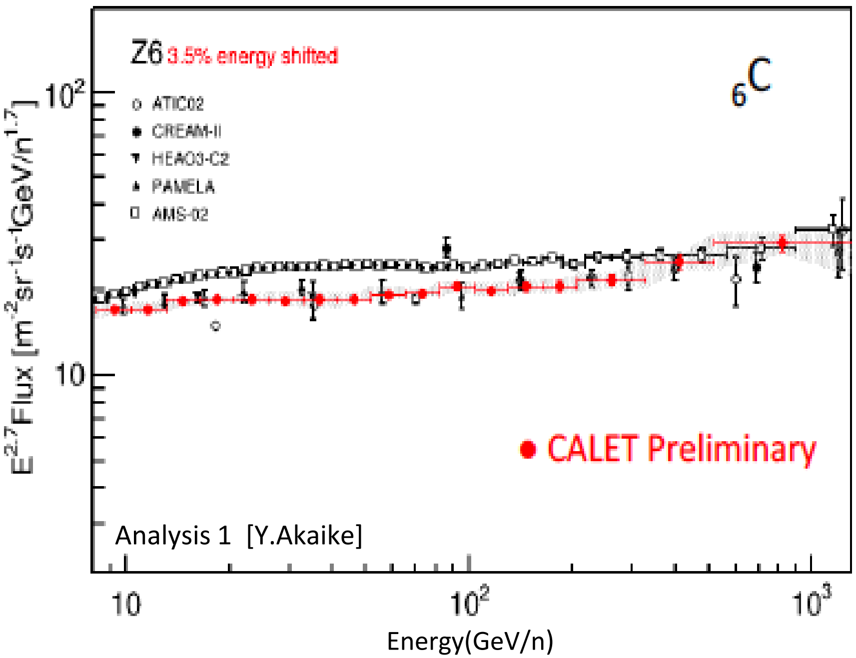

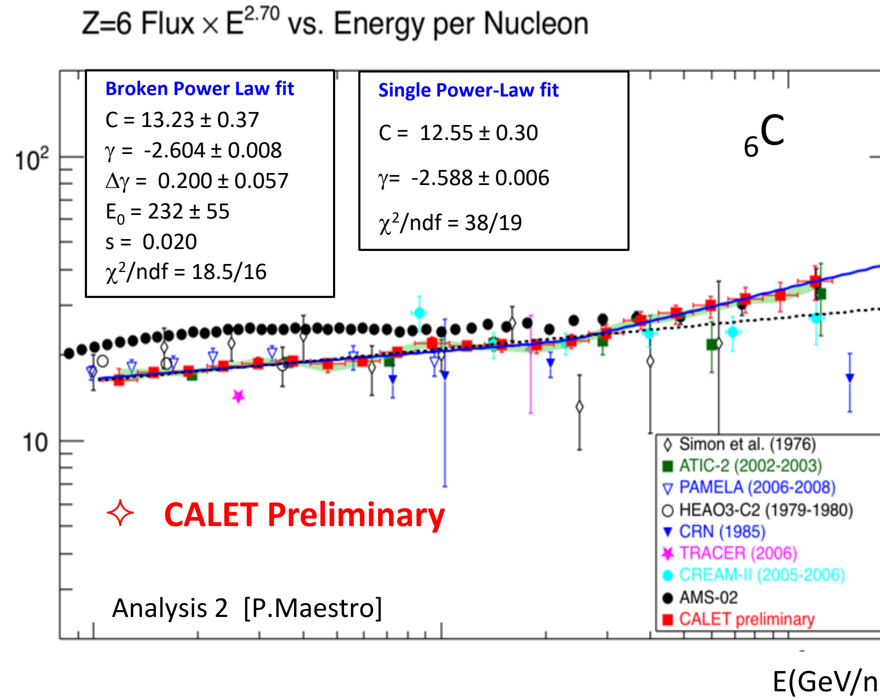

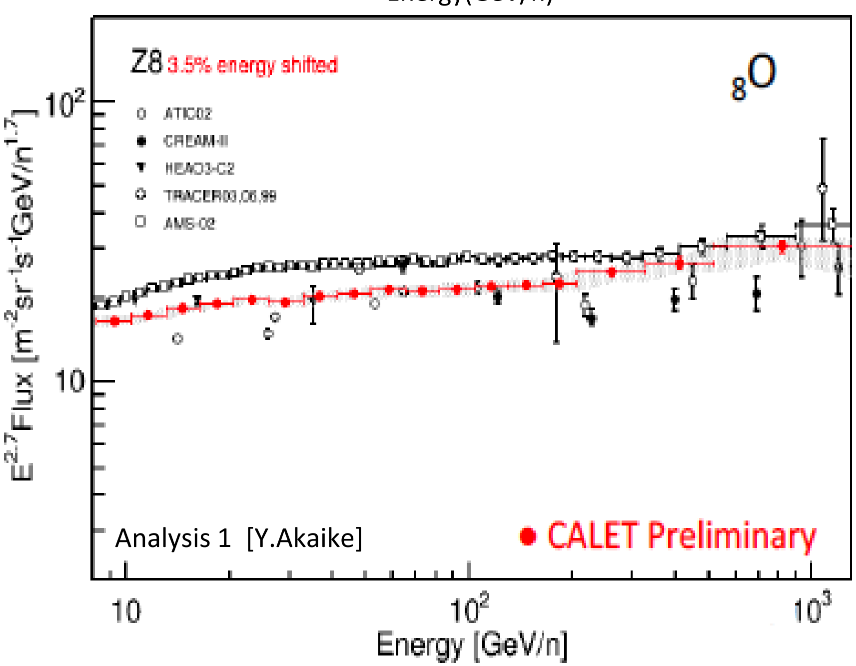

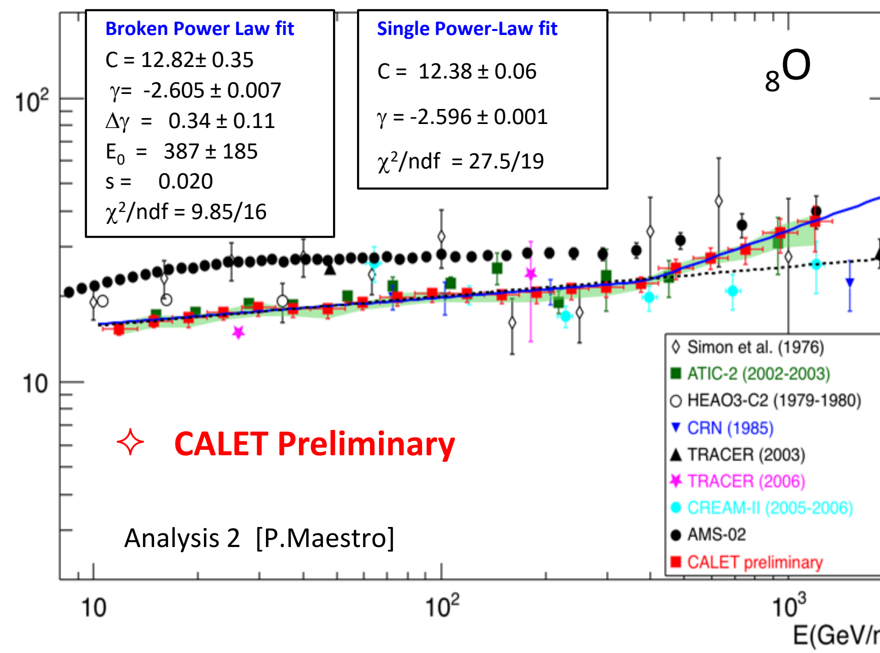

TASC Energy Measurement in Dynamic Range of 1-10^6 MIP

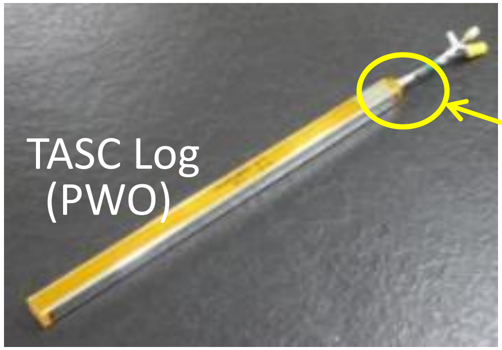

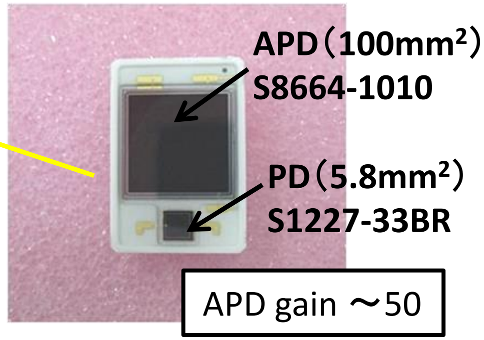

"MIP" peak in PWO: Obs. vs. MC

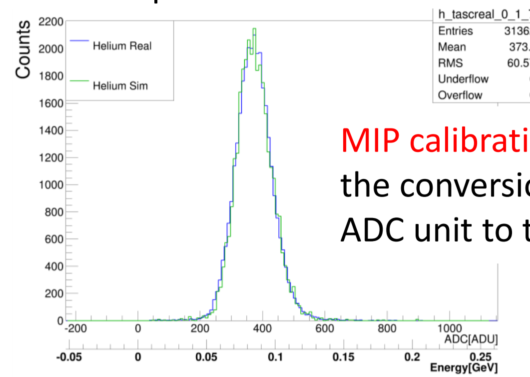

MIP calibration determines the conversion factor from ADC unit to the energy

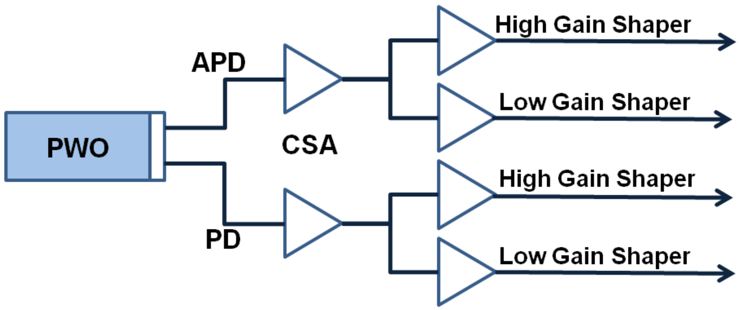

The whole dynamic range was calibrated by UV laser irradiation on ground :

1) The linearity of each gain range is confirmed in the range of 1.4-2.5 %.
2) Each channel covers from 1 MIP to 10^6 MIPs.

APD-H	APD-L	PD-H	PD-L
1.4%	1.5%	2.5%	2.2%

The correlation between adjacent gain ranges is calibrated by using in-flight data in each channel.

APD-H APD-L	APD-L PD-H	PD-H PD-L
0.1%	0.7%	0.1%

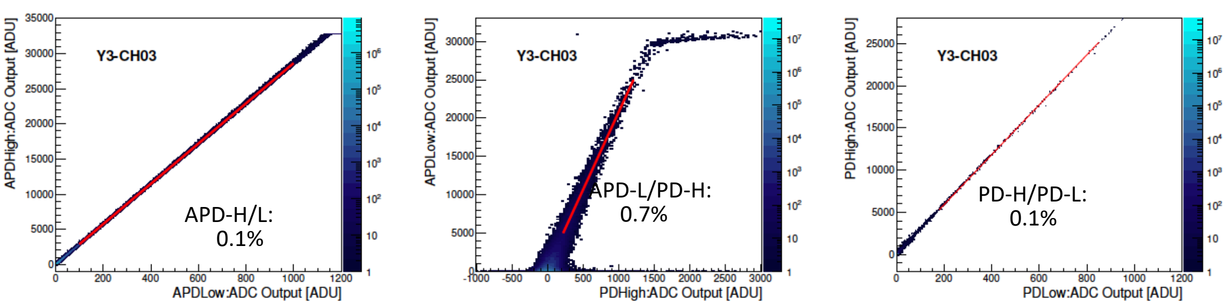

Example of energy distribution in one PWO log

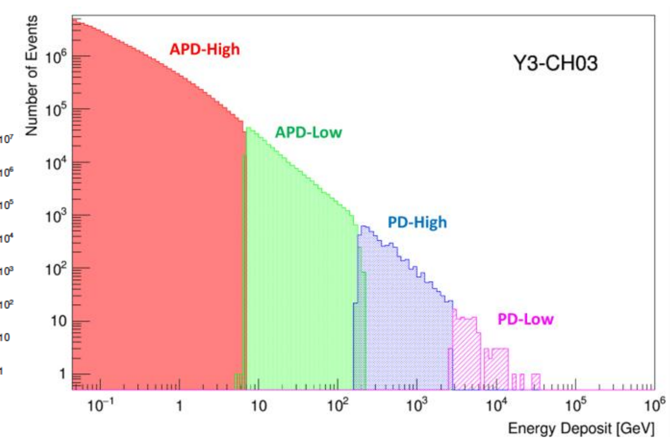

TASC Energy Deposit Distribution of All Triggered-Events by Observation for 962 days

Distribution of deposit energies (ΔE) in TASC

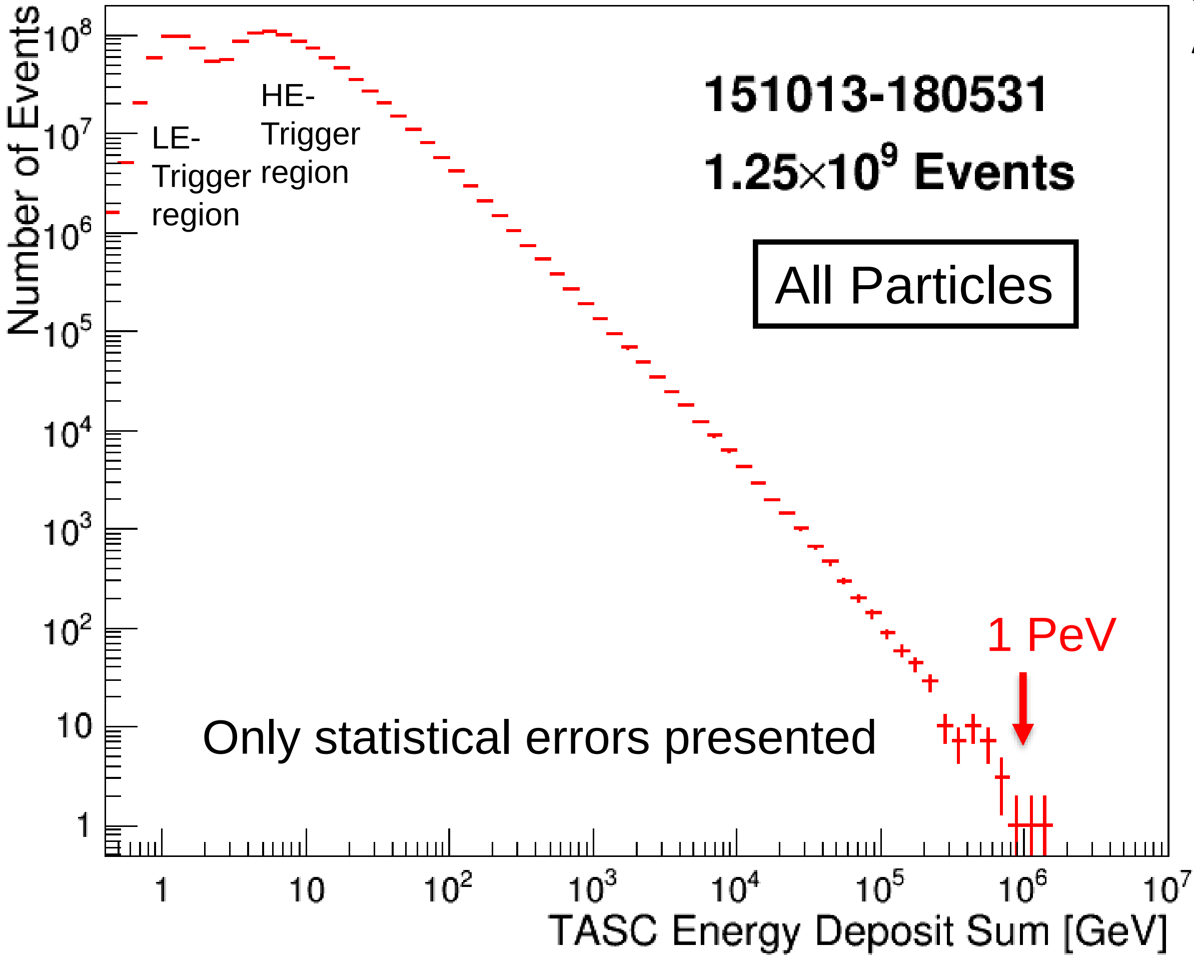

The TASC energy measurements have successfully been carried out in the dynamic range of 1 GeV – 1 PeV.

Y.Asaoka, Y.Akaike, Y.Komiya, R.Miyata, S.Torii et al. (CALET Collaboration), Astropart. Phys. 91 (2017) 1.

Performance of energy measurement in 1GeV-20TeV

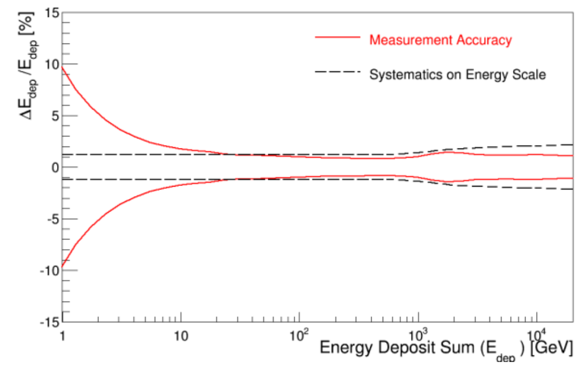

Energy resolution for electrons (TASC+IMC): < 3% over 10 GeV; <2% over 20GeV

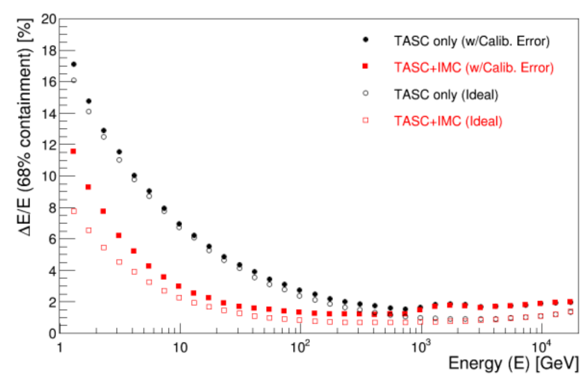

All-Electron (electron + positron) Analysis

CALET is an instrument optimized
for all-electron spectrum measurements.

$\Rightarrow$ CALET is best suited for observation of possible fine structures in the all-electron spectrum up to the trans-TeV region.

3TeV Electron Candidate

Corresponding Proton Background

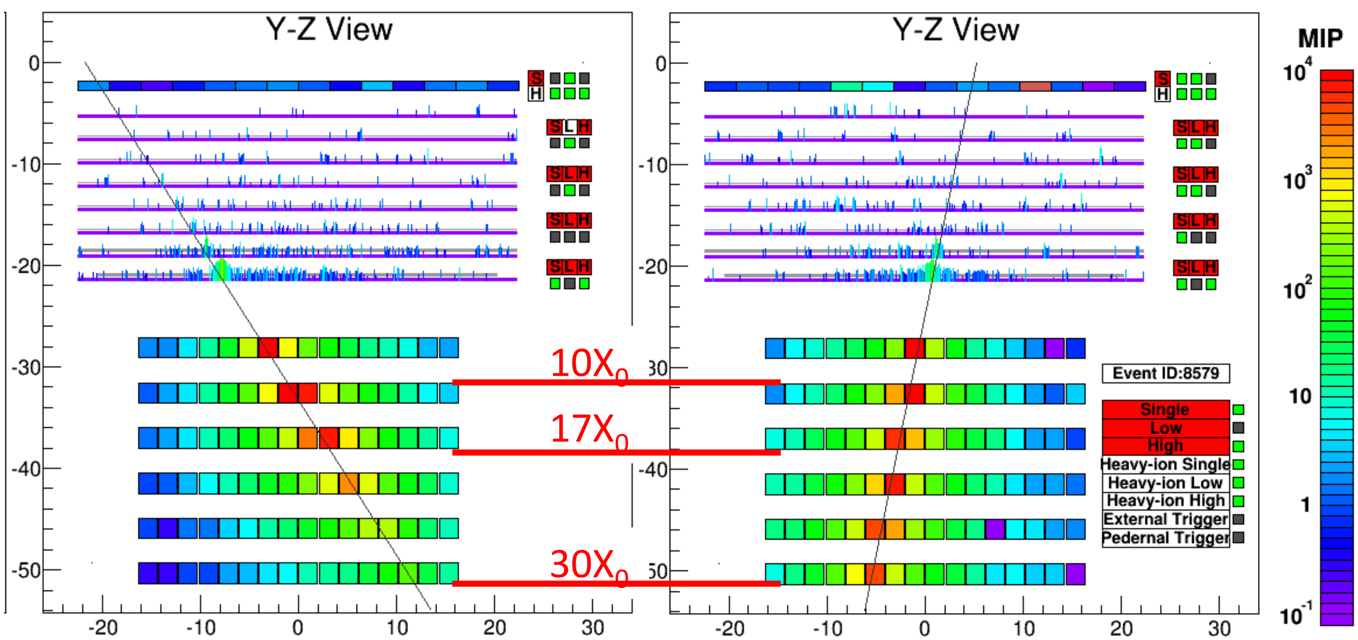

(Flight data; detector size in cm)

1. **Reliable tracking**
   well-developed shower core
2. **Fine energy resolution**
   full containment of TeV showers
3. **High-efficiency electron ID**
   $30X_0$ thickness, closely packed logs

Event Selection

Analyzed Flight Data:

- 627 days (October 13, 2015 to June 30, 2017)
- 55% of full CALET acceptance (Acceptance A+B; 570cm^{2}sr)

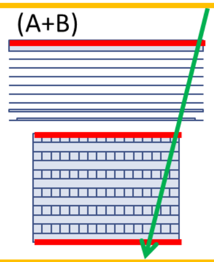

1. Offline Trigger
2. Acceptance Cut
3. Single Charge Selection
4. Track Quality Cut
5. Shower Development Consistency
6. Electron Identification
    1. Simple two parameter cut
    2. Multivariate Analysis using Boosted Decision Trees (BDT)

Event Selection

Analyzed Flight Data:
- 627 days (October 13, 2015 to June 30, 2017)
- 55% of full CALET acceptance (Acceptance A+B; 570cm^{2}sr)

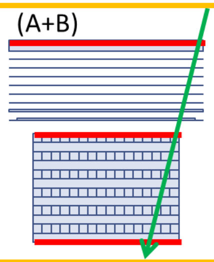

1. Offline Trigger
2. Acceptance Cut
3. Single Charge Selection
4. Track Quality Cut
5. Shower Development Consistency
6. Electron Identification
    1. Simple two parameter cut
    2. Multivariate Analysis using Boosted Decision Trees (BDT)

Pre-selection:
- Select events with successful reconstructions
- Rejecting heavier particles
- Equivalent sample between flight and MC data

Electron Efficiency and Proton Rejection

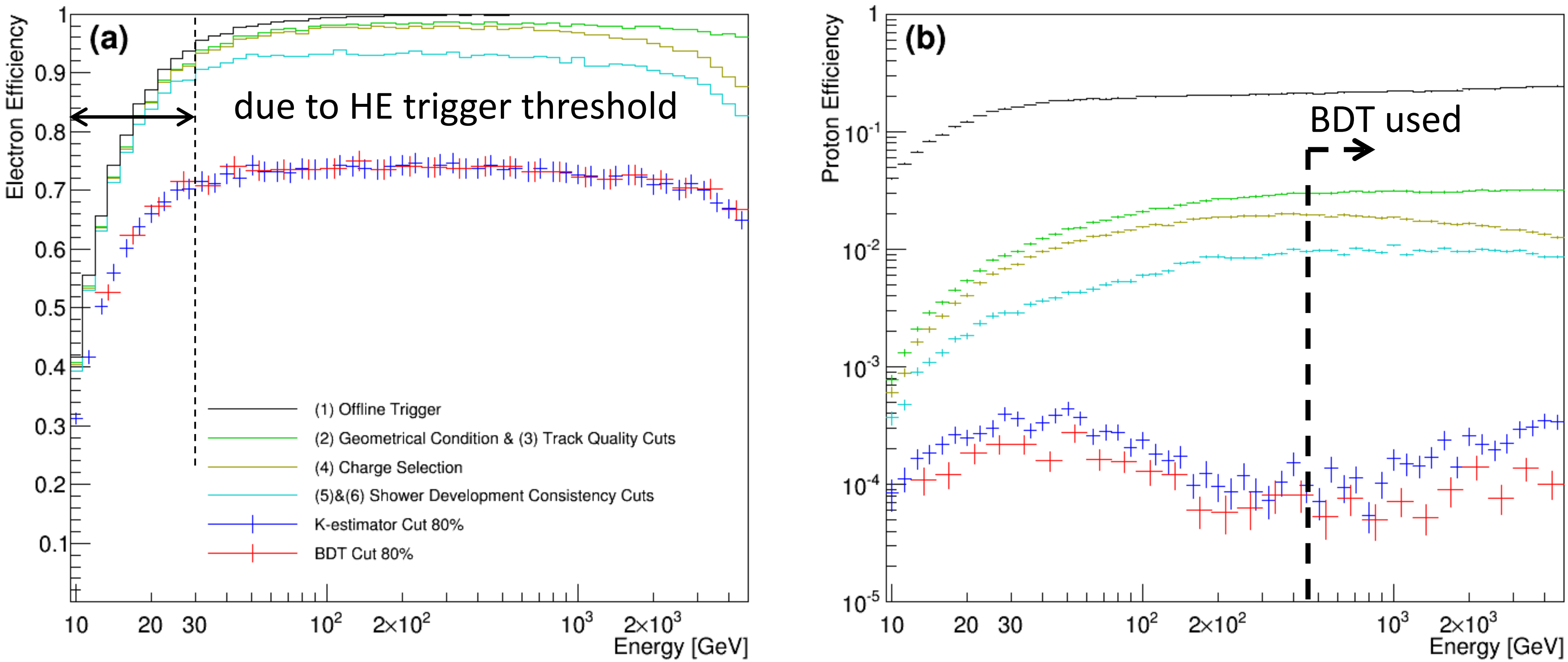

- Constant and high efficiency is the key point in our analysis.
- Simple two parameter (BDT) cut is used in the energy region E<475GeV (E>475GeV) while the small difference in resultant spectrum between two methods are taken into account in the systematic uncertainty.
- Contamination is ~5% up to 1TeV, and 10~20% in the 1—4.8 TeV region.

Spectral Analysis with Extended CALET Result

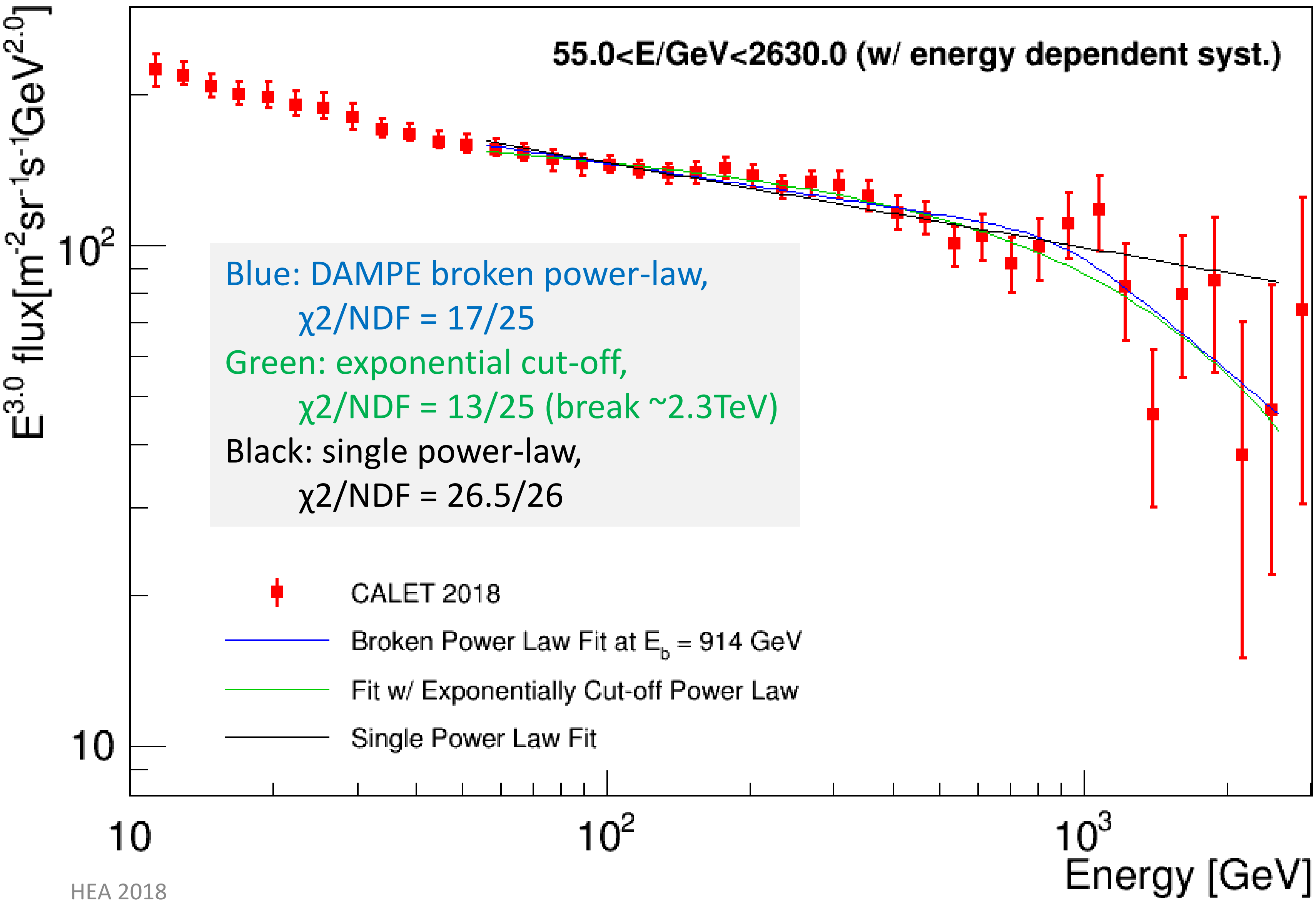

Systematic Uncertainties

(other than energy scale uncertainty)

Stability of resultant flux are analyzed by scanning parameter space

- Normalization:
  - Live time
  - Radiation environment
  - Long-term stability
  - Quality cuts
- Energy dependent:
  - 2 independent tracking
  - charge ID
  - electron ID (K-Cut vs BDT)
  - **BDT stability** (vs efficiency & training)
  - MC model (EPICS vs Geant4)

1. Divided into 4 sub-periods (195days each)
2. spectrum in each sub-period is compared with the one from the whole period.
3. standard deviation of the relative difference distribution is taken as systematic uncertainty (1.4%)

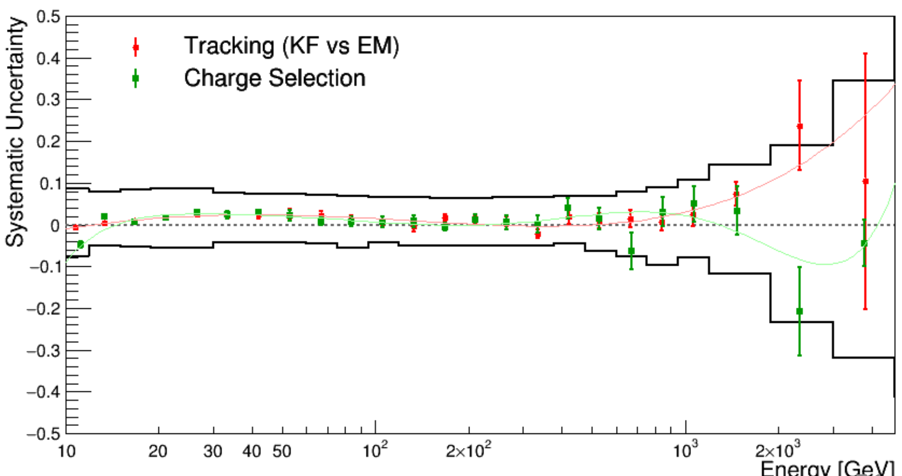

Systematic Uncertainties

(other than energy scale uncertainty)

Stability of resultant flux are analyzed by scanning parameter space

- Normalization:
  - Live time
  - Radiation environment
  - Long-term stability
  - Quality cuts
- Energy dependent:
  - 2 independent tracking
  - charge ID
  - electron ID (K-Cut vs BDT)
  - **BDT stability** (vs efficiency & training)
  - MC model (EPICS vs Geant4)

1. Divided into 4 sub-periods (195days each)
2. spectrum in each sub-period is compared with the one from the whole period.
3. standard deviation of the relative difference distribution is taken as systematic uncertainty (1.4%)

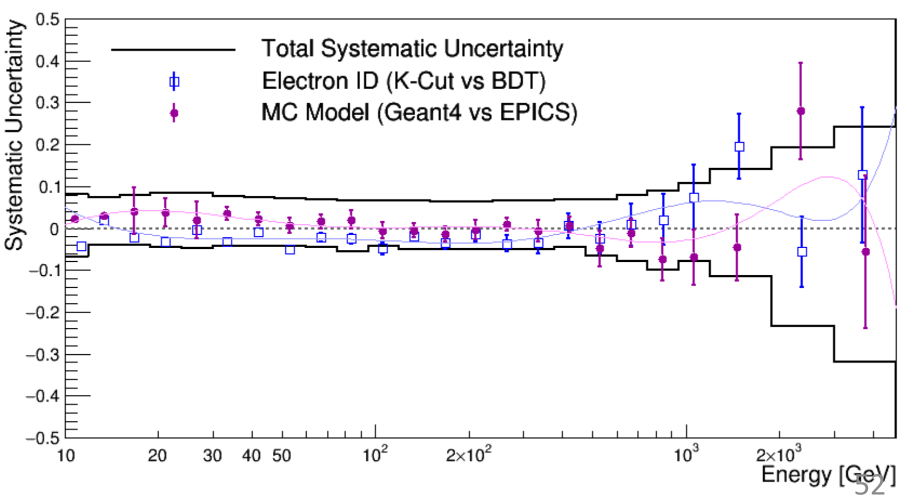

All-Electron Spectrum Comparison w/ DAMPE

and other space based experiments

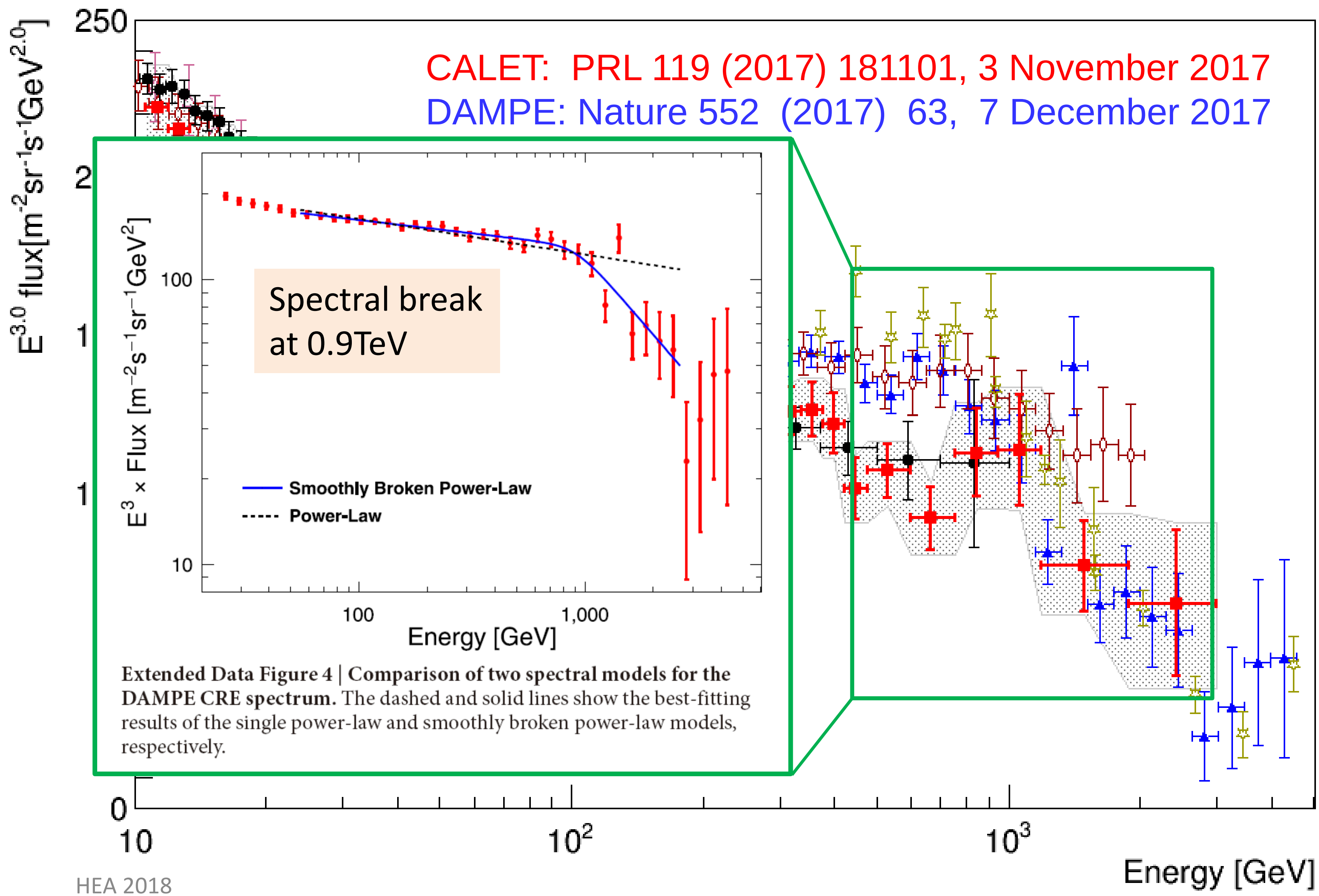

Extended Data Figure 4 | Comparison of two spectral models for the DAMPE CRE spectrum. The dashed and solid lines show the best-fitting results of the single power-law and smoothly broken power-law models, respectively.

All-Electron Spectrum Measured with CALET from 10 GeV to 3 TeV

CALET: PRL 119 (2017) 181101, 3 November 2017

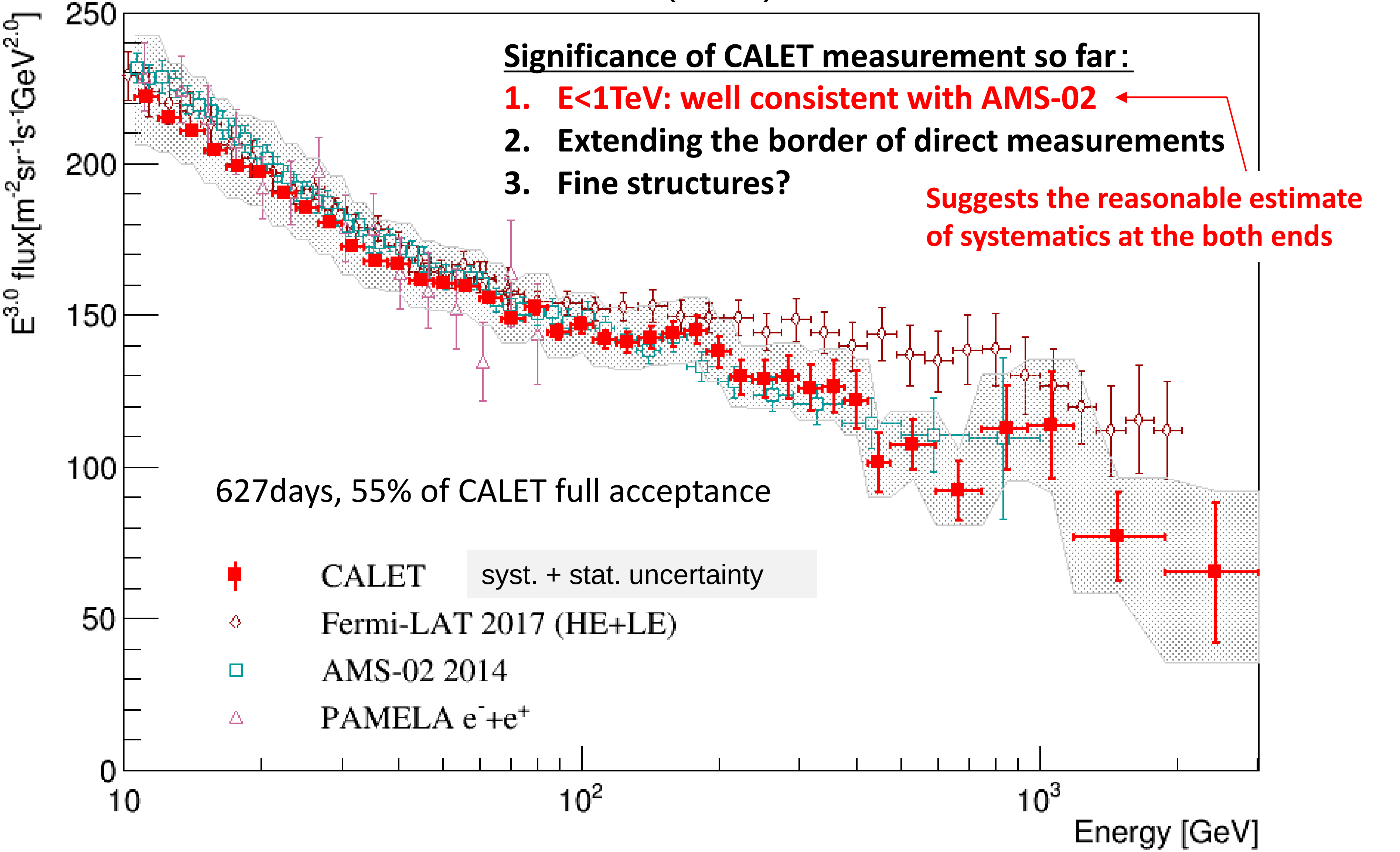

Cosmic-Ray All-Electron Spectrum ($e^+ + e^-$)

Direct measurements reached 1TeV region.

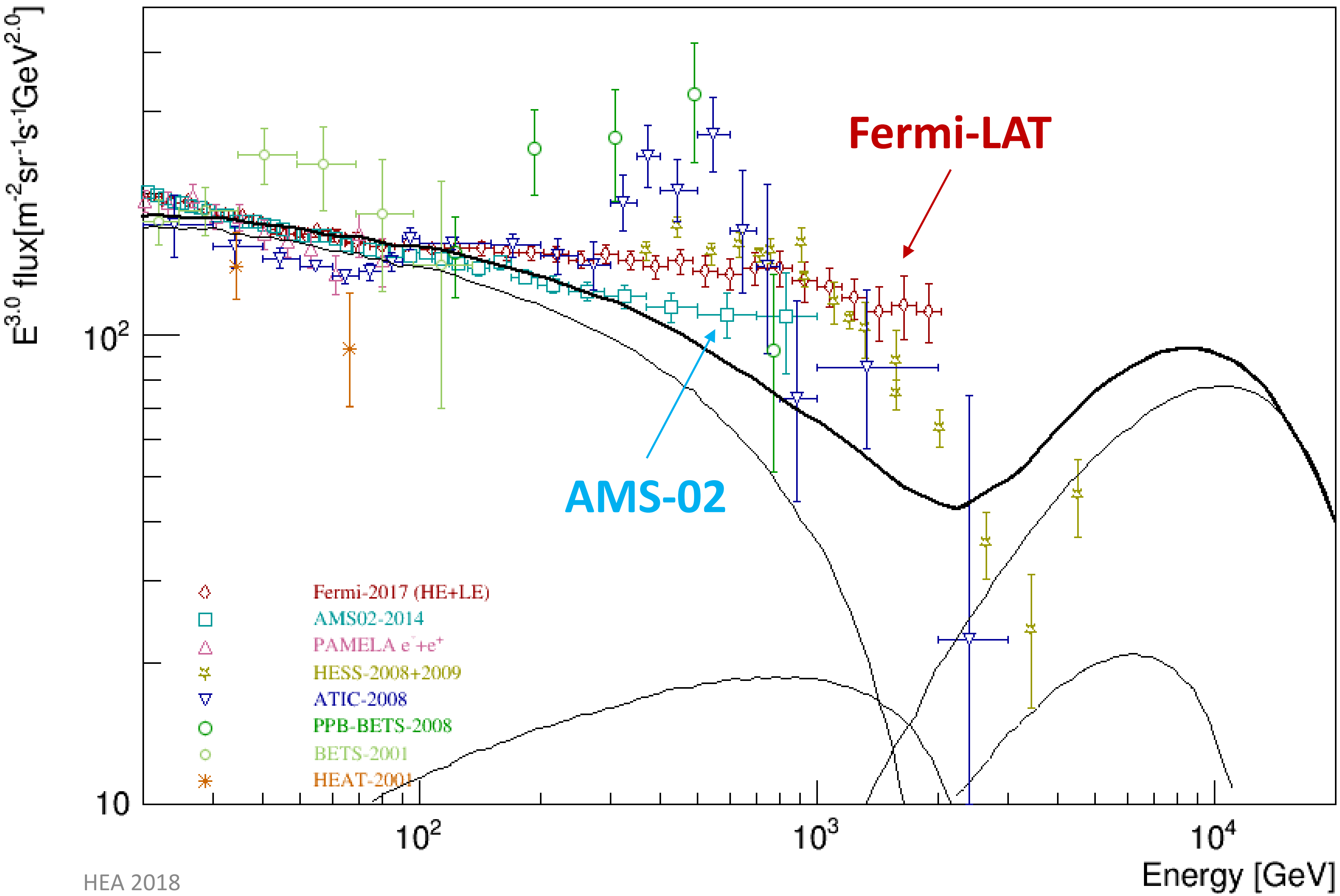

Cosmic-Ray All-Electron Spectrum ($e^+ + e^-$)

https://physics.aps.org/articles/v6/40

$$\frac{e^+}{e^+ + e^-}$$

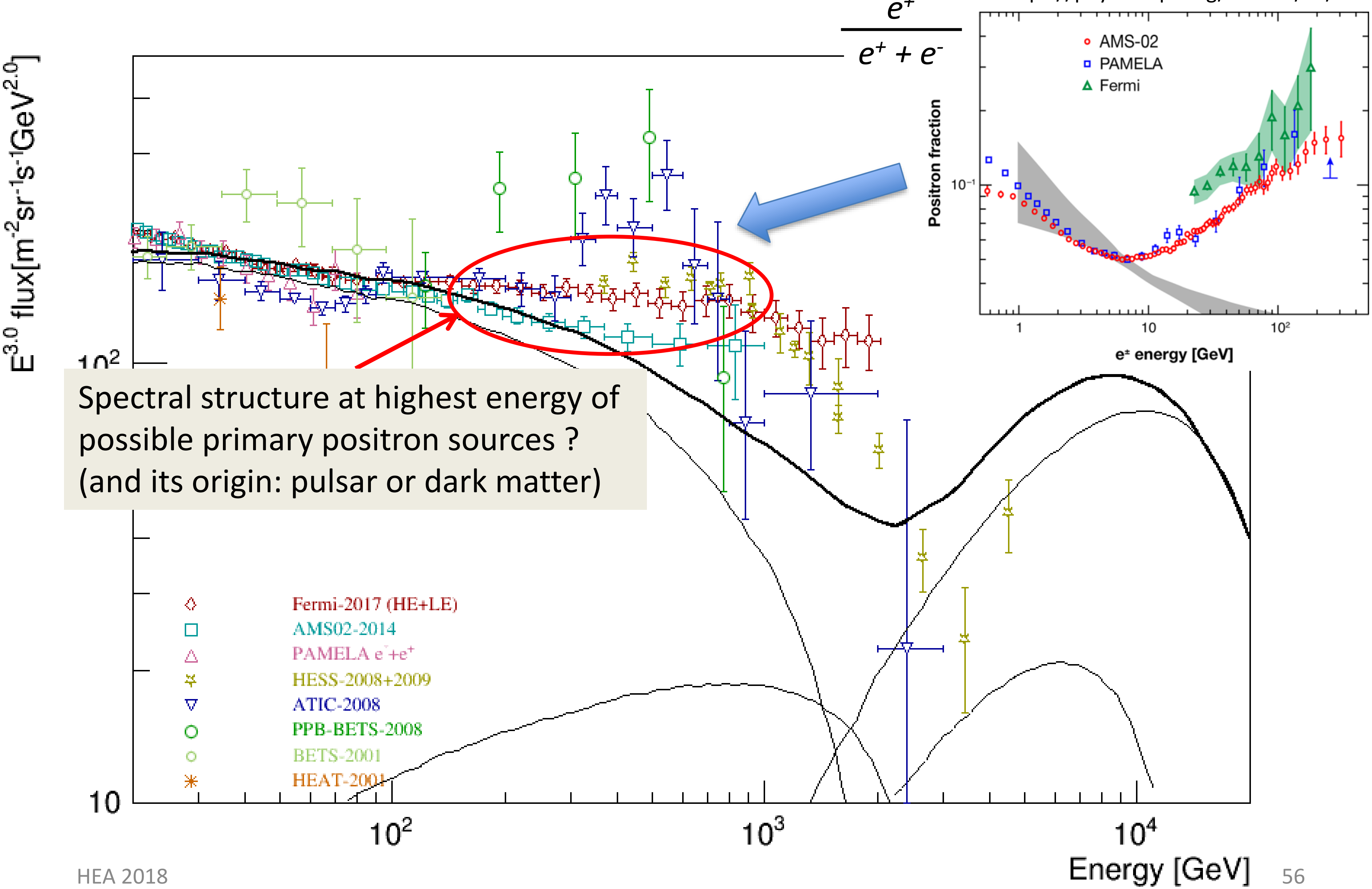

Spectral structure at highest energy of possible primary positron sources ?
(and its origin: pulsar or dark matter)

Cosmic-Ray All-Electron Spectrum ($e^+ + e^-$)

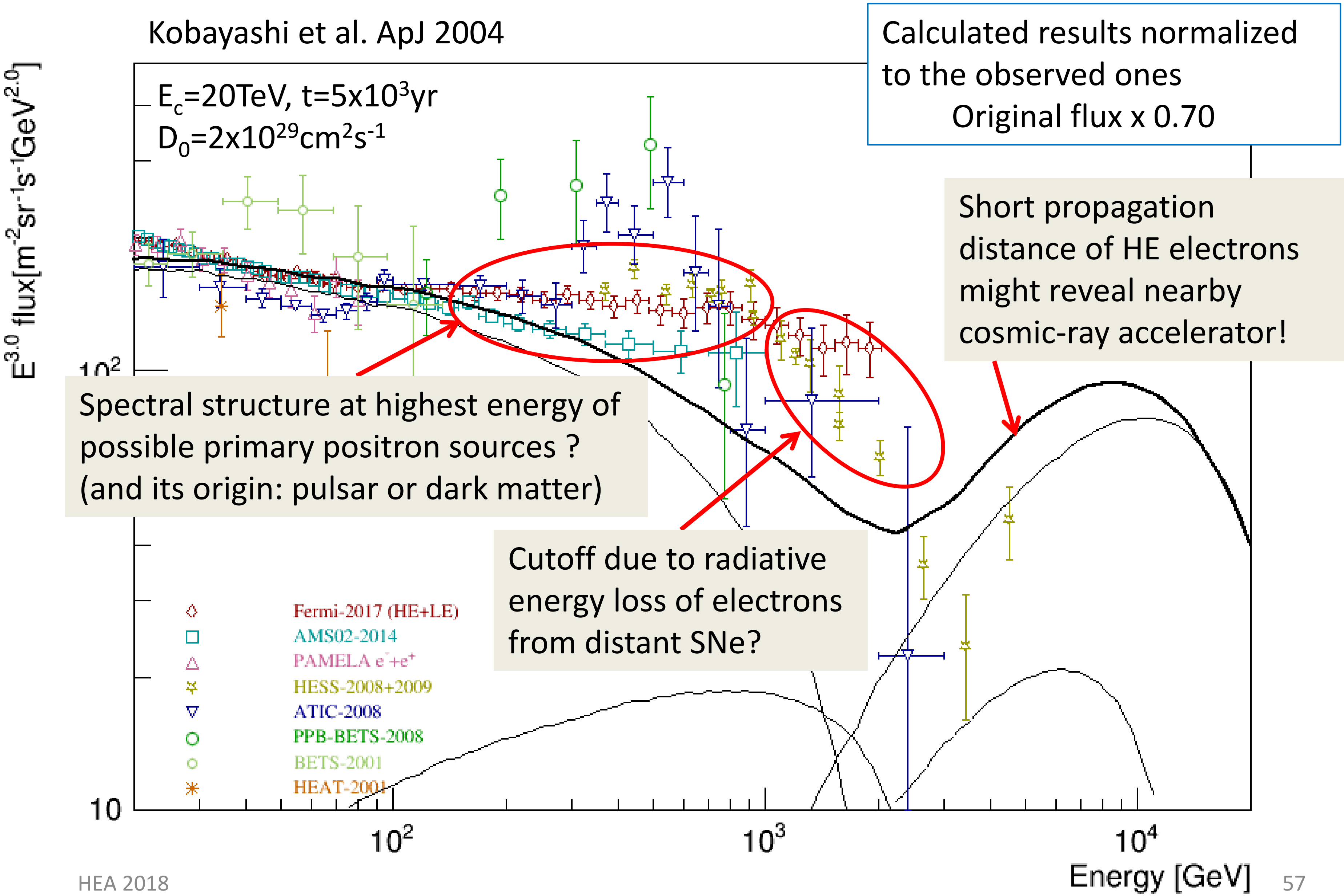

Cosmic-Ray All-Electron Spectrum ($e^+ + e^-$)

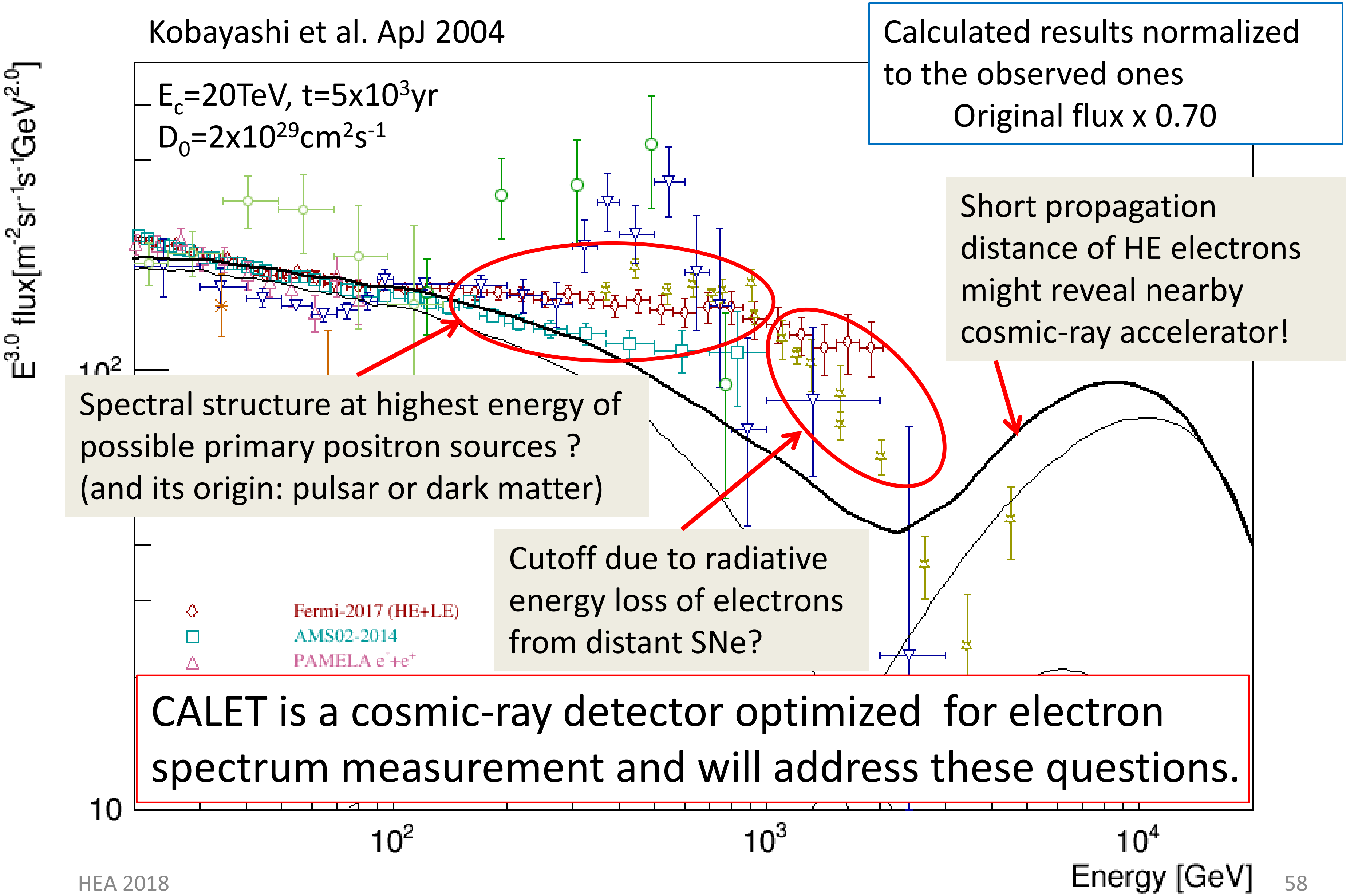

CALET is a cosmic-ray detector optimized for electron spectrum measurement and will address these questions.

Preliminary Energy spectra of Carbon and Oxygen (2 independent CALET analyses)

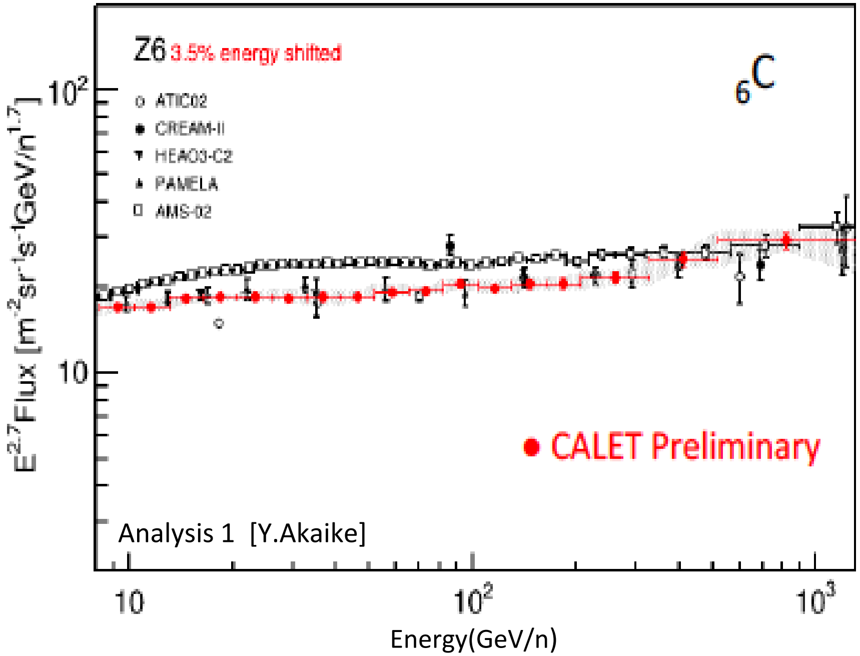

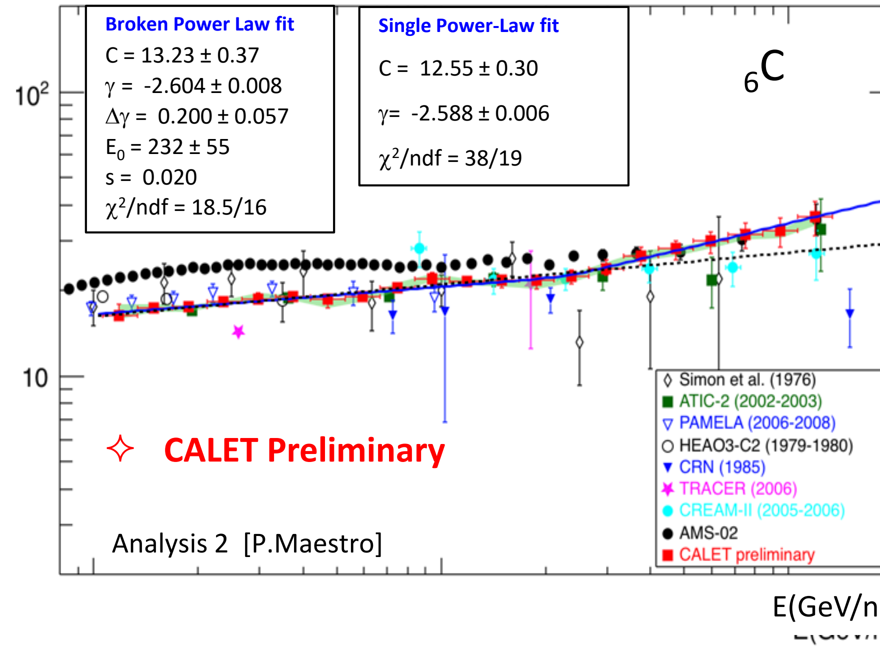

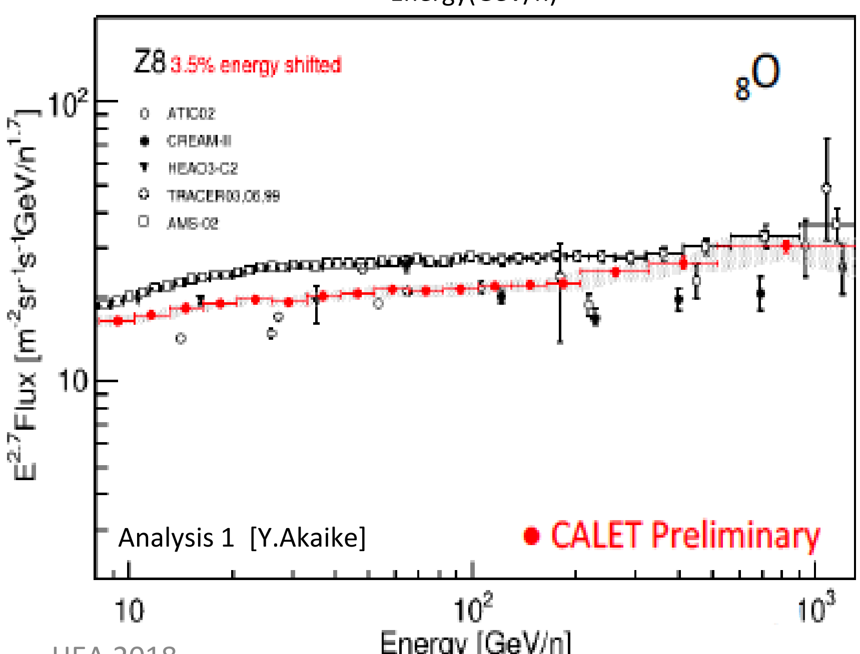

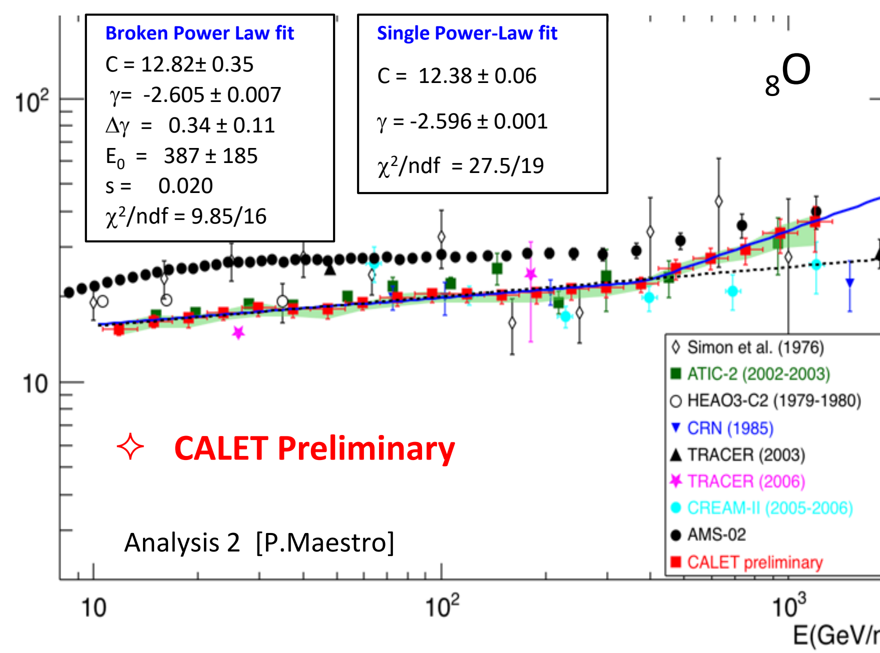

Preliminary Boron-to-Carbon Flux Ratio

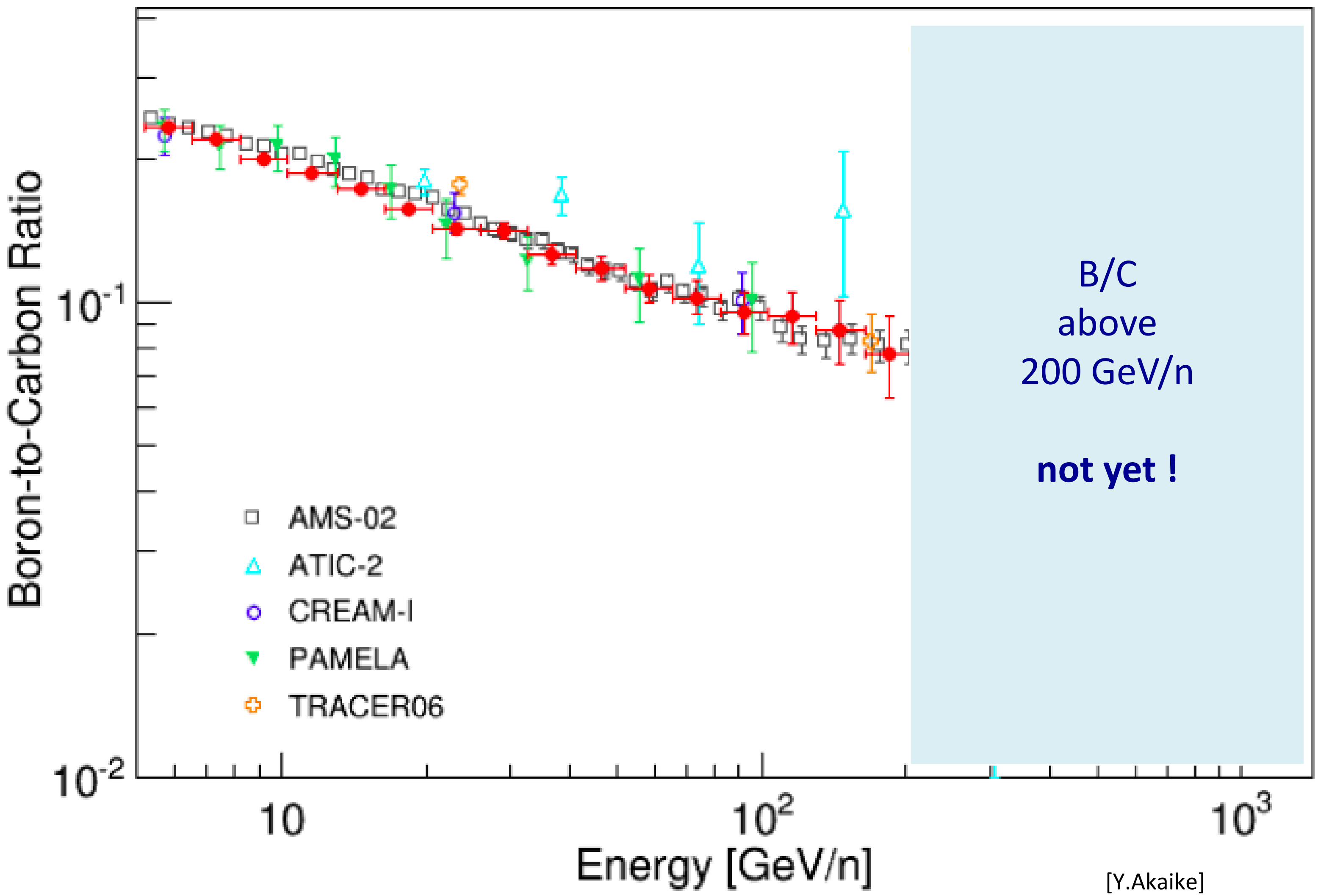

[Y.Akaike]

Preliminary Spectra of Nuclei with **Even** Atomic Number (Z = 10—16)

[Y.Akaike]

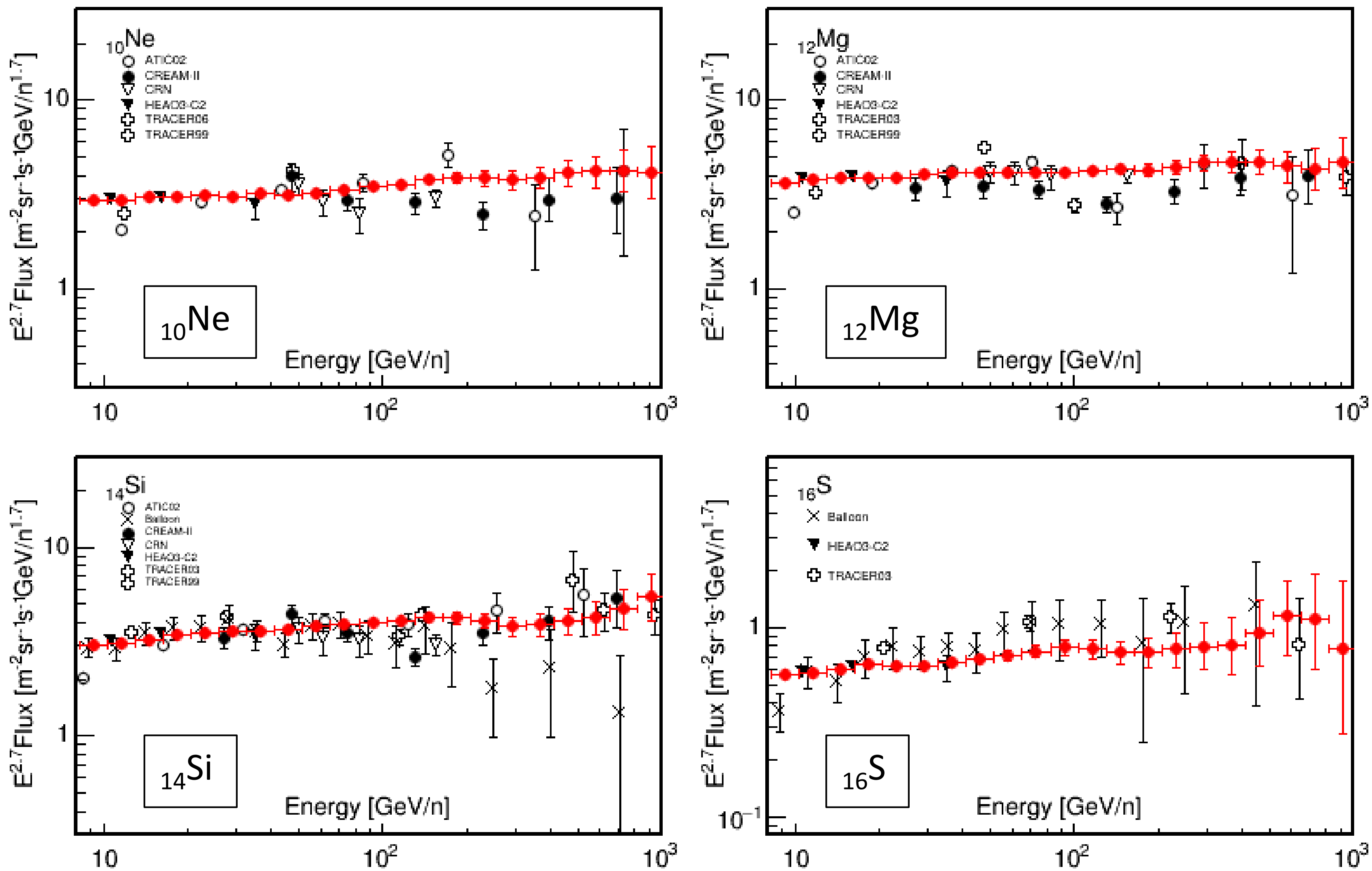

Preliminary Spectra of Nuclei with **Even** Atomic Number (Z = 18—28)

[Y.Akaike]

$_{18}$Ar

$_{20}$Ca

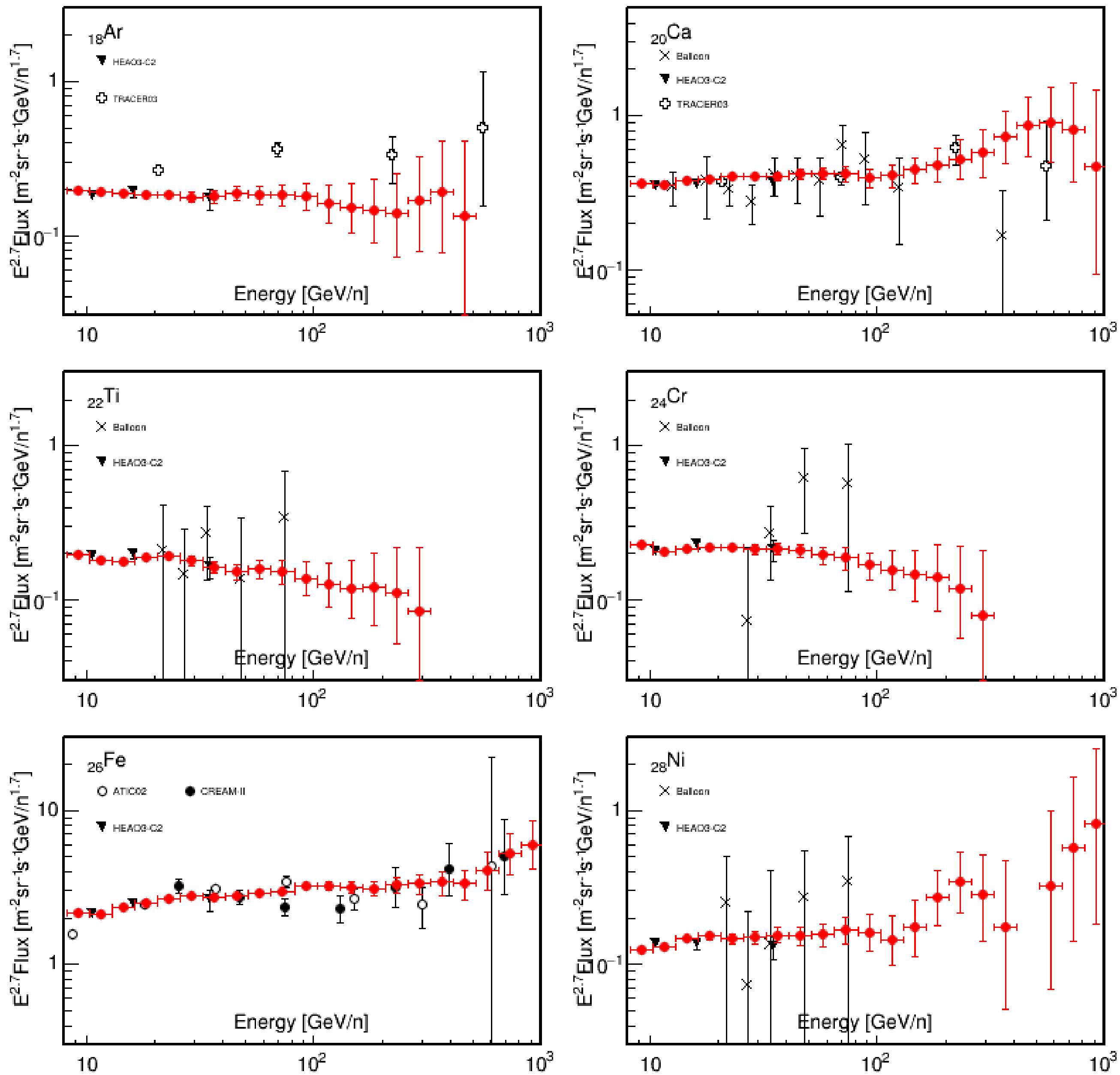

$_{22}$Ti

$_{24}$Cr

$_{26}$Fe

$_{28}$Ni

Preliminary Ultra Heavy Nuclei Measurements   ($26 < Z \le 40$)

Onboard trigger for UH events

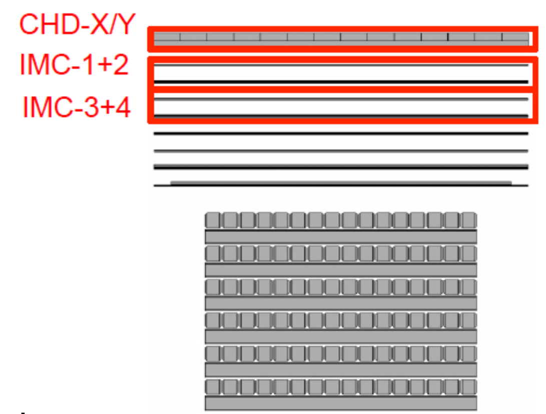

- CALET measures the relative abundances of ultra heavy nuclei through $_{40}Zr$
- Trigger for ultra heavy nuclei:
  - signals of only CHD, IMC1+2 and IMC3+4 are required
  - ➡ an expanded geometrical acceptance (4000 $cm^2 sr$)
- Energy threshold depends on the geomagnetic cutoff rigidity

<u>Data analysis</u>

- ☐ Event Selection: Vertical cutoff rigidity > 4GV & Zenith Angle < 60 degrees
- ☐ Contamination from neighboring charge are determined by multiple-Gaussian function

Charge distribution

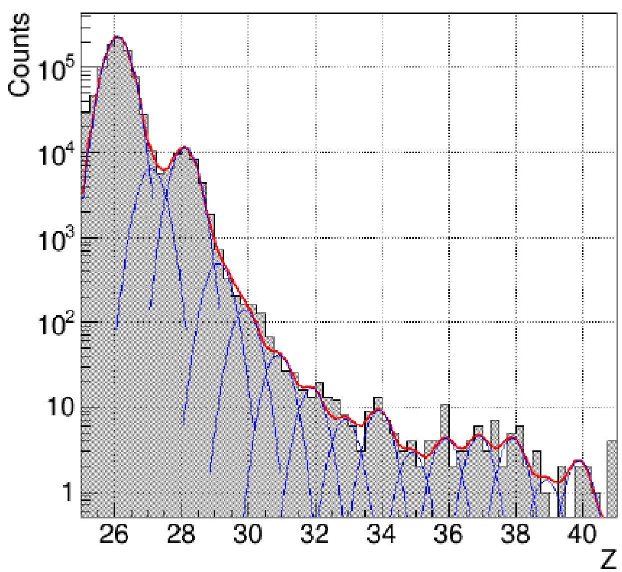

Relative abundance (Fe=1)

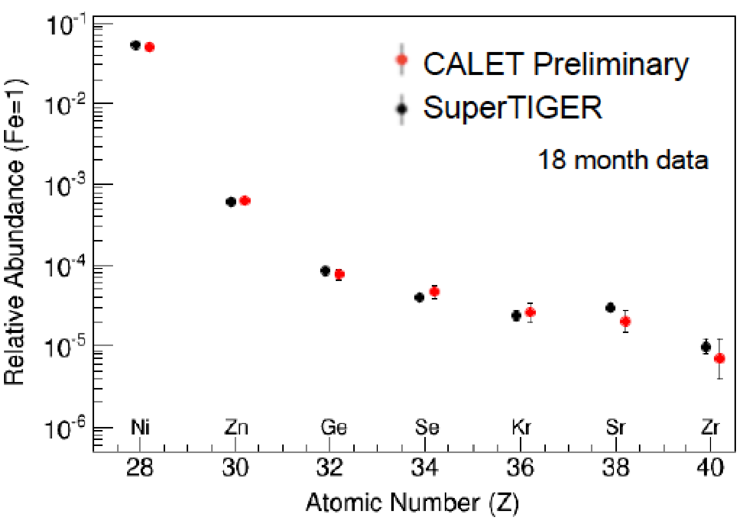

CALET's first publication NOT for Cosmic Rays

Accepted article online 25 APR 2016

Geophysical Research Letters

Relativistic electron precipitation at International Space Station: Space weather monitoring by Calorimetric Electron Telescope

Ryuho Kataoka[1,2], Yoichi Asaoka[3], Shoji Torii[3,4], Toshio Terasawa[5], Shunsuke Ozawa[4], Tadahisa Tamura[6], Yuki Shimizu[6], Yosui Akaike[4], and Masaki Mori[7]

[1]Space and Upper Atmospheric Sciences Group, National Institute of Polar Research, Tachikawa, Japan, [2]Department of Polar Science, School of Multidisciplinary Sciences, SOKENDAI (Graduate University for Advanced Studies), Tachikawa, Japan, [3]Research Institute for Science and Engineering, Waseda University, Shinjuku, Japan, [4]Department of Physics, Waseda University, Shinjuku, Japan, [5]Institute for Cosmic Ray Research, University of Tokyo, Kashiwa, Japan, [6]Institute of Physics, Kanagawa University, Yokohama, Japan, [7]Department of Physical Sciences, Ritsumeikan University, Kusatsu, Japan

Abstract The charge detector (CHD) of the Calorimetric Electron Telescope (CALET) on board the International Space Station (ISS) has a huge geometric factor for detecting MeV electrons and is sensitive to relativistic electron precipitation (REP) events. During the first 4 months, CALET CHD observed REP events mainly at the dusk to midnight sector near the plasmapause, where the trapped radiation belt electrons can be efficiently scattered by electromagnetic ion cyclotron (EMIC) waves. Here we show that interesting 5–20 s periodicity regularly exists during the REP events at ISS, which is useful to diagnose the wave-particle interactions associated with the nonlinear wave growth of EMIC-triggered emissions.

Space Weather is now a new topic of the CALET science !!

Relativistic Electron Precipitation

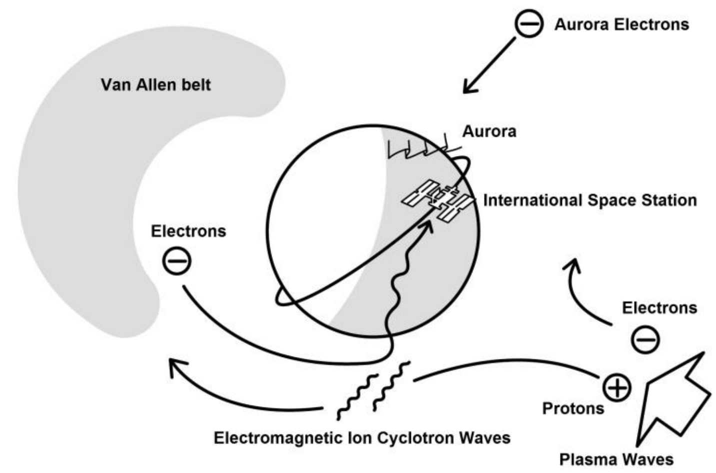

CHD X and Y count rate increase by REP

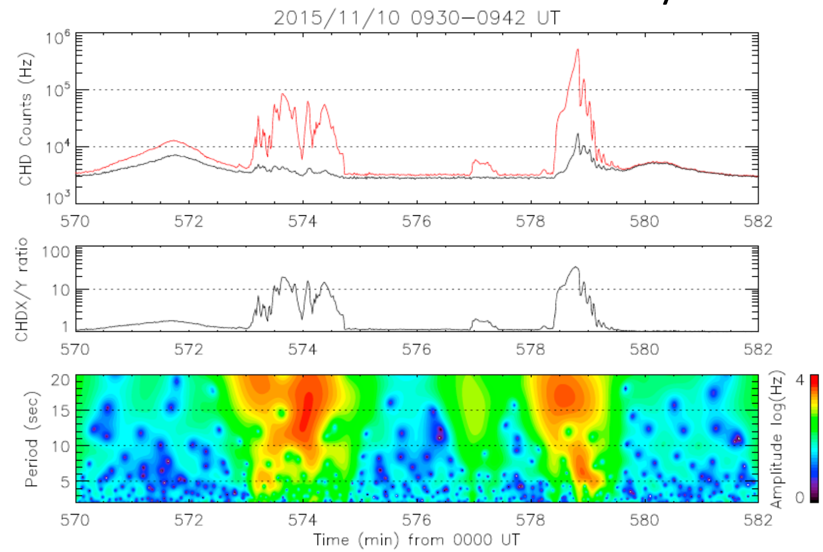

CERN-SPS Beam Test: protons and electrons

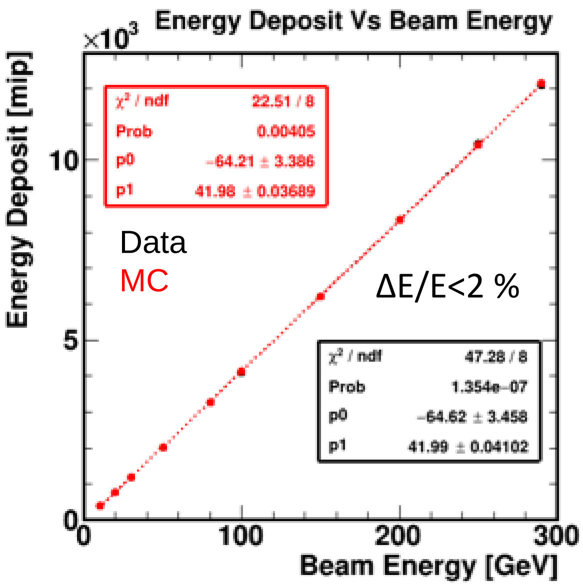

Electron shower transition curve in TASC

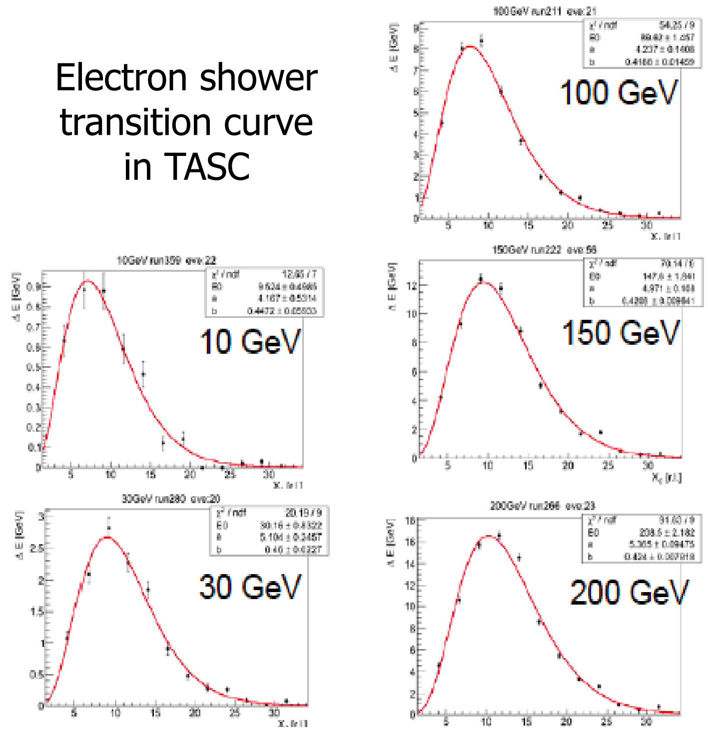

Energy distribution

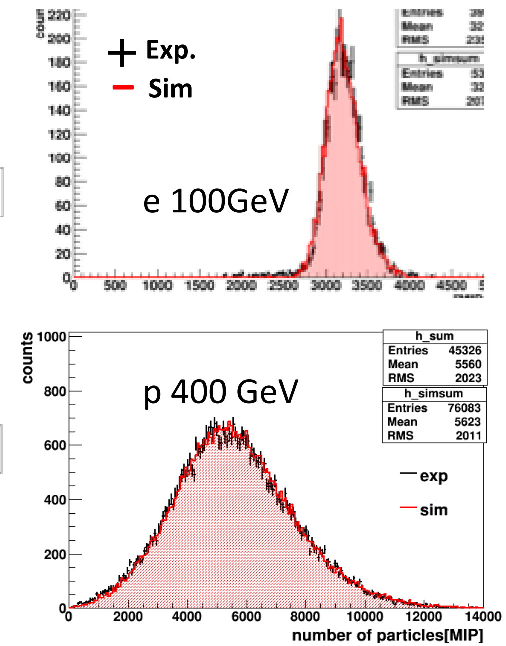

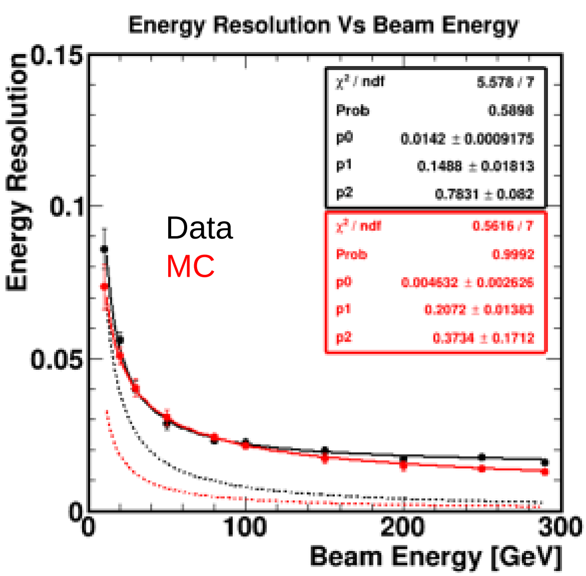

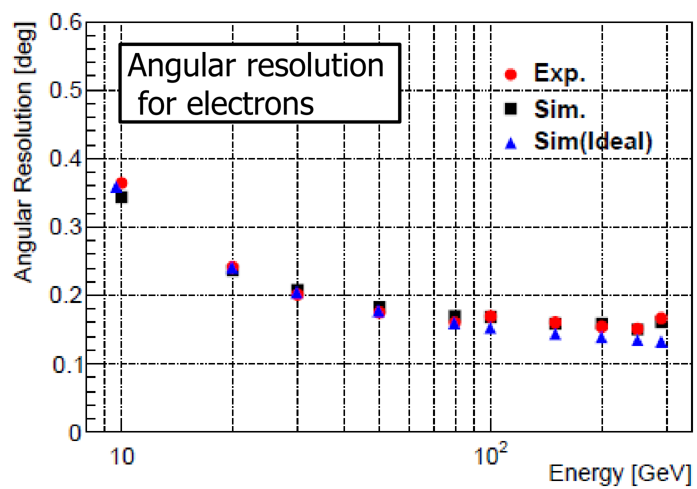

Heavy Ion Beam Test @ CERN 2014 & 2015

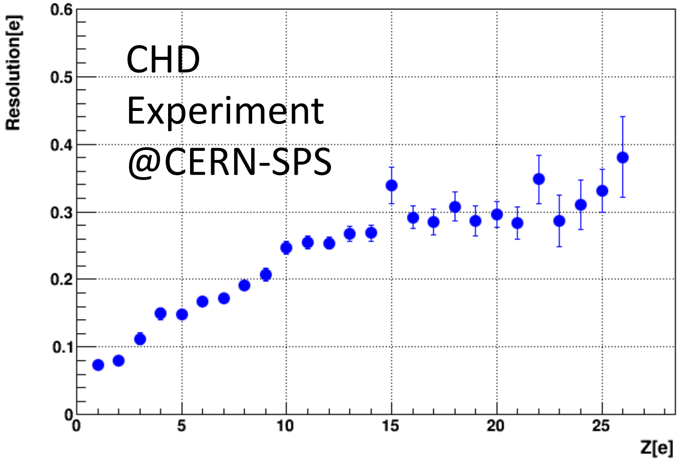

Charge resolution:
σ_Z = 0.15e(@B) – 0.35e(@Fe)

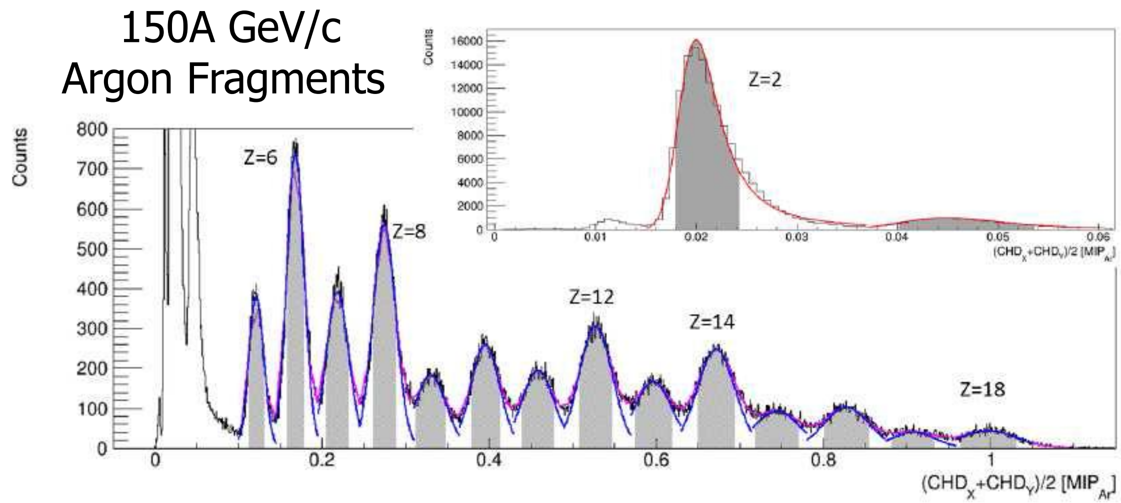

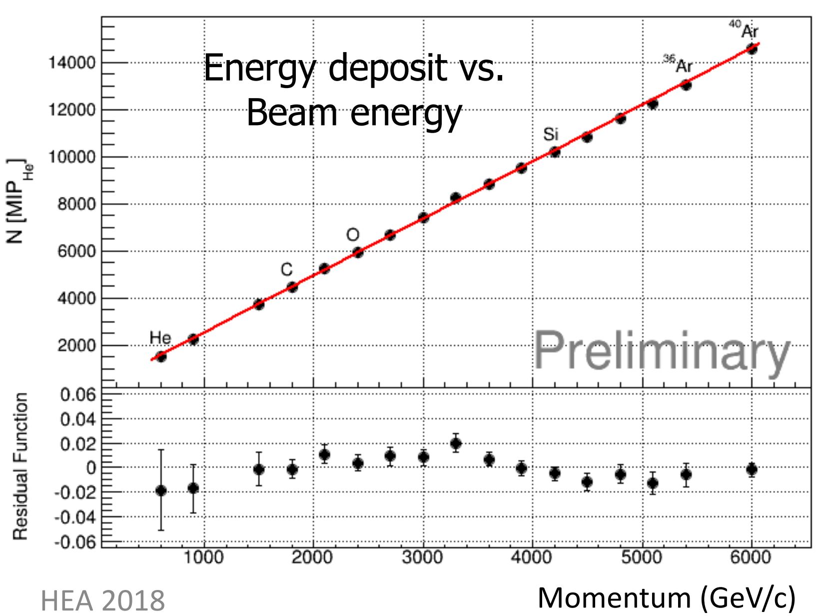

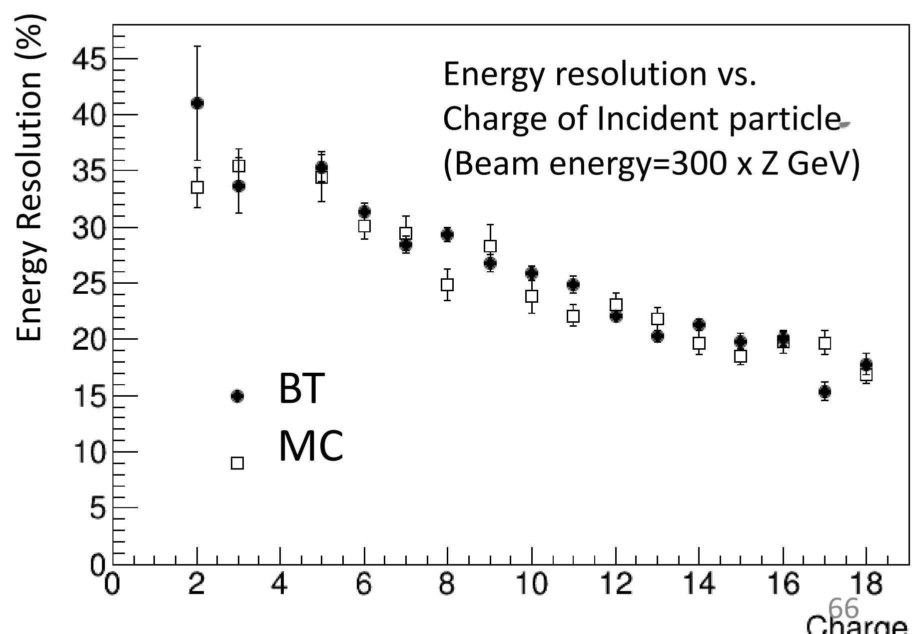

Absolute Calibration of Energy Scale using Geomagnetic Rigidity Cutoff

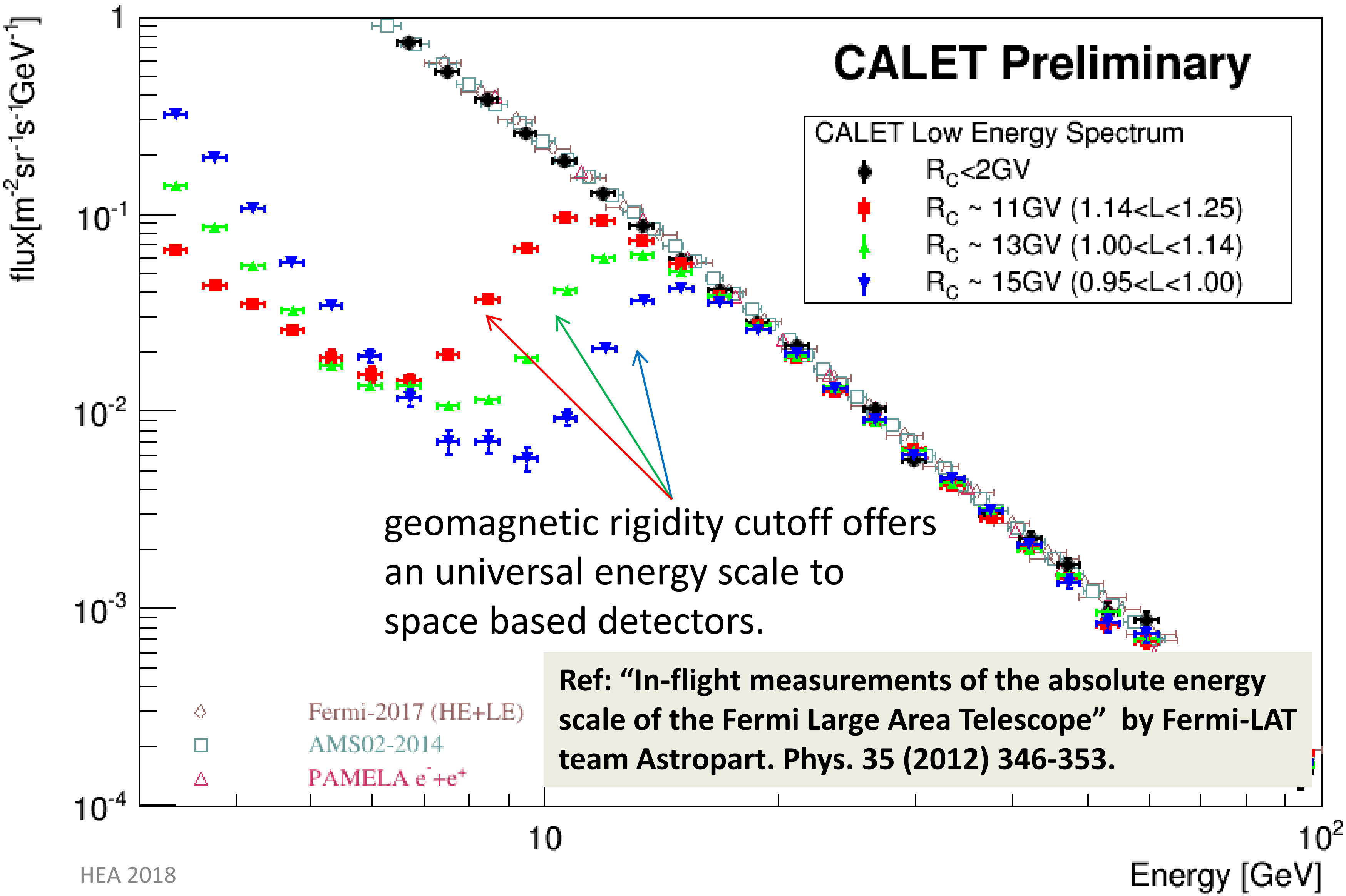

geomagnetic rigidity cutoff offers an universal energy scale to space based detectors.

Ref: “In-flight measurements of the absolute energy scale of the Fermi Large Area Telescope” by Fermi-LAT team Astropart. Phys. 35 (2012) 346-353.

Cutoff Rigidity Measurements and Comparison with Calculation

Measured cutoff rigidity is compared with calculated one (denoted as Tracer) which trace particle in earth's magnetic field (IGRF12).

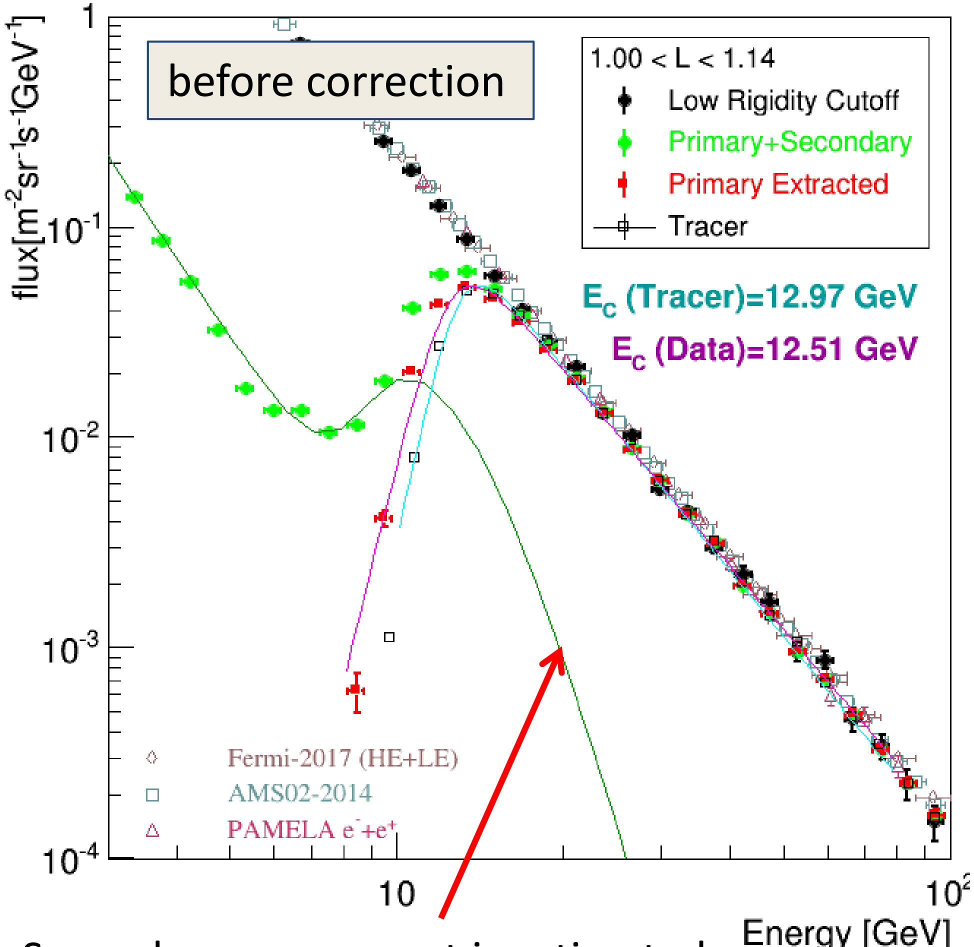

Secondary component is estimated using azimuthal distributions

- Same analysis performed in 3 different rigidity cutoff regions.

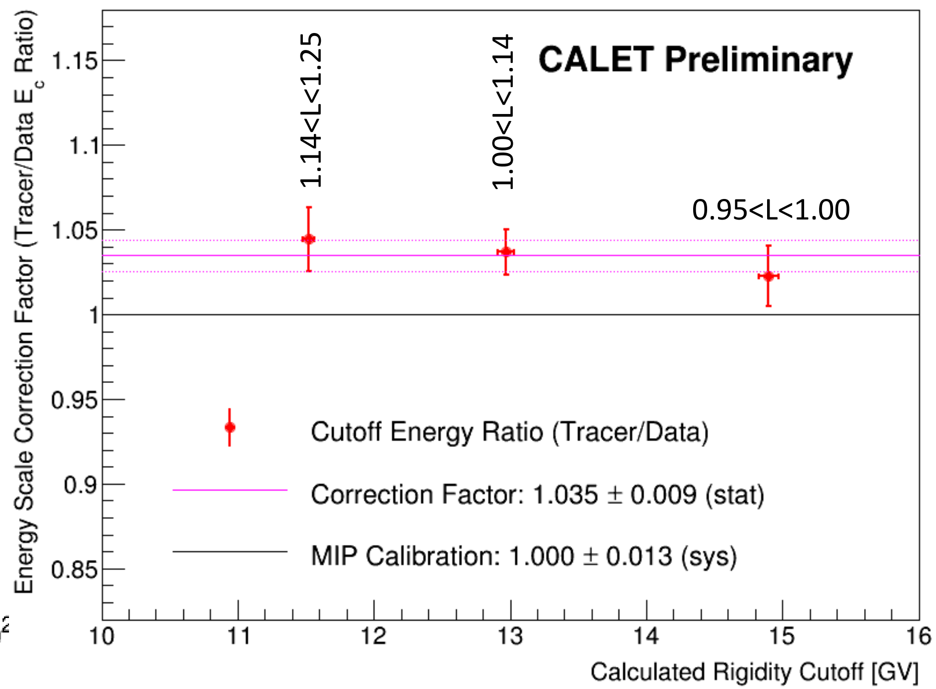

Cutoff Rigidity Measurements and Comparison with Calculation

Measured cutoff rigidity is compared with calculated one (denoted as Tracer) which trace particle in earth's magnetic field (IGRF12).

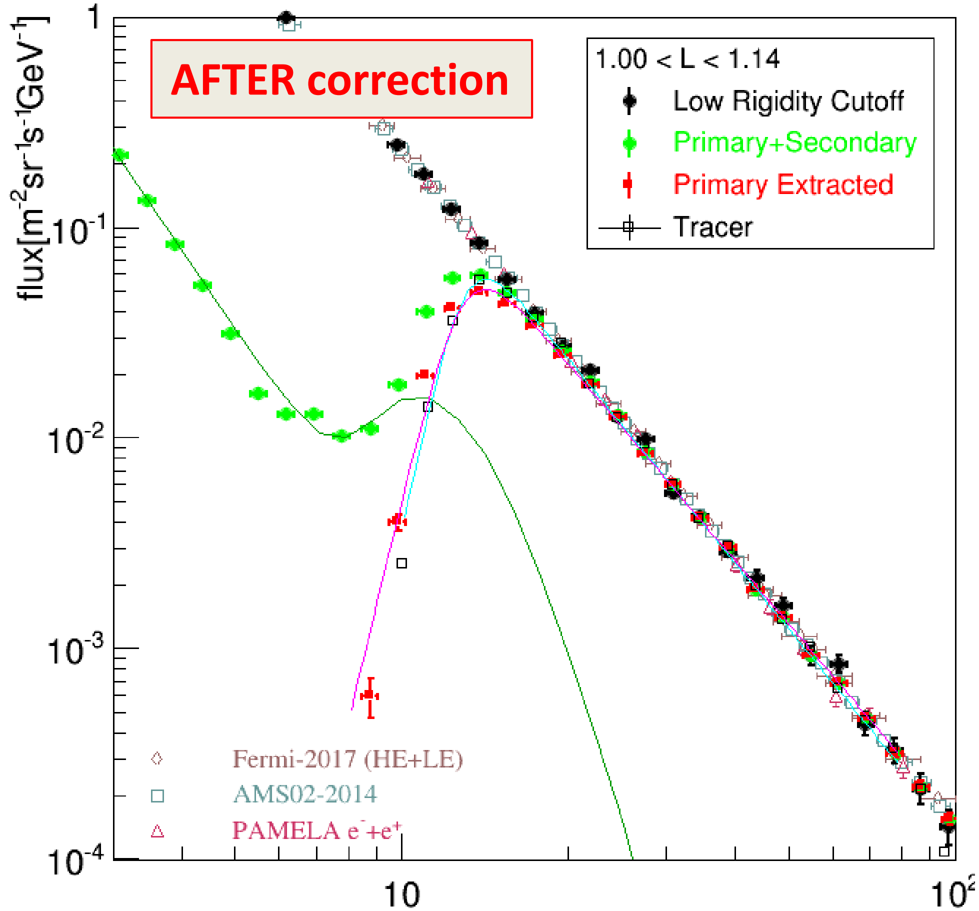

- Same analysis performed in 3 different rigidity cutoff regions.

⇒ Correction factor was found to be **1.035** compared to MIP calibration.

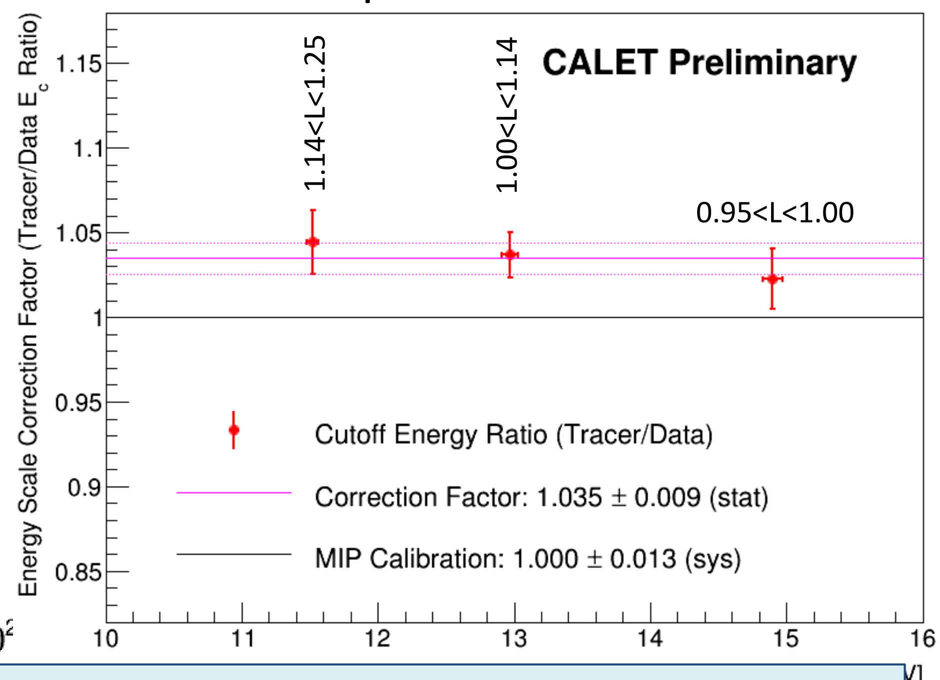

Since universal energy-scale calibration between different instruments is very important, we adopt the energy scale determined by rigidity cutoff to derive our spectrum.

Subtraction of Secondary Components based on Azimuthal Distributions

following Fermi-LAT recipe [Ackermann et al. Astropart. Phys. 35 (2012) 346]

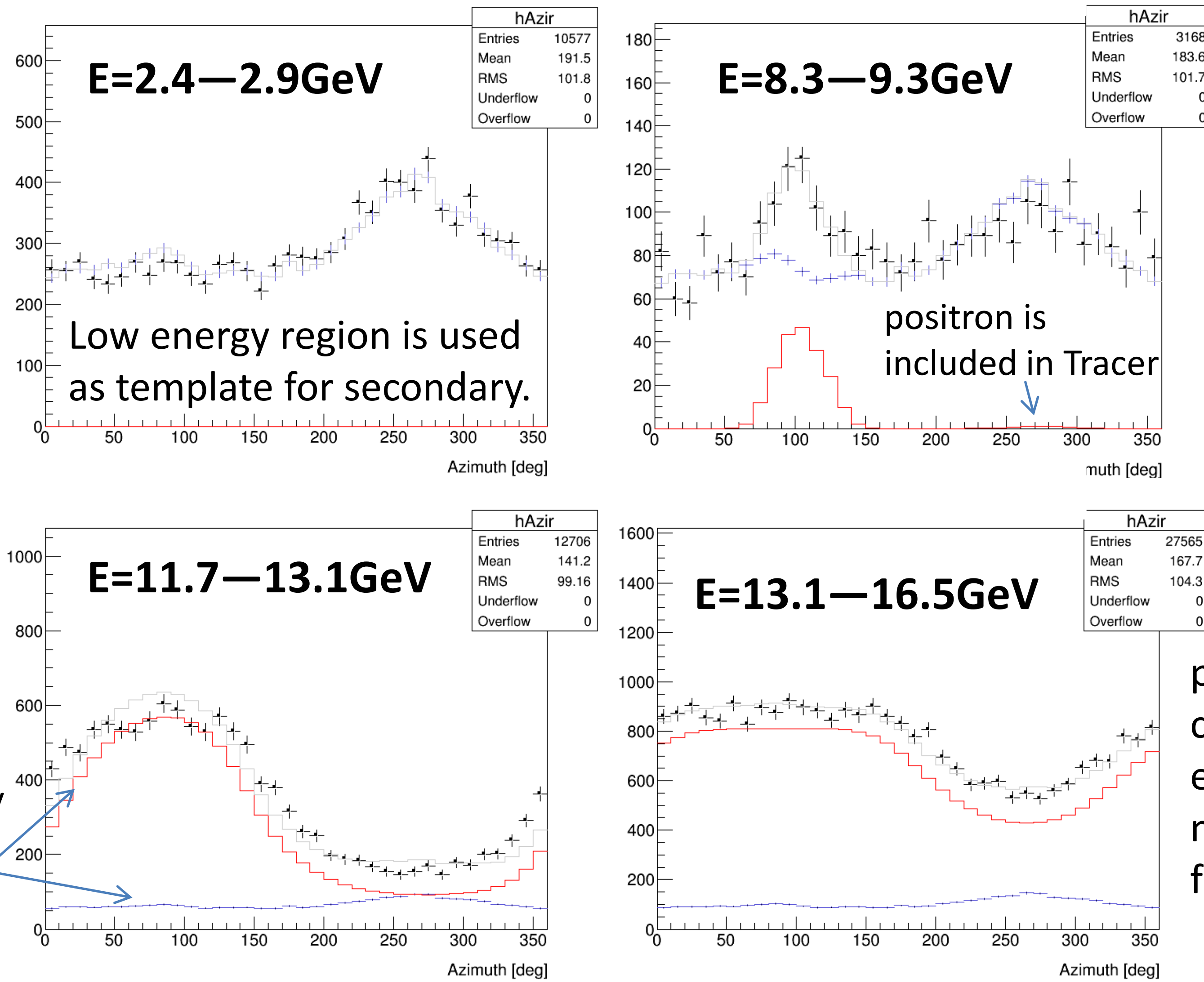

RED: (Tracer) primary
Blue: secondary
Gray: sum
Black: Flight Data

azimuthal dependence of secondary component is fixed at low energy while that of primary changes with energy and is estimated by Tracer.

Tracer:
particle trace code in the earth's magnetic field (IGRF12)

Energy Calibration Using “MIP” in Flight with Tests on Ground

Intrinsic Advantage of the CALET Instrument :

EM Shower Energy Measurement =TASC Energy Sum × “Small” Correction

- Active and thick calorimeter absorbs most of the electromagnetic energy (~95%) up to the TeV region
  - Fine energy resolution of ~ 2 %
  - Capability of measuring shower energy from 1GeV to 1000 TeV in 6 order of magnitude !
- In principle, energy measurement with small systematic error is possible.
- Needs to obtain the ADC unit to energy conversion factor and to calibrate the whole dynamic range channel by channel

On orbit : Energy conversion factor using “MIP” of p or He

- Position and temperature dependence
- Latitude dependence due to rigidity cutoff

On ground: Linearity measurements for the whole dynamic range

- CHD/IMC – Charge injection
- TASC – UV Laser irradiation (end-to-end)

“MIP” peak in PWO: Obs. vs. MC

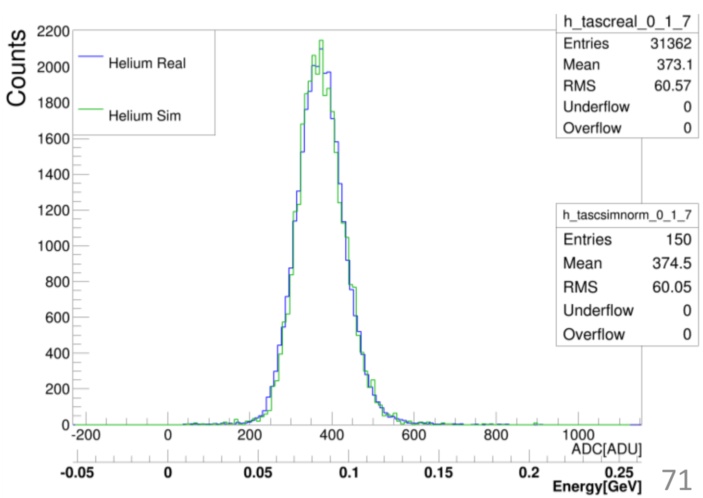

Position and Temperature Calibration, and Long-term Stability

Example of position dependence correction

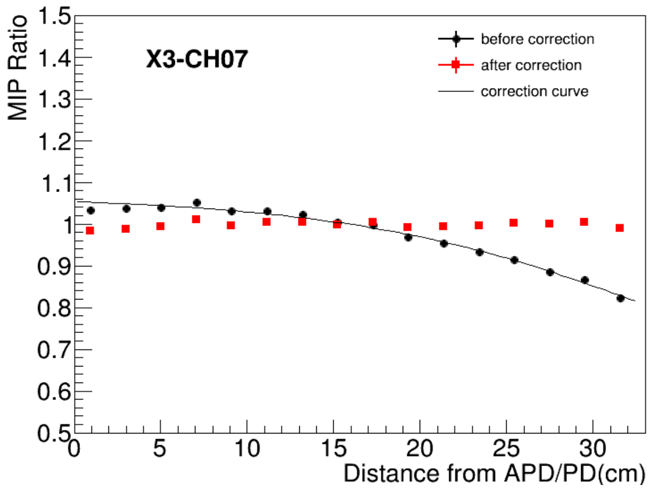

Examples of temperature change correction

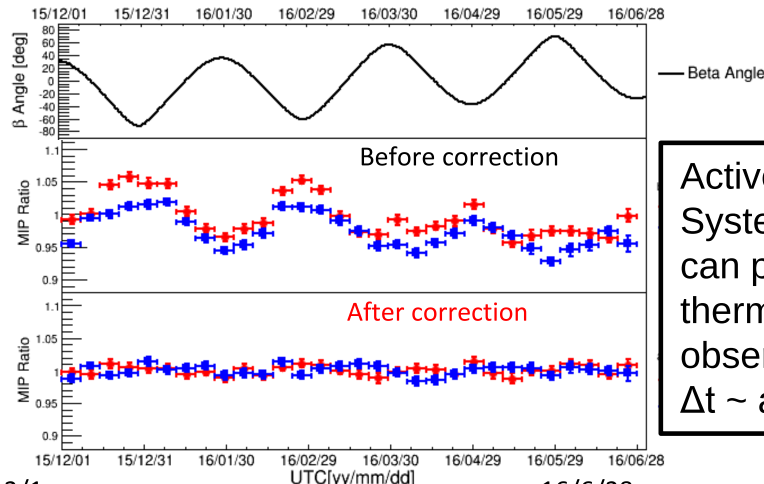

15/12/1 16/6/28

Active Thermal Control System (ATCS) on ISS can provide very stable thermal condition during observations:
Δt ~ a few degrees

Example of long-tem variation correction

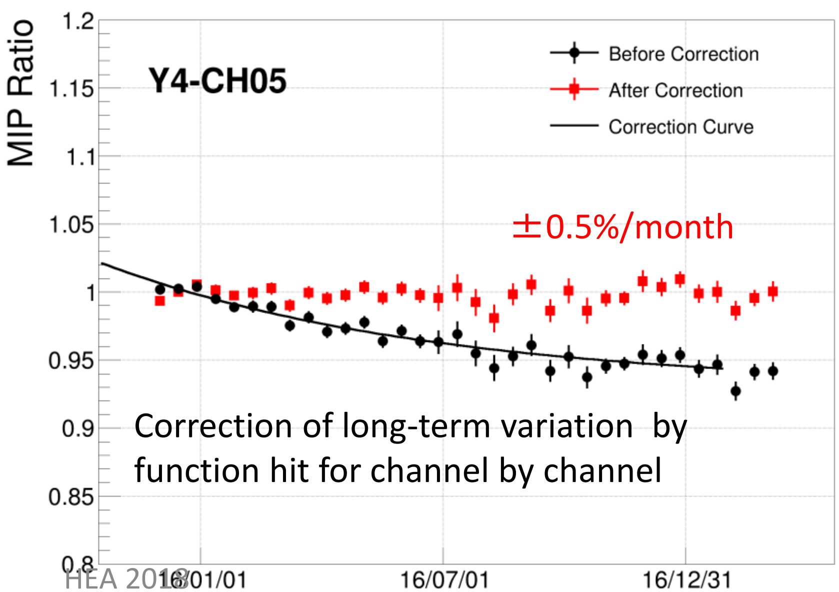

Distribution of MIPs for 192 ch x 16 segmented positions after each correction

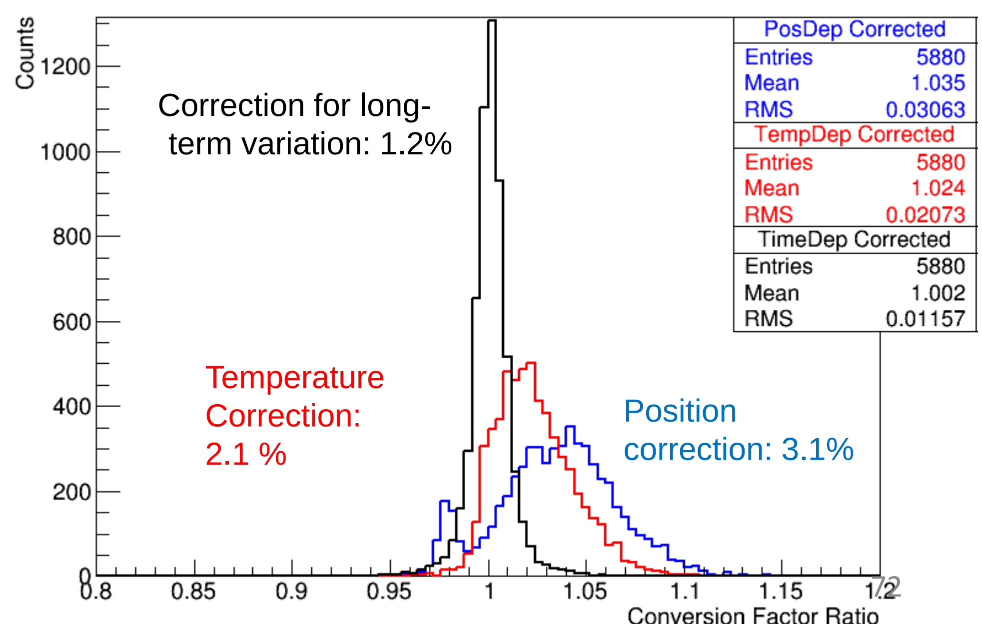

CALET Expected Performance by Simulations –electrons & gamma-rays –

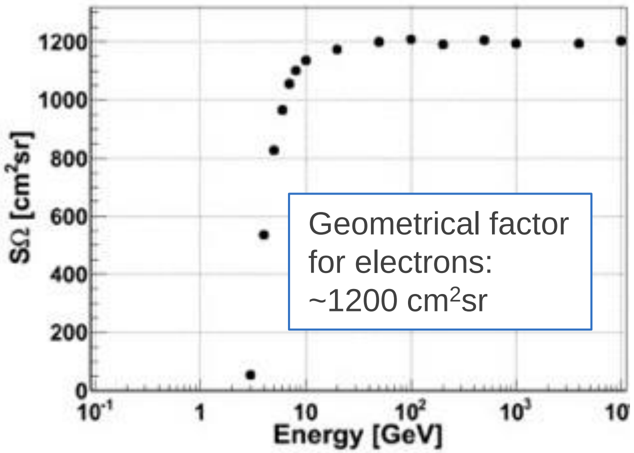

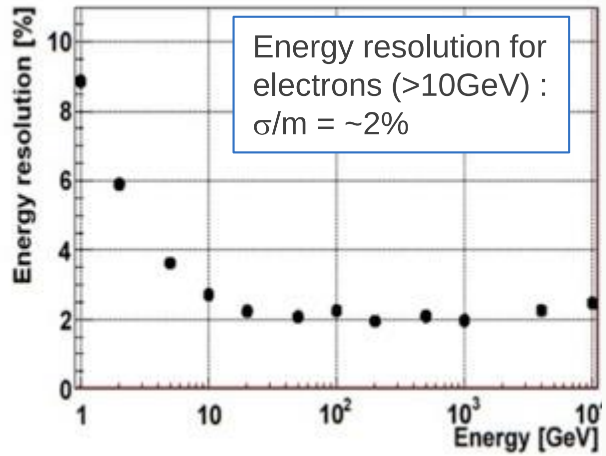

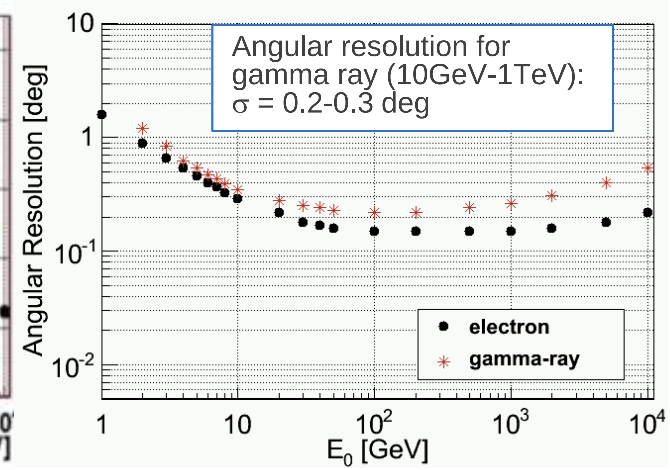

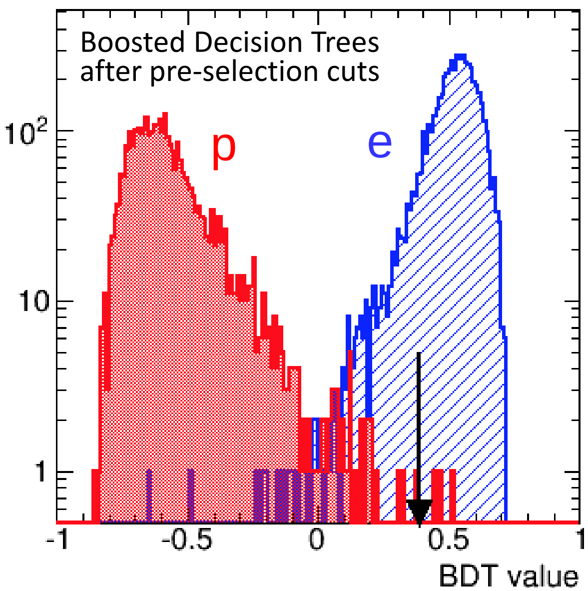

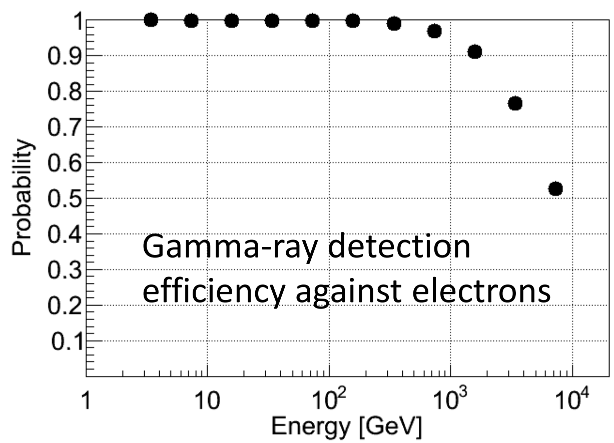

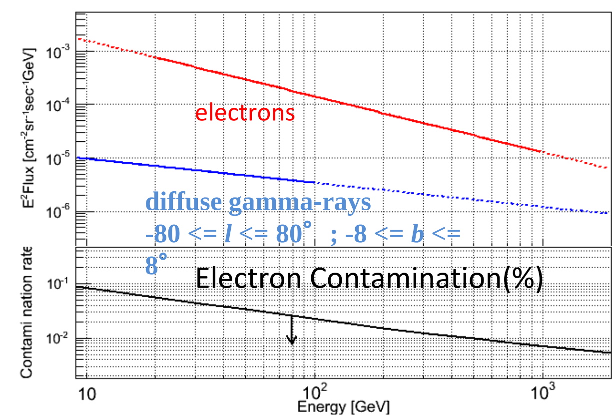

Proton rejection power at 1TeV :
≈1.3x10⁵ with 88% efficiency for electrons

Left: detection efficiency of gamma-rays with electron discrimination power 3.54 x 10^{-4} (90% CL): >95% in 10-900 GeV
Right: electron contamination in galactic diffuse gamma-rays : ~1% @10GeV –1 TeV

Nearby Sources of Electrons in the TeV region

$$\frac{\partial}{\partial t} f(t, E_e, \vec{x}) = \underbrace{D(E_e)\nabla^2 f}_{\text{Diffusion}} + \underbrace{\frac{\partial}{\partial E_e}\left[b E_e^2 f\right]}_{\text{Energy loss by IC \& synchro.}} + \underbrace{q(t, E_e, \vec{x})}_{\text{Injection}}$$

$$b \sim 10^{-16}\,\mathrm{GeV^{-1} s^{-1}}$$

$$D(E_e) \sim 5.8 \times 10^{28}\,\mathrm{cm^2 s^{-1}} \left(1 + \frac{E_e}{4\,\mathrm{GeV}}\right)^{1/3} \leftarrow \text{B/C ratio}$$

T (age) = 2.5 × 10^5 × (TeV/E) yr

R (distance) = 600 × $(\mathrm{TeV/E})^{1/2}$ pc

Contribution to 3 TeV Electrons from Nearby Source Candidates

Kobayashi et al. ApJ 2004

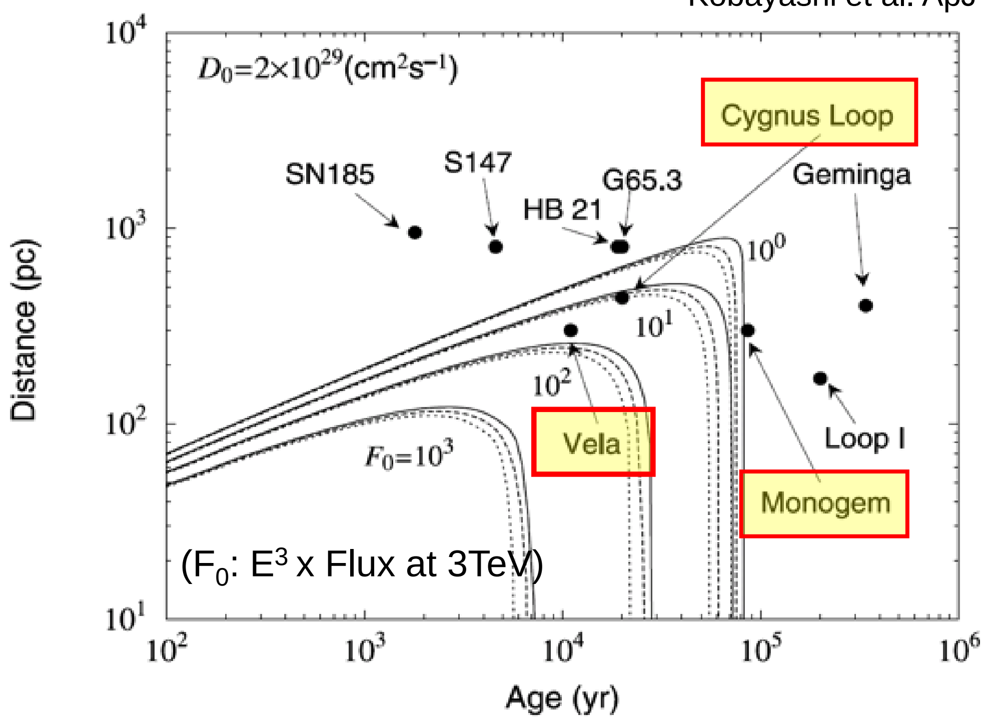

> 1 TeV Electron Source:

- **Age < a few10^5 years**
  very young comparing to ~10^7 year at low energies
- **Distance < 1 kpc**
  nearby source

Source (SNR) Candidates :

Vela Cygnus Loop Monogem

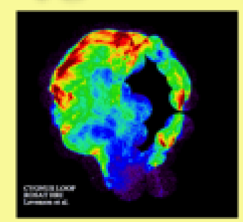

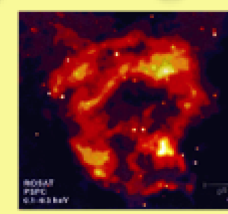

Unobserved Sources?

Overview of Trigger Modes for CALET

High Energy Shower Trigger (HE)

- High energy electrons (10GeV ～20TeV)
- High energy gamma rays (10GeV ～10TeV)
- Nuclei (a few10GeV～1000TeV)

Low Energy Shower Trigger (LE)

- Low energy electron at high latitude (1GeV ～10GeV)
- GeV gamma-rays originated from GRB (1GeV ～)
- Ultra heavy nuclei (combined with heavy mode)

Single Trigger (Single)

- For detector calibration : penetrating particles (mainly non-interacting protons and heliums)

(*) In addition to above 3 trigger modes, heavy modes are defined for each of the above trigger mode. They are omitted here for simple explanation.

Auto Trigger (Pedestal/Test Pulse)

- For calibration:
  - ADC offset measurement (Pedestal)
  - FEC's response measurement (Test pulse)

Data Downlink Using TDRSS and Operations Center

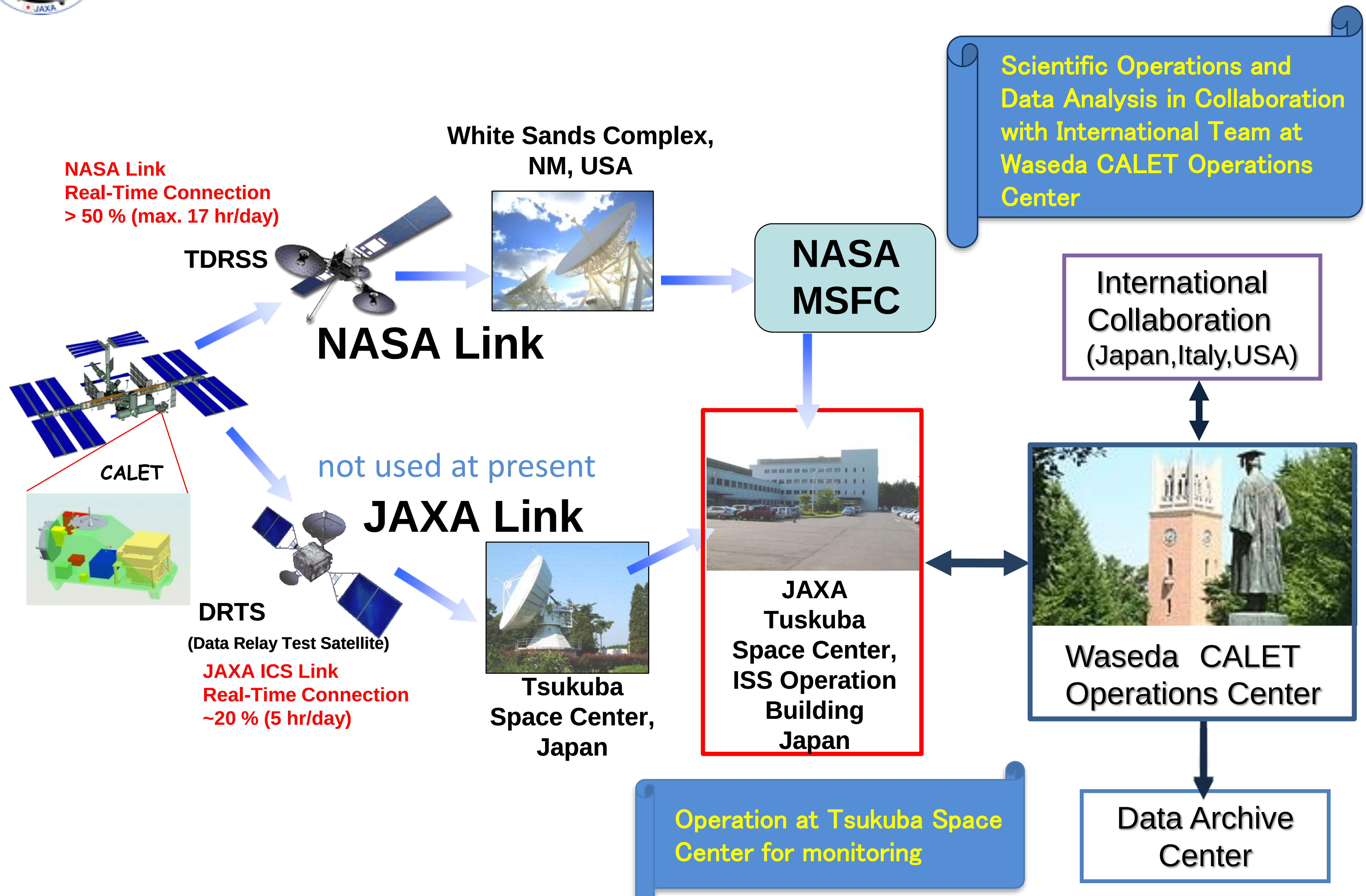

Strong GeV γ-ray Activity from blazar CTA 102

reported to ATEL by AGILE, Fermi, DAMPE in GeV

⇒ Also detected by CALET

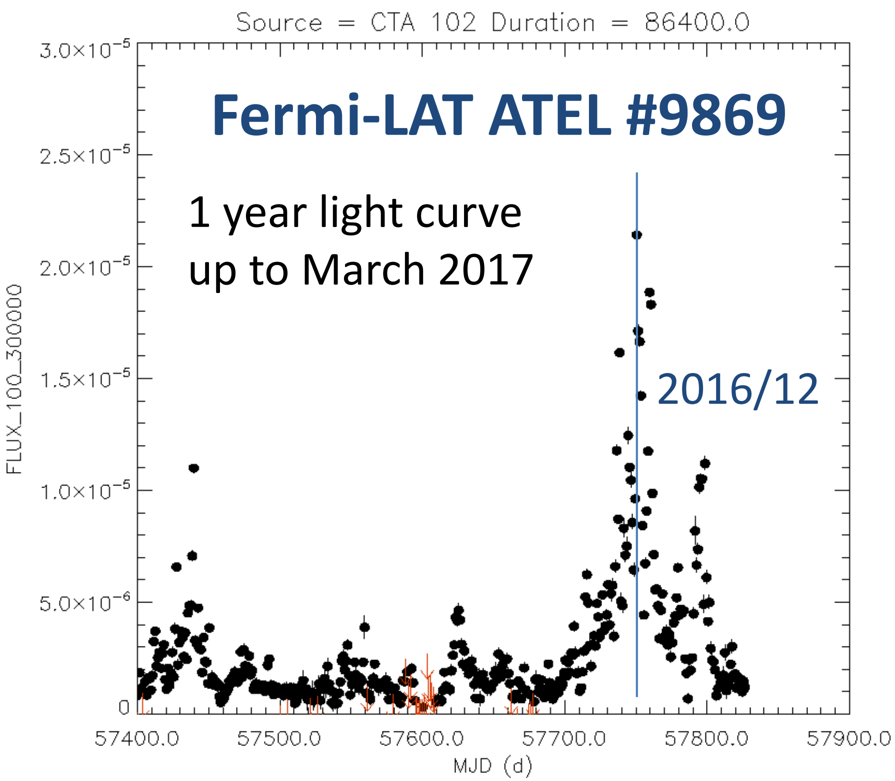

https://fermi.gsfc.nasa.gov/ssc/data/access/lat/msl_lc/source/CTA_102

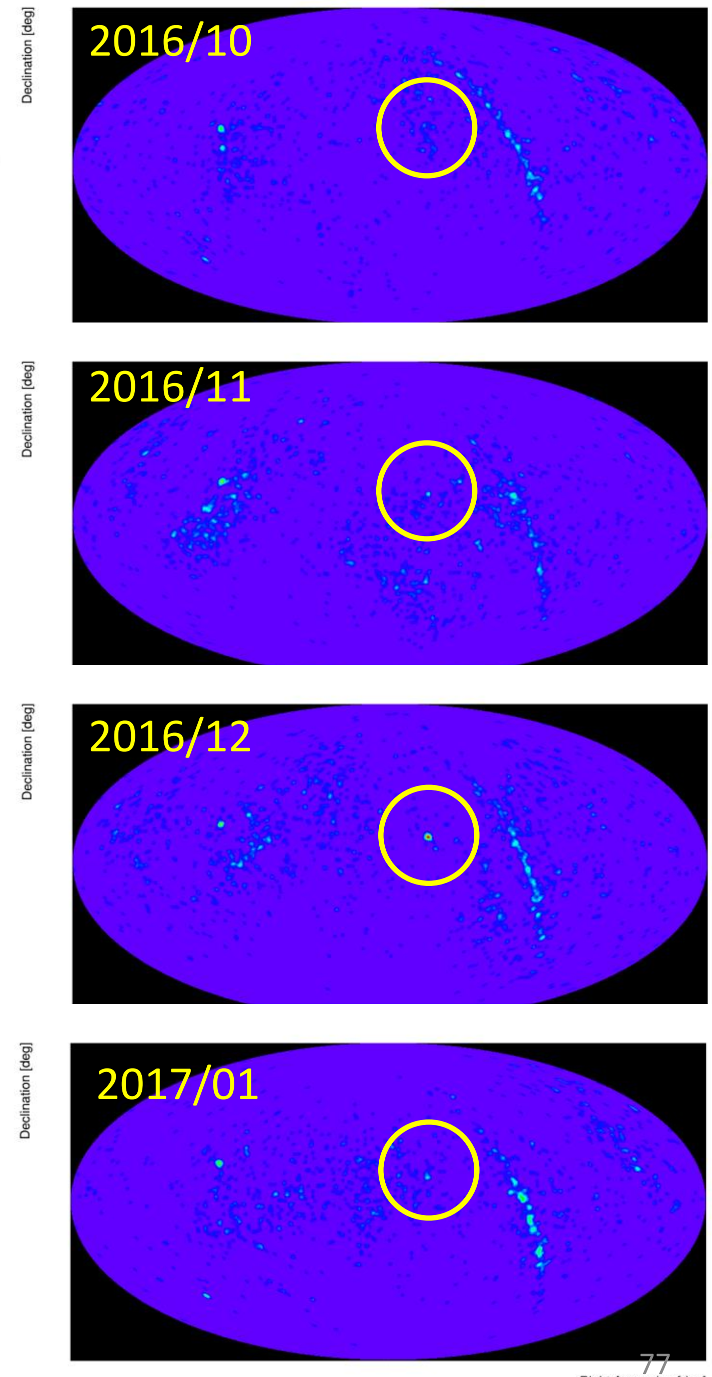

All-Electron Anisotropy Analysis

Nearby SNR and Anisotropy of the All-Electron Flux

- The Vela SNR could cause significant anisotropy in the TeV-region, depending on the cosmic-ray injection and propagation conditions
- With suitable conditions it is possible that the anisotropy signal occurs **only** at high energy, not detected by current measurements (Fermi-LAT)*
- CALET can search for such signals due to good energy determination up to several TeV

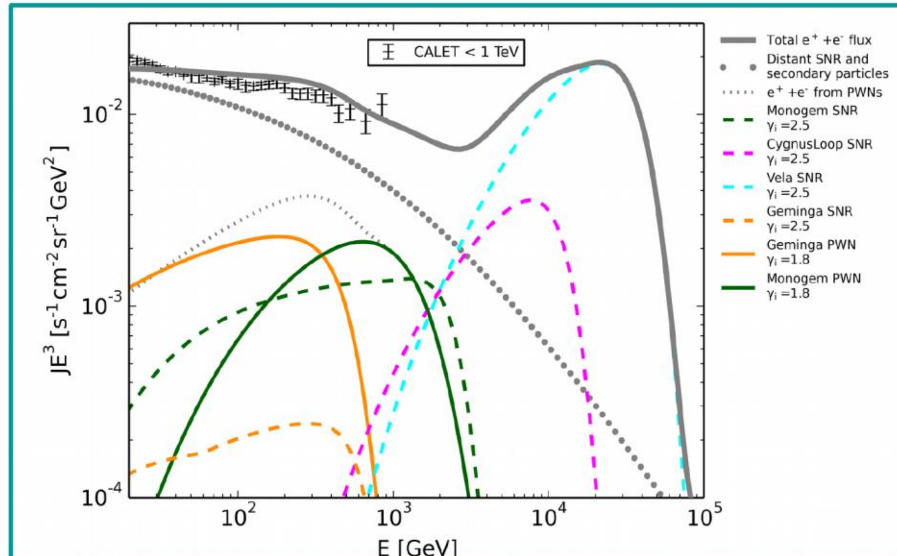

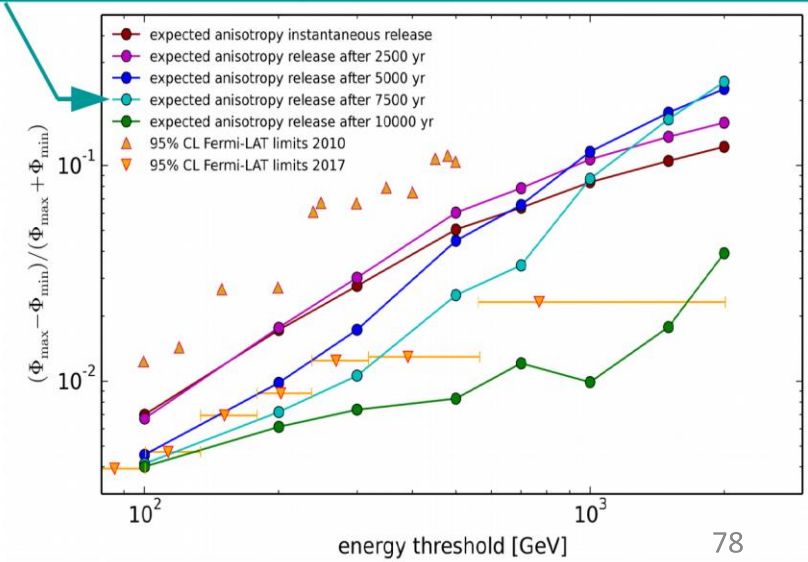

* PoS ICRC 2017, 265

All-Electron Anisotropy Analysis

H.Motz et al., ICRC 2017, PoS 265, & JPS 2017 (13aU31-4)

Analysis Method and Electron + Positron Event Sky Map

- Limits on anisotropy by finding the value of δ for which the probability of the measured and smaller anisotropy is 5% (1-CL; CL=95%).
- Analysis method is based on M. Ackermann et al., Phys. Rev. Lett. 82 (2010) 092003.

$$\delta=\frac{\Phi_{max}-\Phi_{min}}{\Phi_{max}+\Phi_{min}} \;;\; P(\hat{\delta},\delta)=\frac{3\sqrt{6}}{\sqrt{\pi}}\frac{\hat{\delta}^2}{\delta^3}e^{\left(-\frac{3}{2}\frac{\hat{\delta}^2}{\delta^2}\right)} \;;\; \int_0^{\delta_{meas}} P(\hat{\delta},\delta)\,d\hat{\delta}=1-CL$$

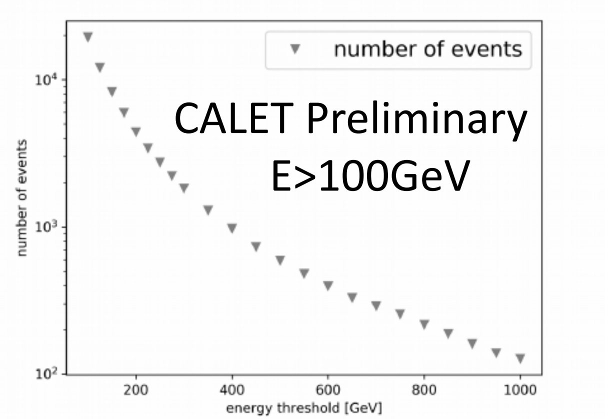

- 627 days of flight data up to 170630.
- Full acceptance of 1040cm^{2}sr (Preliminary)
- Electron identification by using BDT.

CALET Preliminary
E>100GeV

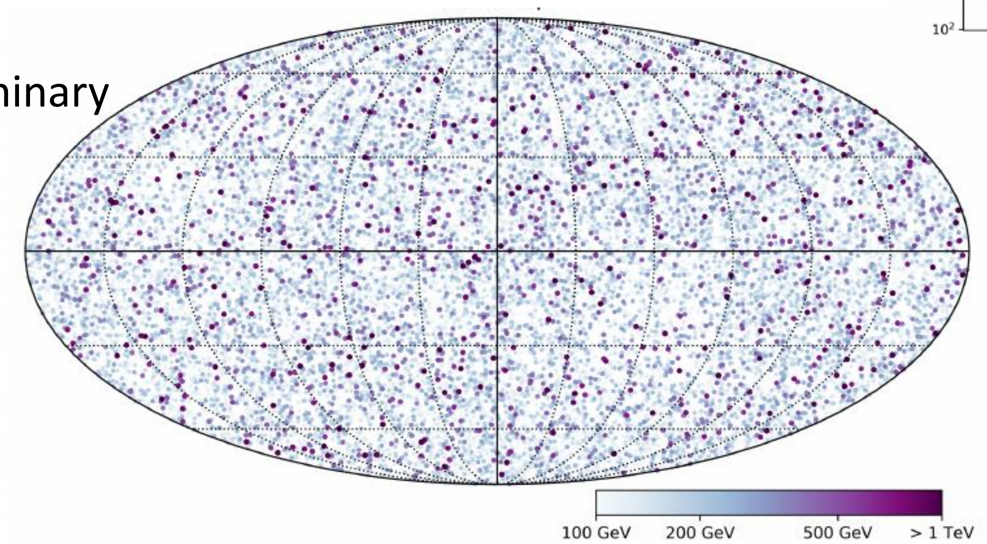

Galactic Coordinates

H.Motz et al., ICRC 2017, PoS 265, & JPS 2017 (13aU31-4)

Correction for Uneven Exposure

- ISS orbit convolved with CALET's energy and direction dependent effective area → exposure in equatorial coordinates
- Converted to galactic coordinates
- Each event receives a weight which is the inverse of this energy and direction dependent exposure, normalized to the average exposure to the sky for the measured spectrum.

Example map for this energy bin

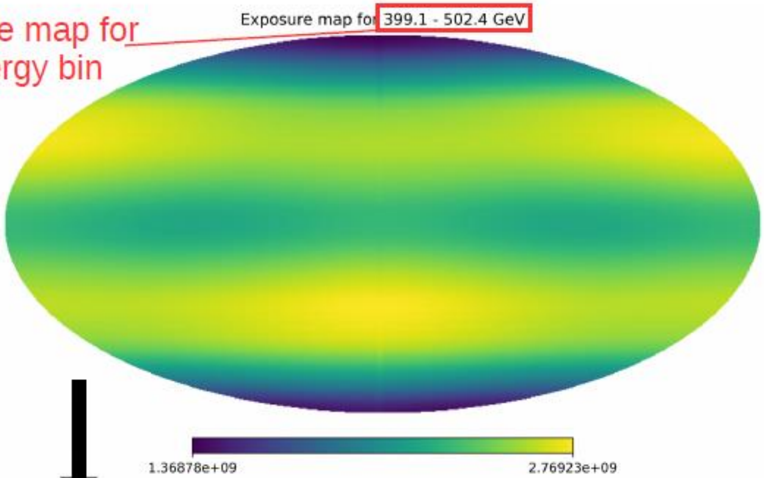

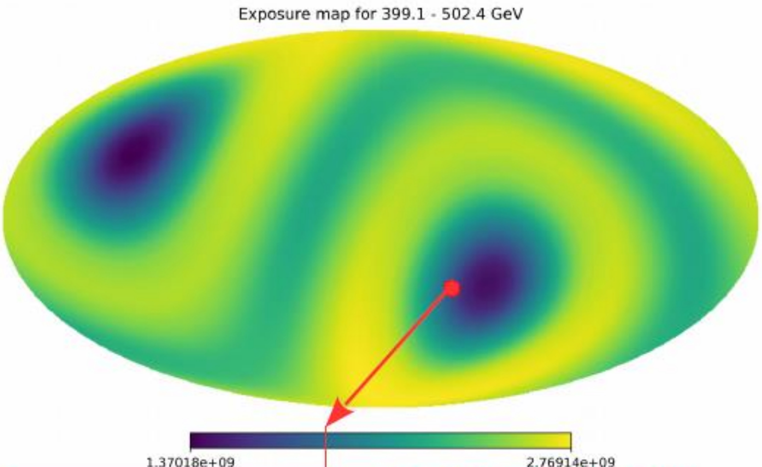

A_i : exposure for event *i*

w_i : weight for event *i*

$$w_i = \frac{1}{A_i}\left(\frac{\sum_{events}\sum_{pixels} A(E, pixel)}{N_{events} N_{pixels}}\right)$$

All-Electron Anisotropy Analysis

H.Motz et al., ICRC 2017, PoS 265, & JPS 2017 (13aU31-4)

Results: Measured Anisotropy

$$\delta = \frac{\Phi_{max} - \Phi_{min}}{\Phi_{max} + \Phi_{min}}$$

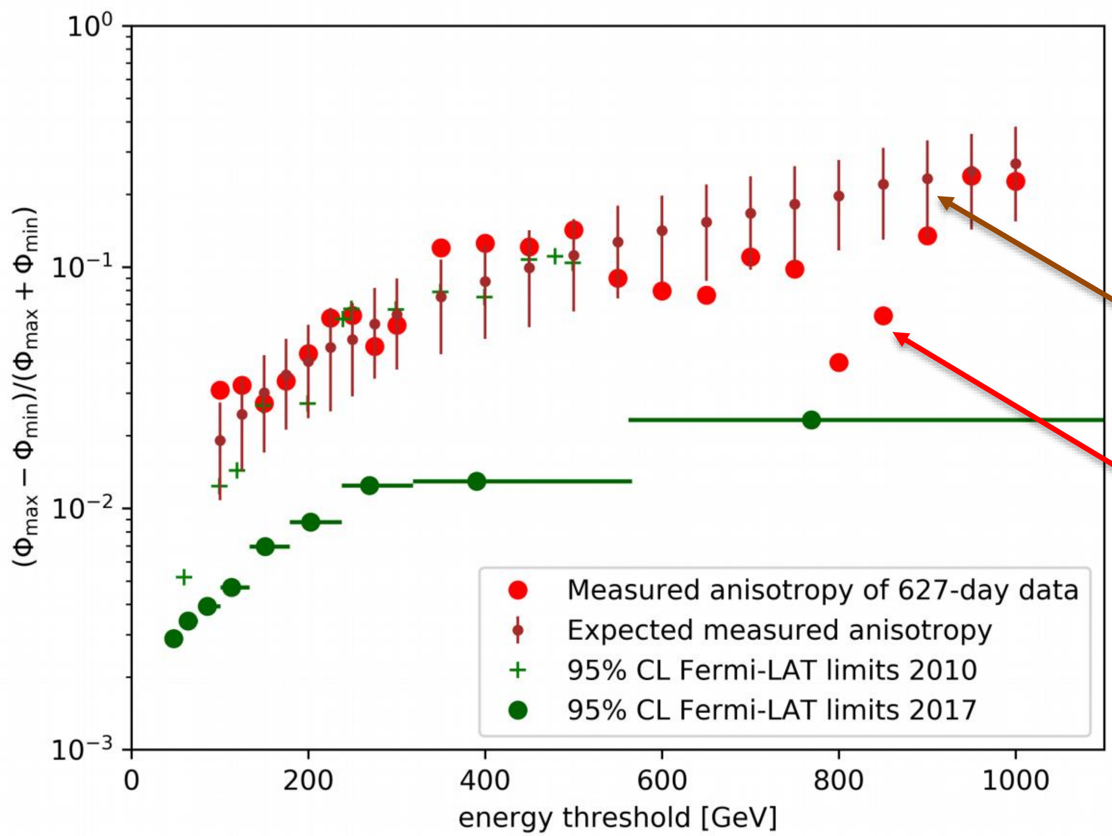

Multiple expansion with *anafast* routines of *Healpix*:

$\delta = \Phi_{dipole} / \Phi_{monopole}$

Expected anisotropy (calculated by simulated uniform sky)

Measured anisotropy is much smaller than expected (1.4% prob.)

⇔ Need to consider trial factor

All-Electron Anisotropy Analysis

H.Motz et al., ICRC 2017, PoS 265, & JPS 2017 (13aU31-4)

Results: 95% Confidence Level Limit

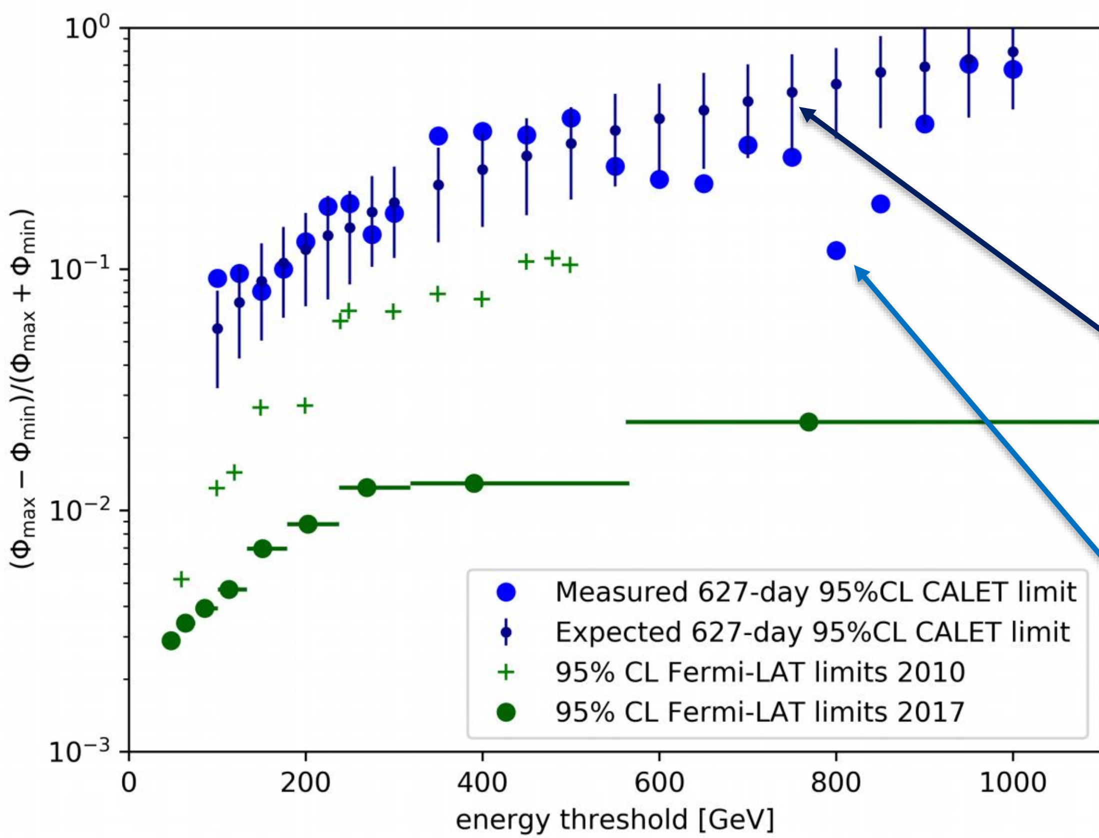

$$P(\hat{\delta},\delta)=\frac{3\sqrt{6}}{\sqrt{\pi}}\frac{\hat{\delta}^2}{\delta^3}e^{\left(-\frac{3}{2}\frac{\hat{\delta}^2}{\delta^2}\right)}$$

$$\int_0^{\delta_{meas}} P(\hat{\delta},\delta)\,d\hat{\delta}=1-CL$$

Upper limit

Expected limit (calculated by simulated uniform sky)

Measured limit is even more uniform than expected (1.4% prob.)
⇔ Need to consider trial factor

Prospects:

1. Proving 1TeV region where significant limit can be set with more statistics
2. A dedicated search directed at the position of Vela (PoS, ICRC2017, 265)